SMAI-JCM
SMAI Journal of Computational Mathematics

Bounded commuting projections for multipatch spaces with non-matching interfaces

Martin Campos Pinto & Frederik Schnack

Volume 11 (2025), p. 85-137.
https://doi.org/10.5802/smai-jcm.120

The SMAI Journal of Computational Mathematics is a member of the Centre Mersenne for Open Scientific Publishing
http://www.centre-mersenne.org/
Submissions at https://smai-jcm.centre-mersenne.org/ojs/submission
e-ISSN: 2426-8399

SMAI Journal of Computational Mathematics
Vol. 11, 85-137 (2025)

Bounded commuting projections for multipatch spaces with non-matching interfaces

Martin Campos Pinto [1]
Frederik Schnack [2]

[1] Max-Planck-Institut für Plasmaphysik, Boltzmannstr. 2, 85748 Garching, Germany
E-mail address: martin.campos-pinto@ipp.mpg.de
[2] Max-Planck-Institut für Plasmaphysik, Boltzmannstr. 2, 85748 Garching, Germany
E-mail address: frederik.schnack@ipp.mpg.de.

Abstract. We present commuting projection operators on de Rham sequences of two-dimensional multipatch spaces with local tensor-product parametrization and non-matching interfaces. Our construction yields projection operators which are local and stable in any L^p norm with $p \in [1, \infty]$: it applies to shape-regular spline patches with different mappings and resolutions, under the assumption that interior vertices are shared by exactly four patches, and that neighboring patches have nested resolutions in a way that excludes local chessboard patterns. Our construction also applies to de Rham sequences with homogeneous boundary conditions. Following a broken-FEEC approach, we first consider tensor-product commuting projections on the single-patch de Rham sequences, and modify the resulting patch-wise operators so as to enforce their conformity and commutation with the global derivatives, while preserving their projection and stability properties with constants independent of both the diameter and inner resolution of the patches.

2020 Mathematics Subject Classification. 65N30, 65N12, 65D07.

Keywords. Commuting projection, finite element exterior calculus, de Rham sequence, multipatch spaces, isogeometric analysis.

1. Introduction

Mixed finite element spaces which preserve the de Rham structure offer a flexible and powerful framework for the approximation of partial differential equations. This discretization paradigm has been extensively studied in the scope of electromagnetic modelling [9, 10, 28] and has given rise to an elegant body of theoretical work which guarantees that compatible spaces of nodal, edge, face and volume type lead to stable and accurate approximations to various differential operators in domains with non-smooth or non-connected boundaries [1, 6, 7, 27].

A notable step has been the unifying analysis of Finite Element Exterior Calculus (FEEC) [2, 3] developed in the general framework of Hilbert complexes. There, the existence of bounded cochain projections, i.e. sequences of commuting projection operators with uniform stability properties, is identified as a key ingredient for the stability, spectral accuracy and structure preservation of the discrete problems. In parallel, L^2 stable commuting projection operators based on composition of finite element interpolation and smoothing operators have been proposed by Schöberl [35, 36] for sequences of compatible Lagrange, Nédélec, Raviart-Thomas and discontinuous finite element spaces, and by Christiansen, Arnold, Falk and Winther in [2, 19, 20] for simplicial finite element spaces of differential forms in arbitrary dimensions. These constructions have later been refined by Ern and Guermond [23] who introduced shrinking-based mollifiers to avoid technical difficulties with the domain boundaries, and derived commuting projections stable in any L^p norm, $p \in [1, \infty]$. Local commuting projection operators have also been proposed: first by Falk and Winther [25] with uniform stability properties

https://doi.org/10.5802/smai-jcm.120

in the domain spaces (H^1, $H(\mathrm{curl})$, ...) and by Arnold and Guzmán [4] with uniform stability in L^2. Let us also mention [22] where the authors derive local stable commuting projections in $H(\mathrm{div})$.

Important extensions of these works have been carried out in the scope of isogeometric analysis methods [30], with structure-preserving spline finite element spaces on multipatch domains proposed by Buffa, Sangalli, Rivas and Vásquez in [13, 14]. These discretizations involve compatible sequences of tensor-product spline spaces defined on a Cartesian parametric domain and transported on mapped subdomains (the patches) using pullback operators such as contravariant and covariant Piola transformations. The parametric tensor-product structure is attractive as it enables fast algorithms at the numerical level, and with the elegant construction of [13] it admits a variety of commuting projection operators starting from general projections for the first space of the sequence. In particular, this process leads to commuting projections with uniform stability properties on single-patch spline spaces.

A difficulty, however, regards the construction of stable commuting projection operators on multipatch spline spaces. Because the tensor-product structure breaks down at the patch interfaces the construction of [13] does not apply, and it is unclear whether the smoothing projection approach of [2, 20, 35] can yield projections which are uniformly stable with respect to the inner grid resolution of the patches, due to the non-locality of spline interpolation operators. Although optimal convergence results for multipatch spline approximations have been established in [11, 16], up to our knowledge no L^2 stable commuting projections have been proposed for these spaces.

Another difficulty regards the extension of these constructions to locally refined spaces. A typical configuration is when adjacent patches are discretized with spline spaces using different knot sequences or polynomial degrees. Then the patches are non-matching in the sense of [16] and the existence of commuting projection operators, let alone stable ones, seems to be an open question. More generally the preservation of the de Rham structure at the discrete level is an active research topic when locally refined splines are involved: let us cite [15, 31] on the construction of discrete de Rham sequences of T-spline and locally refined B-splines, [24] where sufficient and necessary conditions are proposed for the exactness of discrete de Rham sequences on hierarchical spline discretizations, and [33, 38] for de Rham sequences of splines with multiple degrees and mapped domains with polar singularities. We note, however, that none of these works propose commuting projection operators for spline spaces with local refinement.

In this article, we provide a first answer to these questions in the 2D setting, by constructing L^p stable commuting projection operators on multipatch spaces with non-matching interfaces, for any $1 \le p \le \infty$. Under the assumption that the multipatch decomposition is geometrically conforming, that local resolutions across patch interfaces must be nested and that interior vertices are shared by exactly four patches, our construction applies to general discretizations involving parametric tensor-product spaces with locally stable bases. Our commuting projection operators are also local, and their stability holds with constants independent of both the size of the patches and the resolution of the individual patch discretizations.

Our construction follows a broken-FEEC approach reminiscent of [18, 26], where the multipatch finite element spaces are seen as the maximal conforming subspaces of broken spaces defined as the juxtaposition of the single-patch ones. The commuting projections are then obtained by a two-step process: Applying the tensor-product construction of [13] on the individual single-patch spaces (which consists of composing antiderivative operators, stable projections and local derivatives) we first obtain stable projection operators on the broken space which commute with the patch-wise differential operators. The second step is to modify these patch-wise projections close to the patch interfaces so as to enforce the conformity conditions and their commuting properties, while preserving their projection and stability properties. On the first space of the sequence where the conformity amounts to continuity conditions across patch interfaces, this is done by composing the patch-wise commuting projection with a local discrete conforming projection which essentially consists of averaging interface degrees of freedom. On the next spaces the patch-wise commuting projection are modified with additive correction terms which rely on carefully crafted antiderivative, local projection and derivative operators associated with the edge and vertex interfaces. Our main finding is that this constructive process indeed produces local commuting projection operators on the conforming spaces, with uniform L^p stability properties. Moreover, our construction also applies to de Rham sequences with homogeneous boundary conditions. A by-product of this analysis is the optimal convergence and spectral correctness of Hodge–Laplace operators on multipatch spaces with patch-wise refinements.

The outline is as follows: in Section 2 we present the form of our commuting projection operators and state their main properties. The structure of the broken and conforming multipatch spaces are respectively described in Section 3 and 4, together with our assumptions on the multipatch geometry and the local stability of the bases. In Section 5 we define and study stable antiderivative operators associated with patches, edge and vertex interfaces, and our construction is finalized in Section 6 with a statement of our main results. Section 7 is then devoted to proving these results, using the preliminary properties established for the various intermediate operators. We conclude with some perspectives. The appendix presents ours results for the curl-div sequence and describes how the construction is modified in the case of homogeneous boundary conditions.

2. Broken-FEEC approach and main result

In this article, we mainly consider the 2D grad-curl de Rham sequence

$$\mathbb{R} \xrightarrow{\text{id}} V^0 = H^1(\Omega) \xrightarrow{\nabla} V^1 = H(\text{curl};\Omega) \xrightarrow{\text{curl}} V^2 = L^2(\Omega) \xrightarrow{0} \{0\}. \tag{2.1}$$

The curl-div sequence and their counterparts with homogeneous boundary conditions are discussed in the appendices A and B, as they can be treated in almost the same way. We refer to [2, 3] for their description as $L^2(\Omega)$ Hilbert complexes.

Accordingly, we consider a sequence of finite element spaces in 2D

$$V_h^0 \xrightarrow{\nabla} V_h^1 \xrightarrow{\text{curl}} V_h^2$$

included in the spaces (2.1), and a multipatch domain of the form

$$\Omega = \text{int}\left(\bigcup_{k\in\mathcal{K}} \overline{\Omega_k}\right) \quad \text{with} \quad \Omega_k = F_k(\hat{\Omega}) \tag{2.2}$$

with disjoint, geometrically conforming subdomains Ω_k associated with smooth mappings F_k defined on a reference domain $\hat{\Omega} =]0,1[^2$. We further assume that each patch Ω_k is equipped with a sequence of local finite element spaces

$$V_k^0 \xrightarrow{\nabla} V_k^1 \xrightarrow{\text{curl}} V_k^2 \tag{2.3}$$

where $V_k^\ell = \mathcal{F}_k^\ell(\hat{V}_k^\ell)$ is defined as the ℓ-degree pushforward of a logical space $\hat{V}_k^\ell$ with a locally stable tensor-product basis that will be described in the next section.

We further allow different patches to have different logical spaces, which corresponds to local (patch-wise) refinements, under nestedness assumptions which will be specified later on. The global finite element spaces are then defined as

$$V_h^\ell = \{v \in V^\ell(\Omega) : v|_{\Omega_k} \in V_k^\ell \text{ for } k \in \mathcal{K}\} \tag{2.4}$$

where again, the spaces $V^\ell(\Omega)$ are given by (2.1).

Our objective is then to design L^p stable projection operators on these discrete spaces that yield a commuting diagram:

$$\begin{array}{ccccccccc} \mathbb{R} & \xrightarrow{\text{id}} & H^1(\Omega) & \xrightarrow{\nabla} & H(\mathrm{curl};\Omega) & \xrightarrow{\mathrm{curl}} & L^2(\Omega) & \xrightarrow{0} & \{0\} \\ \big\downarrow & & \big\downarrow \Pi^0 & & \big\downarrow \Pi^1 & & \big\downarrow \Pi^2 & & \big\downarrow \\ \mathbb{R} & \xrightarrow{\text{id}} & V_h^0 & \xrightarrow{\nabla} & V_h^1 & \xrightarrow{\mathrm{curl}} & V_h^2 & \xrightarrow{0} & \{0\} \end{array} \tag{2.5}$$

On a single patch Ω_k, the approach of [13] starts from a general tensor-product projection $\hat{\Pi}_k^0 : L^p(\hat{\Omega}) \to \hat{V}_k^0$ on the first logical space, and defines projections on the next spaces of the form

$$\hat{\Pi}_k^1 \hat{\boldsymbol{u}} := \sum_{d\in\{1,2\}} \hat{\nabla}_d \hat{\Pi}_k^0 \hat{\Phi}_d(\hat{\boldsymbol{u}}) \quad \text{ and } \quad \hat{\Pi}_k^2 \hat{f} := \hat{\partial}_1 \hat{\partial}_2 \hat{\Pi}_k^0 \hat{\Psi}(\hat{f}) \tag{2.6}$$

with directional gradient operators $\hat{\nabla}_d$ and antiderivative operators

$$\begin{cases} \hat{\Phi}_1(\hat{\boldsymbol{u}})(\hat{\boldsymbol{x}}) := \displaystyle\int_0^{\hat{x}_1} \hat{u}_1(z, \hat{x}_2)\,\mathrm{d}z \\ \hat{\Phi}_2(\hat{\boldsymbol{u}})(\hat{\boldsymbol{x}}) := \displaystyle\int_0^{\hat{x}_2} \hat{u}_2(\hat{x}_1, z)\,\mathrm{d}z \end{cases} \quad \text{ and } \quad \hat{\Psi}(\hat{f})(\hat{\boldsymbol{x}}) := \int_0^{\hat{x}_1}\int_0^{\hat{x}_2} \hat{f}(z_1,z_2)\,\mathrm{d}z_2\,\mathrm{d}z_1.$$

The projections (2.6) commute with the logical differential operators thanks to the tensor-product structure of $\hat{\Pi}_k^0$, and they preserve its stability due to the intrinsic integrability of the antiderivative operators and a localization argument that relies on the tensor-product product structure, as will be explained below. On the mapped spaces the projections are defined through pullbacks and pushforwards,

$$\Pi_k^\ell = \mathcal{F}_k^\ell \hat{\Pi}_k^\ell (\mathcal{F}_k^\ell)^{-1} : \quad L^p(\Omega_k) \longrightarrow V_k^\ell. \tag{2.7}$$

Their stability and commuting properties respectively follow from the smoothness of the mapping F_k and from the fact that the pullbacks commute with the differential operators, see e.g. [13, 28]. (Note that for $\ell = 1$, the L^p space in (2.7) is implicitly understood as vector-valued: this convention will be adopted throughout the article.)

At patch interfaces where the parametric tensor-product structure breaks down, this construction must be adapted. Our approach is to first consider the patch-wise projections

$$\Pi_{\mathrm{pw}}^\ell = \sum_{k\in\mathcal{K}} \Pi_k^\ell : \quad L^p(\Omega) \longrightarrow V_{\mathrm{pw}}^\ell \tag{2.8}$$

on the broken patch-wise spaces

$$V_{\mathrm{pw}}^\ell := \{v \in L^2(\Omega) : v|_{\Omega_k} \in V_k^\ell \text{ for } k \in \mathcal{K}\} \tag{2.9}$$

which are fully discontinuous at the patch interfaces. These patch-wise operators map to functions which may take different values on the interfaces, corresponding to the different patches. Therefore, we modify them to enforce the conformity conditions at the patch interfaces. On the first space of (2.1) where the H^1 conformity amounts to continuity conditions, in the sense that $V_h^0 = V_{\mathrm{pw}}^0 \cap C^0(\Omega)$, this is done by applying a conforming projection $P : V_{\mathrm{pw}}^0 \to V_h^0$ which averages interface degrees of freedom: we thus set

$$\Pi^0 := P\Pi_{\mathrm{pw}}^0.$$

On the next spaces our modification takes the form of additive correction terms associated with the patch interfaces. The global projection on V_h^1 has the form

$$\Pi^1 := \Pi^1_{\rm pw} + \sum_{e\in\mathcal{E}} \tilde\Pi^1_e + \sum_{\boldsymbol{v}\in\mathcal{V}} \tilde\Pi^1_{\boldsymbol{v}} + \sum_{\boldsymbol{v}\in\mathcal{V}, e\in\mathcal{E}(\boldsymbol{v})} \tilde\Pi^1_{e,\boldsymbol{v}} \tag{2.10}$$

with correction terms that are localized on patch edges and vertices. Like the single-patch projections (2.6), they involve antiderivative operators, local (patch-wise) projections $\Pi^0_{\rm pw}$ and partial derivative operators. In addition, they also involve local projection operators which vanish on conforming functions. Specifically, our correction terms take the following form:

$$\begin{cases} \tilde\Pi^1_e \boldsymbol{u} := \sum_{d\in\{\parallel,\perp\}} \nabla^e_d (P^e - I^e)\Pi^0_{\rm pw}\Phi^e_d(\boldsymbol{u}) \\ \tilde\Pi^1_{\boldsymbol{v}} \boldsymbol{u} := \nabla_{\rm pw}(P^{\boldsymbol{v}} - \bar I^{\boldsymbol{v}})\Pi^0_{\rm pw}\Phi^{\boldsymbol{v}}(\boldsymbol{u}) \\ \tilde\Pi^1_{e,\boldsymbol{v}} \boldsymbol{u} := \sum_{d\in\{\parallel,\perp\}} \nabla^e_d (\bar I^e_{\boldsymbol{v}} - P^e_{\boldsymbol{v}})\Pi^0_{\rm pw}\Phi^{\boldsymbol{v},e}_d(\boldsymbol{u}). \end{cases}$$

Here, $\nabla_{\rm pw}$ is the patch-wise gradient operator and ∇^e_d, $d \in \{\parallel, \perp\}$, are patch-wise gradients along the logical parallel and perpendicular directions relative to a given edge e: they will be defined in Section 3. The various operators P^g, I^g, $\bar I^g, \dots$ are discrete projections on local conforming and broken subspaces associated to patch edges (for $g = e$), vertices (for $g = \boldsymbol{v}$) and edge-vertex pairs (for $g = (\boldsymbol{v}, e)$). These local projection operators will be designed so as to guarantee the grad-commuting properties of Π^1 and Π^0, and to vanish on continuous functions: they will be described in Section 4. Finally, the Φ^g are antiderivative operators associated with edges and vertices: they will be studied in Section 5.

Similarly, the projection on V_h^2 reads

$$\Pi^2 := \Pi^2_{\rm pw} + \sum_{e\in\mathcal{E}} \tilde\Pi^2_e + \sum_{\boldsymbol{v}\in\mathcal{V}, e\in\mathcal{E}(\boldsymbol{v})} \tilde\Pi^2_{e,\boldsymbol{v}}$$

with interface correction terms of the form

$$\begin{cases} \tilde\Pi^2_e f := D^{2,e}(P^e - I^e)\Pi^0_{\rm pw}\Psi^e(f) \\ \tilde\Pi^2_{e,\boldsymbol{v}} f := D^{2,e}(\bar I^e_{\boldsymbol{v}} - P^e_{\boldsymbol{v}})\Pi^0_{\rm pw}\Psi^{\boldsymbol{v},e}(f). \end{cases} \tag{2.11}$$

Here, $D^{2,e}$ is a second order patch-wise derivative and Ψ^e, $\Psi^{\boldsymbol{v},e}$ are bivariate antiderivatives: they will be described in Section 3 and 5.

Our findings can be summarized as follows.

Theorem 2.1. *The operators Π^ℓ_h are local projections on the spaces V^ℓ_h, $\ell = 0, 1, 2$. They yield a commuting diagram* (2.5) *and they are uniformly L^p stable with respect to the size and inner resolution of the patches.*

This result will be formally stated and proven in Section 6. A precise meaning of the uniform stability will be given by listing discretization parameters κ_1, $\kappa_2, \dots$ on which our estimates depend. Throughout the article, we will then write

$$f \lesssim g$$

to mean that $f \le Cg$ holds for a constant that only depends on these constants κ_m while $f \sim g$ indicates that both $f \lesssim g$ and $g \lesssim f$ hold.

3. Broken multipatch spaces

In this section, we describe in more detail the multipatch domains and the finite element spaces to which our construction applies.

3.1. Multipatch geometry

As described above, we consider a domain Ω of the form (2.2), made of disjoint open patches $\Omega_k = F_k(\hat{\Omega})$ with smooth mappings F_k, $k \in \mathcal{K}$. We denote by H_k the diameter of patch Ω_k, and assume that the mappings are C^1 diffeomorphisms with Jacobian matrices satisfying

$$\|DF_k(\hat{\boldsymbol{x}})\| \leq \kappa_1 H_k \quad \text{and} \quad \|(DF_k(\hat{\boldsymbol{x}}))^{-1}\| \leq \kappa_2 (H_k)^{-1}$$

for all $\hat{\boldsymbol{x}} \in \hat{\Omega}$ and $k \in \mathcal{K}$. In particular, it holds

$$\|DF_k(\hat{\boldsymbol{x}})\| \sim H_k, \quad \|(DF_k(\hat{\boldsymbol{x}}))^{-1}\| \sim (H_k)^{-1}, \quad \det(DF_k(\hat{\boldsymbol{x}})) \sim H_k^2. \tag{3.1}$$

We make the following assumptions:

(i) the patch decomposition is geometrically conforming,

(ii) across any interior edge, the patch discretization spaces are nested,

(iii) vertices are shared by at most four patches (exactly four in the case of interior vertices) with specific nestedness properties.

Here, Assumption (i) amounts to saying that the intersection of two closed patches is either empty, or a common vertex, or a common edge. In addition, we assume that the mappings are continuous on the patch edges, in the sense that both sides provide the same parametrization up to a possible change in orientation. Assumption (ii) is standard for locally refined spaces and Assumption (iii) essentially amounts to excluding chessboard refinement patterns around interior vertices; around boundary vertices it prevents boundary patches from being coarser than interior ones. This will be specified in Section 3.5, see Assumption 1 and 2.

3.2. Tensor-product logical spaces

Following [13, 28, 34], we consider discrete spaces on each patch which are obtained by pushing forward tensor-product de Rham sequences on the logical Cartesian domain $\hat{\Omega} =]0,1[^2$. Thus, for a patch Ω_k, $k \in \mathcal{K}$, we consider a logical discrete de Rham sequence on $\hat{\Omega}$,

$$\hat{V}_k^0 \xrightarrow{\ \nabla\ } \hat{V}_k^1 \xrightarrow{\ \mathrm{curl}\ } \hat{V}_k^2$$

with tensor-product spaces of the form

$$\hat{V}_k^0 := \mathbb{V}_k^0 \otimes \mathbb{V}_k^0, \qquad \hat{V}_k^1 := \begin{pmatrix} \mathbb{V}_k^1 \otimes \mathbb{V}_k^0 \\ \mathbb{V}_k^0 \otimes \mathbb{V}_k^1 \end{pmatrix}, \qquad \hat{V}_k^2 := \mathbb{V}_k^1 \otimes \mathbb{V}_k^1. \tag{3.2}$$

The univariate spaces must form de Rham sequences on the reference interval, i.e.

$$\mathbb{V}_k^0 \subset W^{1,1}(]0,1[) \quad \xrightarrow{\ \partial_{\hat{x}}\ } \quad \mathbb{V}_k^1 \subset L^1(]0,1[)$$

and antiderivative operators must map back to the first space,

$$\mathbb{V}_k^0 \quad \xleftarrow{\ \int^{\hat{x}}\ } \quad \mathbb{V}_k^1$$

for arbitrary integration constants, which also implies that constants belong to $\mathbb{V}_k^0$. An important particular case is provided by spline spaces

$$\mathbb{V}_k^0 = \mathbb{S}_{\boldsymbol{\alpha}}^p, \qquad \mathbb{V}_k^1 = \mathbb{S}_{\boldsymbol{\alpha}-1}^{p-1}$$

where p and $\boldsymbol{\alpha}$ are the degree and regularity vector of the first space, as described in [13]. This also includes the case of polynomial spaces $\mathbb{V}_k^0 = \mathbb{P}^p$ and $\mathbb{V}_k^1 = \mathbb{P}^{p-1}$. To simplify the matching of functions across patch interfaces we further assume that the univariate spaces are invariant by a change of orientation, namely

$$\varphi \in \mathbb{V}_k^0 \quad \Longrightarrow \quad \varphi \circ \eta \in \mathbb{V}_k^0 \quad \text{where} \quad \eta(z) = 1 - z.$$

Our next assumption is that the first space is equipped with basis functions

$$\mathbb{V}_k^0 = \mathrm{Span}(\{\lambda_i^k : i = 0, \dots, n_k\})$$

with the following properties:

- interpolation at the endpoints,

$$\lambda_i^k(0) = \delta_{i,0} \qquad \text{and} \qquad \lambda_i^k(1) = \delta_{i,n_k}. \tag{3.3}$$

- bounded overlapping and quasi-uniformity: the functions λ_i^k are supported inside a closed interval $\hat{s}_i^k$ with

$$\kappa_3^{-1}\hat{h}_k \le \mathrm{diam}(\hat{s}_i^k) \le \kappa_3 \hat{h}_k \qquad \text{with} \qquad \hat{h}_k := (n_k + 1)^{-1}, \tag{3.4}$$

  and these intervals overlap in a bounded way, i.e.

$$\#(\{j : \hat{s}_j^k \cap \hat{s}_i^k \neq \emptyset\}) \le \kappa_4 \qquad \text{for } i = 0, \dots, n_k. \tag{3.5}$$

- inverse estimate: for all $\varphi \in \mathbb{V}_k^0$ and all $\hat{s}_i^k$, $0 \le i \le n_k$, it holds

$$\|\partial_{\hat{x}}\varphi\|_{L^\infty(\hat{s}_i^k)} \le \kappa_5 (\hat{h}_k)^{-1} \|\varphi\|_{L^\infty(\hat{s}_i^k)}. \tag{3.6}$$

- local stability: there exist dual basis functions θ_i^k vanishing outside the intervals $\hat{s}_i^k$, such that

$$\int_0^1 \theta_i^k \lambda_j^k \,\mathrm{d}\hat{x} = \delta_{i,j}$$

  holds for all $i, j \in \{0, \dots, n_k\}$, as well as the dual normalization

$$\|\lambda_i^k\|_{L^\infty(\hat{S}_i^k)} \le 1, \qquad \|\theta_i^k\|_{L^\infty(\hat{S}_i^k)} \le \kappa_6 (\hat{h}_k)^{-1}. \tag{3.7}$$

The basis functions for $\hat{V}_k^0$, as well as the dual functions, are then defined as

$$\begin{cases} \hat{\Lambda}_{\boldsymbol{i}}^k(\hat{\boldsymbol{x}}) := \lambda_{i_1}^k(\hat{x}_1)\lambda_{i_2}^k(\hat{x}_2) \\ \hat{\Theta}_{\boldsymbol{i}}^k(\hat{\boldsymbol{x}}) := \theta_{i_2}^k(\hat{x}_1)\theta_{i_2}^k(\hat{x}_2) \end{cases} \qquad \text{for } \hat{\boldsymbol{x}} \in \hat{\Omega}, \quad \boldsymbol{i} \in \boldsymbol{\mathcal{I}}^k := \{0, \dots, n_k\}^2$$

and both functions are supported in the Cartesian domains

$$\hat{S}_{\boldsymbol{i}}^k = \hat{s}_{i_1}^k \times \hat{s}_{i_2}^k \tag{3.8}$$

which, according to (3.5), also overlap in a bounded way. From (3.4) and the normalization (3.7) we infer

$$\|\hat{\Lambda}_{\boldsymbol{i}}^k\|_{L^p(\hat{S}_i^k)} \lesssim \hat{h}_k^{2/p}, \qquad \|\hat{\Theta}_{\boldsymbol{i}}^k\|_{L^q(\hat{S}_i^k)} \lesssim \hat{h}_k^{2/q-2} \tag{3.9}$$

where we have denoted $\frac{1}{q} = 1 - \frac{1}{p}$ for $p \in [1, \infty]$. Note that in the case of splines, the inverse estimates hold [5] and such dual functionals are standard: they can be obtained from the perfect B-spline of de Boor [21] or as piecewise polynomials [12, 17]. Using these dual functions, we define a projection operator

$$\hat{\Pi}_k^0 : L^p(\hat{\Omega}) \longrightarrow \hat{V}_k^0, \qquad \hat{\phi} \longmapsto \sum_{\boldsymbol{i} \in \boldsymbol{\mathcal{I}}^k} \langle \hat{\Theta}_{\boldsymbol{i}}^k, \hat{\phi} \rangle \hat{\Lambda}_{\boldsymbol{i}}^k \tag{3.10}$$

where $\langle\cdot,\cdot\rangle$ is the usual L^q-L^p duality product in $\hat\Omega$. Our assumptions classically imply that the projection $\hat\Pi^0_k$ is locally stable. Specifically, denoting $\phi^k_{\boldsymbol{i}} = \langle \hat\Theta^k_{\boldsymbol{i}}, \hat\phi\rangle$ for $k \in \mathcal{K}$ and $\boldsymbol{i} \in \boldsymbol{\mathcal{I}}^k$, one easily infers from (3.9) that

$$\hat h_k^{2/p} |\phi^k_{\boldsymbol{i}}| \lesssim \|\hat\phi\|_{L^p(\hat S^k_{\boldsymbol{i}})}. \tag{3.11}$$

A key property of the tensor-product structure is the preservation of directional invariance. The proof is straightforward, using that constants belong to the univariate spaces $\hat{\mathbb{V}}^0_k$.

Lemma 3.1. *If $\hat\phi \in L^p(\hat\Omega)$ satisfies $\hat\partial_d\hat\phi = 0$ for some $d \in \{1,2\}$, then $\hat\partial_d \hat\Pi^0_k\hat\phi = 0$.*

3.3. Pushforward spaces on the mapped patches

On each patch $\Omega_k = F_k(\hat\Omega)$, the local spaces are defined as the image of the logical ones by the pushforward operators associated with F_k, i.e. $V^\ell_k := \mathcal{F}^\ell_k(\hat V^\ell_k)$. In 2D these operators read

$$\begin{cases} \mathcal{F}^0_k : \hat\phi \longmapsto \phi := \hat\phi \circ F_k^{-1} \\ \mathcal{F}^1_k : \hat{\boldsymbol{u}} \longmapsto \boldsymbol{u} := (DF_k^{-T}\hat{\boldsymbol{u}}) \circ F_k^{-1} \\ \mathcal{F}^2_k : \hat f \longmapsto f := (J_{F_k}^{-1}\hat f) \circ F_k^{-1} \end{cases} \tag{3.12}$$

where $DF_k = \big(\partial_b(F_k)_a(\hat{\boldsymbol{x}})\big)_{1\le a,b\le 2}$ is the Jacobian matrix of F_k, and J_{F_k} its (positive) metric determinant, see e.g. [11, 28, 29, 32]. These operators define isomorphisms between $L^p(\hat\omega)$ and $L^p(\omega)$ for any open domain $\hat\omega \subset \hat\Omega$ with image $\omega = F_k(\hat\omega)$. Specifically, for all $\hat\phi$, $\hat{\boldsymbol{u}}$, $\hat f \in L^p(\hat\Omega)$ the pushforwards $\phi := \mathcal{F}^0_k\hat\phi$, $\boldsymbol{u} := \mathcal{F}^1_k\hat{\boldsymbol{u}}$ and $f := \mathcal{F}^2_k\hat f$ satisfy

$$\begin{cases} \|\phi\|_{L^p(\omega)} \sim H_k^{2/p}\|\hat\phi\|_{L^p(\hat\omega)}, \\ \|\boldsymbol{u}\|_{L^p(\omega)} \sim H_k^{2/p-1}\|\hat{\boldsymbol{u}}\|_{L^p(\hat\omega)}, \\ \|f\|_{L^p(\omega)} \sim H_k^{2/p-2}\|\hat f\|_{L^p(\hat\omega)}. \end{cases} \tag{3.13}$$

A key property is the commutation with the differential operators, namely

$$\nabla \mathcal{F}^0_k\hat\phi = \mathcal{F}^1_k\hat\nabla\hat\phi, \qquad \operatorname{curl}\mathcal{F}^1_k\hat{\boldsymbol{u}} = \mathcal{F}^2_k\widehat{\operatorname{curl}}\hat{\boldsymbol{u}}$$

which holds for all $\hat\phi \in H^1(\hat\Omega)$ and $\hat{\boldsymbol{u}} \in H(\widehat{\operatorname{curl}};\hat\Omega)$. In particular, the mapped spaces also form de Rham sequences (2.3).

3.4. Broken basis functions and patch-wise projection on V^0_{pw}

Basis functions for the single-patch spaces $V^\ell_k = \mathcal{F}^\ell_k\hat V^\ell_k$ are obtained by pushing forward the reference basis functions. Outside Ω_k, we implicitly extend $\mathcal{F}^\ell_k$ by zero, so that these functions also provide a basis for the broken spaces (2.9). Of particular importance to us is the corresponding basis for V^0_{pw},

$$\Lambda^k_{\boldsymbol{i}}(\boldsymbol{x}) := \mathcal{F}^0_k(\hat\Lambda^k_{\boldsymbol{i}}) = \begin{cases} \hat\Lambda^k_{\boldsymbol{i}}(\hat{\boldsymbol{x}}^k) & \text{for } \boldsymbol{x} \in \Omega_k \\ 0 & \text{elsewhere} \end{cases} \quad \text{for } k \in \mathcal{K},\ \boldsymbol{i} \in \boldsymbol{\mathcal{I}}^k = \{0,\dots,n_k\}^2 \tag{3.14}$$

where $\hat{\boldsymbol{x}}^k := (F_k)^{-1}(\boldsymbol{x})$. These functions have local supports mapped from (3.8),

$$\operatorname{supp}(\Lambda^k_{\boldsymbol{i}}) \subset S^k_{\boldsymbol{i}} := F_k(\hat S^k_{\boldsymbol{i}}) \tag{3.15}$$

and we define the *single-patch extension* of a support domain $S^k_{\boldsymbol{i}} \subset \Omega$ as

$$E_k(S^k_{\boldsymbol{i}}) := \bigcup_{\boldsymbol{j}\in\boldsymbol{\mathcal{I}}^k(S^k_{\boldsymbol{i}})} S^k_{\boldsymbol{j}} \quad \text{where} \quad \boldsymbol{\mathcal{I}}^k(S^k_{\boldsymbol{i}}) := \{\boldsymbol{j} \in \boldsymbol{\mathcal{I}}^k : S^k_{\boldsymbol{j}} \cap S^k_{\boldsymbol{i}} \neq \emptyset\} \tag{3.16}$$

see Figure 3.1. The patch-wise projection onto the broken space $V^0_{\rm pw}$ is then defined as

$$\Pi^0_{\rm pw} \coloneqq \sum_{k\in\mathcal{K}} \Pi^0_k \ : \quad L^p(\Omega) \longrightarrow V^0_{\rm pw} \tag{3.17}$$

with single-patch projections obtained by pushing forward the logical ones (3.10),

$$\Pi^0_k : \phi \longmapsto \mathcal{F}^0_k \hat{\Pi}^0_k (\mathcal{F}^0_k)^{-1}(\phi|_{\Omega_k}). \tag{3.18}$$

Lemma 3.2. *Given $\phi \in L^p(\Omega)$, write $\Pi^0_k\phi = \sum_{\boldsymbol{i}\in\mathcal{I}^k} \phi^k_{\boldsymbol{i}}\Lambda^k_{\boldsymbol{i}}$ for $k \in \mathcal{K}$. We have*

$$|\phi^k_{\boldsymbol{i}}|\|\Lambda^k_{\boldsymbol{i}}\|_{L^p(\Omega)} \lesssim \|\phi\|_{L^p(S^k_{\boldsymbol{i}})} \tag{3.19}$$

for all $\boldsymbol{i} \in \mathcal{I}^k$, and the single-patch projection satisfies

$$\|\Pi^0_k\phi\|_{L^p(S^k_{\boldsymbol{i}})} \lesssim \|\phi\|_{L^p(E_k(S^k_{\boldsymbol{i}}))} \tag{3.20}$$

with E_k the single-patch extension defined in (3.16).

Proof. Observe that $\phi^k_{\boldsymbol{i}} = \langle \hat{\Theta}^k_{\boldsymbol{i}}, \hat{\phi}^k\rangle$ holds with $\hat{\phi}^k = (\mathcal{F}^0_k)^{-1}(\phi|_{\Omega_k})$. From (3.11) and the scaling relations (3.13) we infer that

$$h_k^{2/p}|\phi^k_{\boldsymbol{i}}| \lesssim \|\phi\|_{L^p(S^k_{\boldsymbol{i}})} \tag{3.21}$$

holds with a local mesh size

$$h_k \coloneqq H_k\hat{h}_k = \frac{\mathrm{diam}(\Omega_k)}{n_k+1}.$$

Using next (3.9) and again (3.13) we find $\|\Lambda^k_{\boldsymbol{i}}\|_{L^p(\Omega)} \lesssim h_k^{2/p}$, which yields (3.19). The bound (3.20) follows by combining these estimates and the bounded overlapping of the domains $S^k_{\boldsymbol{i}}$. ■

Remark 3.3. Using (3.20) and the fact that any constant function belongs to $\hat{V}^0_k$, and hence to V^0_k, one easily shows that

$$\phi = c \text{ on } E_k(S^k_{\boldsymbol{i}}) \quad \Longrightarrow \quad \Pi^0_k\phi = c \text{ on } S^k_{\boldsymbol{i}} \tag{3.22}$$

holds for any $c \in \mathbb{R}$.

3.5. **Edges and vertices**

In this section, we introduce some notation relative to edges and vertices, and specify the nestedness assumptions (ii) and (iii) mentioned in Section 3.1.

We first denote by $\mathcal{E}$ the set of patch edges, and for a given $e \in \mathcal{E}$ we gather the indices of contiguous patches in

$$\mathcal{K}(e) = \{k \in \mathcal{K} : e \subset \partial\Omega_k\}.$$

and define the corresponding domain as

$$\Omega(e) \coloneqq \mathrm{int}\Big(\bigcup_{k\in\mathcal{K}(e)} \overline{\Omega_k}\Big). \tag{3.23}$$

Due to the geometric conformity of the patch decomposition, $\mathcal{K}(e)$ contains two patches if e is an interior edge, and only one patch if it is a boundary edge ($e \subset \partial\Omega$). Our edge-nestedness assumption (ii) from Section 3.1 then reads:

Assumption 1. *For any interior edge, $\mathcal{K}(e)$ consists of two adjacent patches $k^-(e)$, $k^+(e)$ of nested resolutions, in the sense that*

$$\mathbb{V}^0_{k^-(e)} \subset \mathbb{V}^0_{k^+(e)}. \tag{3.24}$$

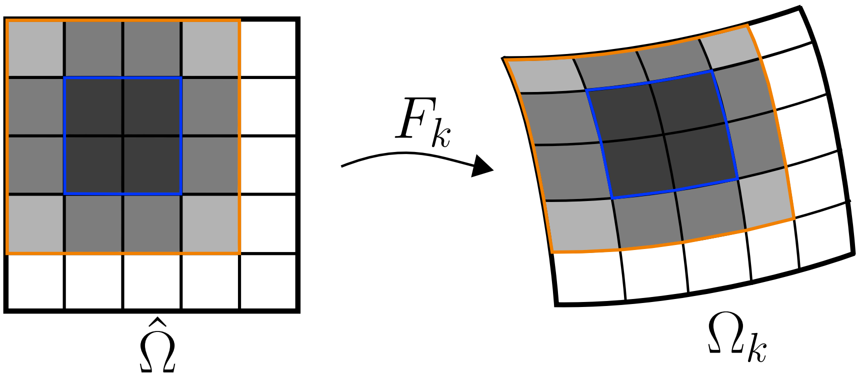

Figure 3.1. A support domain $\hat{S}_{\boldsymbol{i}}^k$ in the logical domain $\hat{\Omega}$ (left) and its mapped image $S_{\boldsymbol{i}}^k = F_k(\hat{S}_{\boldsymbol{i}}^k)$ on a patch Ω_k (right), as defined by equations (3.8) and (3.15), both enclosed by blue boundaries. Here a bilinear spline basis is used for illustration purposes, with support domains consisting of 2×2 cells. The domain extension $E_k(S_{\boldsymbol{i}}^k)$ defined in Equation (3.16), as well as its logical counterpart, are delimited by the orange boundaries. We use different shadings to show different numbers of overlapping basis function supports contributing to the domain extensions.

For boundary edges it will be convenient to denote the unique patch of $\mathcal{K}(e)$ by $k^-(e)$. Given two adjacent patches, the above assumption implies that any coarse basis function can be decomposed in the fine basis, namely an equality of the form

$$\lambda_i^- = \sum_{j \in \mathcal{I}_e^+(i)} c_{i,j}^e \lambda_j^+ \tag{3.25}$$

holds for all $i = 0, \dots, n_{k^-(e)}$, and we further assume that the refinements are graded, in the sense that the decomposition (3.25) involves a bounded number of fine functions:

$$\#(\mathcal{I}_e^+(i)) \le \kappa_7 \qquad \text{for } e \in \mathcal{E},\ i = 0, \dots, n_{k^-(e)}. \tag{3.26}$$

For simplicity, we also assume that the coarse support interval matches the fine ones, in the sense that $\hat{s}_i^- = \bigcup_{j \in \mathcal{I}_e^+(i)} \hat{s}_j^+$, and that the fine and coarse supports are nested, in the sense that

$$\forall j \in \{0, \dots, n_{k^+(e)}\}, \quad \exists i \in \{0, \dots, n_{k^-(e)}\} \quad \text{such that} \quad \hat{s}_j^+ \subset \hat{s}_i^-. \tag{3.27}$$

Observe that the above assumptions imply that the resolutions and diameters of two adjacent patches are similar, namely

$$1 \le \frac{n_{k^+(e)}}{n_{k^-(e)}} \le \kappa_8 \quad \text{and} \quad \kappa_9^{-1} \le \frac{H_{k^+(e)}}{H_{k^-(e)}} \le \kappa_9. \tag{3.28}$$

Given an edge e and some $\boldsymbol{x} \in \Omega_k$, $k \in \mathcal{K}(e)$, we denote by $(\hat{x}_\parallel^k, \hat{x}_\perp^k)$ the components of the logical point $\hat{\boldsymbol{x}}^k = (\hat{x}_1^k, \hat{x}_2^k) := F_k^{-1}(\boldsymbol{x})$ in the directions parallel and perpendicular to the logical edge $\hat{e}^k := (F_k)^{-1}(e)$. In other terms, we set

$$(\hat{x}_\parallel^k, \hat{x}_\perp^k) = (\hat{x}_{\parallel(e)}^k, \hat{x}_{\perp(e)}^k) := \begin{cases} (\hat{x}_1^k, \hat{x}_2^k) & \text{if } \hat{e}^k \text{ is parallel to the } \hat{x}_1 \text{ axis} \\ (\hat{x}_2^k, \hat{x}_1^k) & \text{if } \hat{e}^k \text{ is parallel to the } \hat{x}_2 \text{ axis} \end{cases} \tag{3.29}$$

and it will be convenient to denote the corresponding reordering function by

$$\hat{X}_e^k : (\hat{x}_\parallel^k, \hat{x}_\perp^k) \longmapsto \hat{\boldsymbol{x}}^k \quad \text{and} \quad X_e^k := F_k(\hat{X}_e^k) : (\hat{x}_\parallel^k, \hat{x}_\perp^k) \longmapsto \boldsymbol{x}. \tag{3.30}$$

Using this notation, a logical edge is always of the form

$$\hat{e}^k = \{\hat{\boldsymbol{x}} \in \hat{\Omega} : \hat{x}_\perp = \hat{e}^k_\perp\} \tag{3.31}$$

where $\hat{e}^k_\perp \in \{0,1\}$ is the logical coordinate of $\hat{e}^k$ along its perpendicular axis.

Next, denoting $\mathcal{V}$ the set of all patch vertices, we gather for any $\boldsymbol{v} \in \mathcal{V}$ the indices of the contiguous patches in the set

$$\mathcal{K}(\boldsymbol{v}) = \{k \in \mathcal{K} : \boldsymbol{v} \in \partial\Omega_k\}.$$

We define the corresponding domain as the union of the contiguous patches,

$$\Omega(\boldsymbol{v}) \coloneqq \operatorname{int}\Big(\bigcup_{k\in\mathcal{K}(\boldsymbol{v})} \overline{\Omega_k}\Big), \tag{3.32}$$

and also denote by $\mathcal{E}(\boldsymbol{v})$ the set of contiguous edges. Conversely, we denote by $\mathcal{V}(e) = \{v \in \mathcal{V} : e \in \mathcal{E}(v)\}$ the set of vertices contiguous to a given edge $e \in \mathcal{E}$.

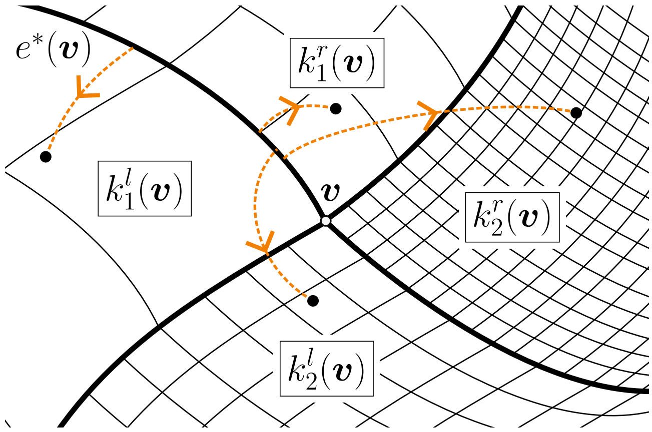

Figure 3.2. Adjacent nested patches around a vertex $\boldsymbol{v}$ corresponding to the decomposition (3.33), with $n(\boldsymbol{v}, l) = n(\boldsymbol{v}, r) = 2$ since $\boldsymbol{v}$ is an interior vertex, and dashed curves connecting arbitrary points $\boldsymbol{x} \in \Omega(\boldsymbol{v})$ to a coarse edge $e^*(\boldsymbol{v})$, according to Assumption 2. Observe that here the edge shared by patches k_1^l and k_2^l could also be used as a coarse edge. The plotted cells correspond to the minimal intersections of the overlapping supports $S^k_{\boldsymbol{i}}$ defined in (3.15).

To specify the vertex-nestedness assumption (iii) from Section 3.1, we say that a point $\boldsymbol{x}$ can be connected to an edge e with a *monotonic curve of length* L if there exists a continuous curve $\gamma : [0,1] \to \Omega$ such that $\gamma(0) \in e$, $\gamma(1) = \boldsymbol{x}$, γ intersects L patches without touching any vertex and for any $t_1 < t_2$, the patches $\Omega_{k_i} \ni \gamma(t_i)$ satisfy $\mathbb{V}^0_{k_1} \subset \mathbb{V}^0_{k_2}$. Our nestedness assumption on vertices then reads as follows.

Assumption 2. *For any interior vertex $\boldsymbol{v}$, $\mathcal{K}(\boldsymbol{v})$ contains exactly four patches and there exists an edge $e^*(\boldsymbol{v}) \in \mathcal{E}(\boldsymbol{v})$ such that any $\boldsymbol{x} \in \Omega(\boldsymbol{v})$ can be connected to $e^*(\boldsymbol{v})$ with a monotonic curve of length $L \le 2$: we call such an edge a* coarse edge *of $\boldsymbol{v}$. For any boundary vertex, $\mathcal{K}(\boldsymbol{v})$ contains no more than four patches, and there also exists a coarse edge $e^*(\boldsymbol{v})$ in the sense just defined.*

An illustration is provided in Figure 3.2 for interior vertices, and Figure 3.3 for boundary vertices.

This assumption allows to decompose any $\mathcal{K}(\boldsymbol{v})$ in two sequences of adjacent patches with nested resolutions (one of which may be empty), namely

$$\mathcal{K}(\boldsymbol{v}) = \{k_i^l(\boldsymbol{v}) : 1 \le i \le n(\boldsymbol{v}, l)\} \cup \{k_i^r(\boldsymbol{v}) : 1 \le i \le n(\boldsymbol{v}, r)\} \tag{3.33}$$

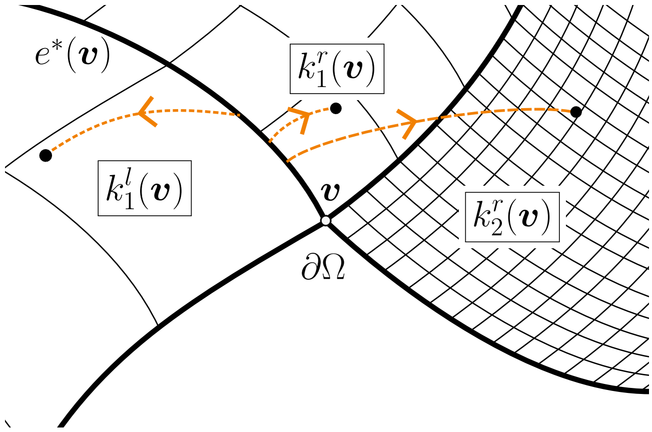

Figure 3.3. Adjacent patches around a boundary vertex $\boldsymbol{v}$ and dashed curves connecting arbitrary points $\boldsymbol{x} \in \Omega(\boldsymbol{v})$ to one coarse edge $e^*(\boldsymbol{v})$, according to Assumption 2. We show a decomposition of the form (3.33) for the adjacent nested patches.

(rotating left and right, for instance) with integers $0 \le n(\boldsymbol{v}, l), n(\boldsymbol{v}, r) \le 2$, such that if $n(\boldsymbol{v}, s) = 2$ for $s = l$ or r, the patches $\Omega_{k_1^s(\boldsymbol{v})}$ and $\Omega_{k_2^s(\boldsymbol{v})}$ are adjacent and their FEM spaces satisfy

$$\mathbb{V}^0_{k_1^s(\boldsymbol{v})} \subset \mathbb{V}^0_{k_2^s(\boldsymbol{v})}.$$

If $\boldsymbol{v}$ is an interior vertex, we must have $n(\boldsymbol{v}, l) = n(\boldsymbol{v}, r) = 2$ and the coarse, resp. fine patches of both sequences (i.e. the patches $k_i^l(\boldsymbol{v})$ and $k_i^r(\boldsymbol{v})$ for $i = 1$, resp. $i = 2$) must be adjacent. Note that since both sequences are independent of each other, the fine patch in one sequence may be coarser than the coarse patch in the other one (that is, in Figure 3.2 one could also use the edge between patches k_1^l and k_2^l as coarse edge e^*). In practice, our assumptions exclude chessboard patterns where two patches facing each other across a vertex are finer than the other two: For instance, in Figure 3.2 one may switch the resolutions of the patches k_2^l and k_2^r, but not those of k_2^l and k_1^l.

If $\boldsymbol{v}$ is a boundary vertex then different configurations may occur: if $\boldsymbol{v}$ is shared by one or two patches only, then we can decompose $\mathcal{K}(\boldsymbol{v})$ in a single sequence of nested, adjacent patches. If $\boldsymbol{v}$ is shared by three or four patches then both sequences are non-empty, and the coarser patches ($k_1^l(\boldsymbol{v})$ and $k_1^r(\boldsymbol{v})$) must be adjacent but the finer ones ($k^l_{n(\boldsymbol{v},l)}(\boldsymbol{v})$ and $k^r_{n(\boldsymbol{v},r)}(\boldsymbol{v})$) do not need to be.

For later purpose we denote by $k^*(\boldsymbol{v})$ the index of one (coarse but not necessarily the coarsest) patch adjacent to the coarse edge $e^*(\boldsymbol{v})$.

3.6. Patch-wise differential operators

Using the pushforward and pullback we also define patch-wise gradient operators. Given $k \in \mathcal{K}$ and $d \in \{1, 2\}$, we define the single-patch directional gradients as

$$\nabla_d^k : H^1(\Omega_k) \longrightarrow L^2(\Omega_k), \qquad \phi \longmapsto \mathcal{F}_k^1(\hat{\boldsymbol{\tau}}_d \hat{\partial}_d (\mathcal{F}_k^0)^{-1}(\phi)) \tag{3.34}$$

where $\hat{\boldsymbol{\tau}}_d$ is the unit vector of $\mathbb{R}^2$ along $\hat{x}_d$, and we observe that on Ω_k the usual gradient writes $\nabla^k = \nabla_1^k + \nabla_2^k$. Like $\mathcal{F}_k^1$, these single-patch gradients are implicitly extended by zero outside their patch. The patch-wise (broken) gradient is then

$$\nabla_{\rm pw} : \left(\bigoplus_{k \in \mathcal{K}} H^1(\Omega_k) \right) \longrightarrow L^2(\Omega), \qquad \phi \longmapsto \sum_{k \in \mathcal{K}} \nabla^k (\phi|_{\Omega_k}). \tag{3.35}$$

We observe that $\nabla_{\rm pw}$ maps $V^0_{\rm pw}$ to $V^1_{\rm pw}$, and on $H^1(\Omega)$ it coincides with the usual gradient ∇. For an edge $e \in \mathcal{E}$, we define broken gradients along the parallel and perpendicular directions: for $d \in \{\|, \perp\}$,

$$\nabla^e_d : \Big(\bigoplus_{k \in \mathcal{K}(e)} H^1(\Omega_k) \Big) \longrightarrow L^2(\Omega(e)), \quad \phi \longmapsto \sum_{k \in \mathcal{K}(e)} \mathcal{F}^1_k (\hat{\boldsymbol{\tau}}^k_d \hat{\partial}_d (\mathcal{F}^0_k)^{-1} (\phi|_{\Omega_k})) \tag{3.36}$$

where now $\hat{\boldsymbol{\tau}}^k_d$ is the unit vector of $\mathbb{R}^2$ along $\hat{x}^k_d$, the parallel or perpendicular logical directions respective to e according to (3.29). Observe that these operators satisfy

$$\nabla^e_\| + \nabla^e_\perp = \sum_{k \in \mathcal{K}(e)} \nabla^k = \nabla_{\rm pw} \quad \text{on} \quad \Omega(e), \tag{3.37}$$

see (3.23). To design our commuting projection on V^2_h, we will need broken second order (mixed) derivative operators: a single-patch operator

$$D^{2,k} := \mathcal{F}^2_k \hat{\partial}_1 \hat{\partial}_2 (\mathcal{F}^0_k)^{-1} : \quad V^0_k \longrightarrow V^2_k, \qquad k \in \mathcal{K} \tag{3.38}$$

and a patch-wise operator $D^{2,e} : V^0_{\rm pw} \to V^2_{\rm pw}$ associated with any edge $e \in \mathcal{E}$. We define the latter by its values on the local domain $\Omega(e)$, as

$$D^{2,e}\phi|_{\Omega_k} := (\det \hat{X}^k_e) \mathcal{F}^2_k (\hat{\partial}^k_\| \hat{\partial}^k_\perp \hat{\phi}^k), \qquad k \in \mathcal{K}(e) \tag{3.39}$$

where we have denoted $\hat{\phi}^k := (\mathcal{F}^0_k)^{-1}\phi \in \hat{V}^0_k$, recalling the reordering function (3.30). Outside $\Omega(e)$, we set $D^{2,e}\phi = 0$. Note that $\det \hat{X}^k_e = \pm 1$, so that $D^{2,e}\phi|_{\Omega_k}$ indeed belongs to V^2_k. Finally, consider the patch-wise curl operator defined by

$$\operatorname{curl}_{\rm pw} : \Big(\bigoplus_{k \in \mathcal{K}} H(\operatorname{curl}; \Omega_k) \Big) \longrightarrow L^2(\Omega), \quad \boldsymbol{u} \longmapsto \sum_{k \in \mathcal{K}} \operatorname{curl}^k (\boldsymbol{u}|_{\Omega_k})$$

where again the local curl^k operator is extended by 0 outside Ω_k. We observe that $\operatorname{curl}_{\rm pw}$ maps $V^1_{\rm pw}$ into $V^2_{\rm pw}$, and on $H(\operatorname{curl}; \Omega)$ it coincides with the usual curl operator. Moreover, the following relation holds.

Lemma 3.4. *Let $\psi_\|$, $\psi_\perp$ be functions in $V^0_{\rm pw}$ which vanish outside $\Omega(e)$. We have*

$$\operatorname{curl}_{\rm pw} \Big(\sum_{d \in \{\|, \perp\}} \nabla^e_d \psi_d \Big) = D^{2,e}(\psi_\perp - \psi_\|).$$

Proof. Let $\boldsymbol{w} := \sum_{d \in \{\|, \perp\}} \nabla^e_d \psi_d$. On each patch Ω_k, $k \in \mathcal{K}(e)$, its pullback reads

$$\hat{\boldsymbol{w}}^k := (\mathcal{F}^1_k)^{-1} \boldsymbol{w} = \sum_{d \in \{\|, \perp\}} \hat{\boldsymbol{\tau}}^k_d \hat{\partial}^k_d \hat{\psi}^k_d = \begin{cases} (\hat{\partial}^k_\| \hat{\psi}^k_\|, \hat{\partial}^k_\perp \hat{\psi}^k_\perp) & \text{if } \det \hat{X}^k_e = 1 \\ (\hat{\partial}^k_\perp \hat{\psi}^k_\perp, \hat{\partial}^k_\| \hat{\psi}^k_\|) & \text{if } \det \hat{X}^k_e = -1 \end{cases}$$

where we have denoted $\hat{\psi}^k_d := (\mathcal{F}^0_k)^{-1}\psi_d$. In particular, we have

$$\operatorname{curl}_{\rm pw} \boldsymbol{w}|_{\Omega_k} = \mathcal{F}^2_k (\widehat{\operatorname{curl}}\, \hat{\boldsymbol{w}}^k) = (\det \hat{X}^k_e) \mathcal{F}^2_k (\hat{\partial}^k_\| \hat{\partial}^k_\perp (\hat{\psi}^k_\perp - \hat{\psi}^k_\|)) = D^{2,e}(\psi_\perp - \psi_\|)|_{\Omega_k}. \qquad \blacksquare$$

4. Conforming multipatch spaces

In this section, we specify a basis for the first conforming space V^0_h, and we construct several projection operators on local broken and conforming spaces that will play a central role in the construction of our commuting projection operators, as presented in Section 2.

We remind that the coarse and fine patches across an edge are denoted by k^- and k^+. To alleviate notation when these indices appear as an exponent, we replace them by the simpler $-$ and $+$ signs respectively.

4.1. Conforming constraints on patch interfaces

The finite element spaces (2.4) are the maximal conforming subspaces of the broken spaces (2.9), namely

$$V_h^0 = V_{\rm pw}^0 \cap H^1(\Omega), \qquad V_h^1 = V_{\rm pw}^1 \cap H(\mathrm{curl};\Omega), \qquad V_h^2 = V_{\rm pw}^2 \cap L^2(\Omega) = V_{\rm pw}^2.$$

Since each local space V_k^ℓ consists of continuous functions, the conforming subspaces are characterized by continuity constraints on the patch interfaces. Specifically, a function $\phi \in V_{\rm pw}^0$ belongs to $H^1(\Omega)$, and hence to V_h^0, if and only if we have

$$\phi|_{\Omega_{k^-}} = \phi|_{\Omega_{k^+}} \qquad \text{on every edge } e = \partial\Omega_{k^-} \cap \partial\Omega_{k^+} \tag{4.1}$$

and a function $\boldsymbol{u} \in V_{\rm pw}^1$ belongs to $H(\mathrm{curl};\Omega)$, and hence to V_h^1, if and only if

$$\boldsymbol{\tau}\cdot\boldsymbol{u}|_{\Omega_{k^-}} = \boldsymbol{\tau}\cdot\boldsymbol{u}|_{\Omega_{k^+}} \qquad \text{on every edge } e = \partial\Omega_{k^-} \cap \partial\Omega_{k^+} \tag{4.2}$$

where $\boldsymbol{\tau}$ denotes an arbitrary vector tangent to the edge. For the last space of the sequence there are no constraints since $V_h^2 = V_{\rm pw}^2$.

It is possible to reformulate these interface constraints on the pullback fields. To do so, we consider the parametrization of an edge $e \in \mathcal{E}$ according to the k^- and k^+ patches, namely

$$\boldsymbol{x}_e^k : [0,1] \longrightarrow e, \quad z \longmapsto F_k(\hat{\boldsymbol{x}}_e^k(z)) \quad \text{ with } \quad \hat{\boldsymbol{x}}_e^k(z) := \hat{X}_e^k(z, \hat{e}_\perp^k)$$

where $\hat{e}_\perp^k$ is as in (3.31). We remind that the continuity assumption on the mappings (see Section 3.1) implies that these parametrizations coincide up to a possible change in orientation, namely an affine bijection $\eta_e : [0,1] \mapsto [0,1]$ such that

$$\boldsymbol{x}_e^-(z) = \boldsymbol{x}_e^+(\eta_e(z)) \quad \text{ where } \quad \eta_e(z) := \begin{cases} z & \text{if orientations coincide} \\ 1-z & \text{if they differ.} \end{cases} \tag{4.3}$$

For later purpose, we denote

$$\eta_e^-(z) := z \quad \text{ and } \quad \eta_e^+(z) := \eta_e(z). \tag{4.4}$$

The continuity condition (4.1) expressed on the pullbacks $\hat\phi^k := (\mathcal{F}_k^0)^{-1}(\phi|_{\Omega_k})$ then reads

$$\hat\phi^-(\hat{\boldsymbol{x}}_e^-(z)) = \hat\phi^+(\hat{\boldsymbol{x}}_e^+(\eta_e(z))), \quad z \in [0,1].$$

To specify the curl-conforming condition (4.2), we consider the tangent vectors to e oriented according to the k^- and k^+ patches, namely

$$\boldsymbol{\tau}_e^k(\boldsymbol{x}) := \frac{\mathrm{d}\boldsymbol{x}_e^k(z)}{\mathrm{d}z} = DF_k(\hat{\boldsymbol{x}}_e^k(z))\hat{\boldsymbol{\tau}}_\parallel^k$$

where $\boldsymbol{x} = \boldsymbol{x}_e^k(z) = F_k(\hat{\boldsymbol{x}}_e^k(z)) \in e$ and $\hat{\boldsymbol{\tau}}_\parallel^k$ is the positive unit vector parallel to the reference edge $\hat{e}^k = F_k^{-1}(e)$. According to (4.3), these vectors coincide up to their orientation, namely

$$\boldsymbol{\tau}_e^+(\boldsymbol{x}) = (\eta_e)'\boldsymbol{\tau}_e^-(\boldsymbol{x}) \quad \text{ with } \quad (\eta_e)' = \pm 1.$$

Expressed on the pullbacks $\hat{\boldsymbol{u}}^k(\hat{\boldsymbol{x}}^k) := (\mathcal{F}_k^1)^{-1}(\boldsymbol{u}|_{\Omega_k})(\hat{\boldsymbol{x}}^k) = DF_k^T(\hat{\boldsymbol{x}}^k)\boldsymbol{u}|_{\Omega_k}(\hat{\boldsymbol{x}})$, the curl-conformity condition (4.2) then reads

$$\hat{\boldsymbol{\tau}}_\parallel^- \cdot \hat{\boldsymbol{u}}^-(\hat{\boldsymbol{x}}_e^-(z)) = (\eta_e)'\hat{\boldsymbol{\tau}}_\parallel^+ \cdot \hat{\boldsymbol{u}}^+(\hat{\boldsymbol{x}}_e^+(\eta_e(z))), \quad z \in [0,1].$$

A useful observation is that $\boldsymbol{\tau}^k_e \cdot \mathcal{F}^1_k(\hat{\boldsymbol{\tau}}^k_\perp \hat{u}) = (DF_k \hat{\boldsymbol{\tau}}^k_\parallel) \cdot DF_k^{-T}(\hat{\boldsymbol{\tau}}^k_\perp \hat{u}) = 0$ holds for all function $\hat{u}$. In particular, for both $\boldsymbol{\tau}_e = \boldsymbol{\tau}^\pm_e$ we find that the perpendicular derivative operator (3.36) satisfies

$$\boldsymbol{\tau}_e \cdot \nabla^e_\perp = 0 \qquad \text{on } \Omega(e). \tag{4.5}$$

4.2. **Continuous basis functions**

A basis for the space V^0_h can be obtained as a collection of

- patch-interior functions $\Lambda^k_{\boldsymbol{i}}$ which vanish outside a single patch Ω_k,
- edge-based functions Λ^e_i which vanish outside an edge domain $\Omega(e)$,
- vertex-based functions $\Lambda^{\boldsymbol{v}}$ which vanish outside a vertex domain $\Omega(\boldsymbol{v})$,

see (3.23) and (3.32).

4.2.1. *Patch-interior continuous functions.*

The patch-interior functions are simply the single-patch basis functions $\Lambda^k_{\boldsymbol{i}}$ with indices $\boldsymbol{i}$ in the set

$$\boldsymbol{\mathcal{I}}^k_0 \coloneqq \{1, \dots, n_k - 1\}^2. \tag{4.6}$$

According to the interpolation property (3.3) these are indeed the basis functions which vanish at the patch boundaries, and they are continuously extended by 0 outside Ω_k.

4.2.2. *Edge-based continuous functions.*

For an edge $e \in \mathcal{E}$, we define the edge-based function of index $i \in \{0, \dots, n_e\}$, with $n_e \coloneqq n_{k^-(e)}$, as

$$\Lambda^e_i(\boldsymbol{x}) \coloneqq \begin{cases} \hat{\lambda}^-_i(\hat{x}^-_\parallel)\hat{\lambda}^-_{i^-_\perp(e)}(\hat{x}^-_\perp) & \text{for } \boldsymbol{x} \in \Omega_k \text{ with } k = k^-(e) \\ \hat{\lambda}^-_i(\eta_e(\hat{x}^+_\parallel))\hat{\lambda}^+_{i^+_\perp(e)}(\hat{x}^+_\perp) & \text{for } \boldsymbol{x} \in \Omega_k \text{ with } k = k^+(e) \\ 0 & \text{elsewhere} \end{cases} \tag{4.7}$$

where $\boldsymbol{x} = F_k(\hat{\boldsymbol{x}}) = X^k_e(\hat{x}^k_\parallel, \hat{x}^k_\perp)$ for $k \in \mathcal{K}(e)$, see (3.30), and where

$$i^k_\perp(e) \coloneqq n_k \hat{e}^k_\perp \in \{0, n_k\} \tag{4.8}$$

is the index corresponding to the (constant) perpendicular coordinate of e in the patch $k \in \mathcal{K}(e)$, see (3.31). The functions Λ^e_i belong to V^0_{pw} thanks to (3.25), moreover they are continuous across e, i.e. their values on the adjacent patches $k^-(e)$ and $k^+(e)$ coincide on e. For $0 < i < n_e$ they further vanish on $\partial\Omega(e) \setminus e$, so they are actually continuous on the whole domain Ω.

We denote the corresponding index sets by

$$\mathcal{I}^e \coloneqq \{0, \dots, n_e\} \quad \text{and} \quad \mathcal{I}^e_0 \coloneqq \{1, \dots, n_e - 1\} \tag{4.9}$$

and for later purposes we let

$$\boldsymbol{\mathcal{I}}^k_e \coloneqq \{\boldsymbol{i} \in \boldsymbol{\mathcal{I}}^k : i^k_\perp = i^k_\perp(e)\}$$

denote the (single-patch) multi-indices associated with the edge e, see (4.8). Notice that $\boldsymbol{\mathcal{I}}^-_e$ is isomorphic to $\mathcal{I}^e$, while $\boldsymbol{\mathcal{I}}^+_e$ may have more elements. In particular, using the reordering coordinate function $\hat{X}^k_e$ defined by (3.30), we have

$$\boldsymbol{\mathcal{I}}^k_e = \{\boldsymbol{i}^k_e(j) : j \in \{0, \dots, n_k\}\} \quad \text{with} \quad \boldsymbol{i}^k_e(j) \coloneqq \hat{X}^k_e(j, i^k_\perp(e)). \tag{4.10}$$

4.2.3. *Edge-based domains and extensions.*

For $i \in \mathcal{I}^e$, the function Λ^e_i is supported in a domain of the form

$$S^e_i := S^{e,-}_i \cup S^{e,+}_i \subset \overline{\Omega(e)} \tag{4.11}$$

where $S^{e,k}_i := \{X^k_e(\hat{x}_\parallel, \hat{x}_\perp) \in \overline{\Omega_k} : \eta^k_e(\hat{x}_\parallel) \in s^-_i, \hat{x}_\perp \in s^k_{i^k_\perp(e)}\}$, see Figure 4.1. We define the (edge-based) domain extension as

$$E_e(S^e_i) := \bigcup_{j \in \mathcal{I}^e(S^e_i)} S^e_j \quad \text{where} \quad \mathcal{I}^e(S^e_i) := \{j \in \mathcal{I}^e : S^e_j \cap S^e_i \neq \emptyset\} \tag{4.12}$$

Note that this is similar to the definition of an extended single patch support $E_k(S^k_{\boldsymbol{i}})$, see (3.16). We further observe that the nested assumption on the supports (3.27) yields the inclusion

$$S^k_{\boldsymbol{i}} \subset E_e(S^e_i) \qquad \text{for all } i \in \mathcal{I}^e \text{ and } \boldsymbol{i} \in \boldsymbol{\mathcal{I}}^k_e(S^e_i) \tag{4.13}$$

where we have set

$$\boldsymbol{\mathcal{I}}^k_e(S^e_i) := \{\boldsymbol{i} \in \boldsymbol{\mathcal{I}}^k_e : S^k_{\boldsymbol{i}} \cap S^e_i \neq \emptyset\}. \tag{4.14}$$

An illustration is provided in Figure 4.1.

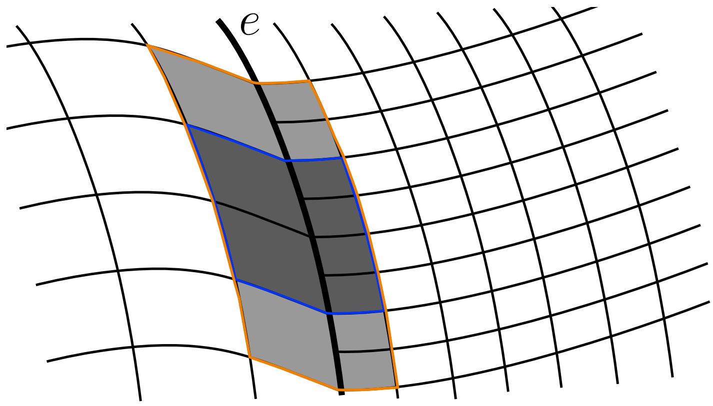

Figure 4.1. An edge-based support domain S^e_i is shown for one edge e, as defined in (4.11) and delimited by the blue boundary. Its domain extension $E_e(S^e_i)$, defined in (4.12), is enclosed by the orange boundary. As in Figure 3.1 a bilinear spline basis is used for the illustration, with support domains consisting of 2 (coarse) cells in the parallel direction and 1 in the perpendicular direction, since the corresponding basis functions are boundary splines. Again, we use different shadings to show different numbers of overlapping basis function supports contributing to the domain extensions.

The following property is an analog of (3.22) in the case of an interface.

Lemma 4.1. *Let $\phi \in L^p(\Omega)$. For any constant $c \in \mathbb{R}$, we have*

$$\phi = c \text{ on } E_e(S^e_j) \quad \Longrightarrow \quad \Pi^0_{\rm pw}\phi = c \text{ on } e \cap S^e_j.$$

Proof. For $k \in \mathcal{K}(e)$, write $\phi^k_h = \Pi^0_k \phi = \sum_{\boldsymbol{i} \in \boldsymbol{\mathcal{I}}^k} \phi^k_{\boldsymbol{i}} \Lambda^k_{\boldsymbol{i}}$ where $\phi^k_{\boldsymbol{i}} = \langle \hat{\Theta}^k_{\boldsymbol{i}}, \hat{\phi}^k \rangle$ holds with $\hat{\phi}^k = (\mathcal{F}^0_k)^{-1}(\phi|_{\Omega_k})$. Using the interpolation property of the basis functions at the endpoints (3.3), we first observe that $\Lambda^k_{\boldsymbol{i}}$ vanishes on e for $\boldsymbol{i} \notin \boldsymbol{\mathcal{I}}^k_e$. For $\boldsymbol{x} \in e \cap S^e_j$, we thus have

$$\phi^k_h(\boldsymbol{x}) = \sum_{\boldsymbol{i} \in \boldsymbol{\mathcal{I}}^k_e} \phi^k_{\boldsymbol{i}} \Lambda^k_{\boldsymbol{i}}(\boldsymbol{x}) = \sum_{\boldsymbol{i} \in \boldsymbol{\mathcal{I}}^k_e(S^e_j)} \phi^k_{\boldsymbol{i}} \Lambda^k_{\boldsymbol{i}}(\boldsymbol{x})$$

where we have used the set (4.14). According to (3.19) the latter sum only involves the values of ϕ on the domains $S^k_{\boldsymbol{i}}$ with $\boldsymbol{i} \in \boldsymbol{\mathcal{I}}^k_e(S^e_j)$, which are all contained in $E_e(S^e_j)$, see (4.12). Now if $\phi = c$ on this domain, we may replace it by c on the whole Ω_k without changing $\phi^k_h(\boldsymbol{x})$: the projection property yields then $\phi^k_h(\boldsymbol{x}) = c$. ∎

4.2.4. *Vertex-based continuous functions.*

For a vertex $\boldsymbol{v} \in \mathcal{V}$, we define

$$\Lambda^{\boldsymbol{v}} := \sum_{e \in \mathcal{E}(\boldsymbol{v})} \Lambda^e_{\boldsymbol{v}} - \sum_{k \in \mathcal{K}(\boldsymbol{v})} \Lambda^k_{\boldsymbol{v}} \tag{4.15}$$

where

$$\Lambda^k_{\boldsymbol{v}} := \Lambda^k_{\boldsymbol{i}^k(\boldsymbol{v})} \qquad \text{and} \qquad \Lambda^e_{\boldsymbol{v}} := \Lambda^e_{i^e(\boldsymbol{v})}.$$

Here, we have respectively denoted by

$$\boldsymbol{i}^k(\boldsymbol{v}) := n_k \hat{\boldsymbol{v}}^k \in \{0, n_k\}^2 \quad \text{and} \quad i^e(\boldsymbol{v}) := i^-_{\parallel}(\boldsymbol{v}) \in \{0, n_e\} \tag{4.16}$$

the multi-index of $\boldsymbol{v}$ in a patch k (with $\hat{\boldsymbol{v}}^k := F_k^{-1}(\boldsymbol{v}) \in \{0,1\}^2$), and its single index on an edge e (with a numbering corresponding to the coarse patch $k = k^-(e)$).

To verify that $\Lambda^{\boldsymbol{v}}$ is continuous on the edges $e \in \mathcal{E}(\boldsymbol{v})$, let us write an explicit expression on a patch Ω_k. To alleviate notation we assume that the logical vertex is the origin $\hat{\boldsymbol{v}}^k = 0$. Writing e_1, e_2 the edges contiguous to $\boldsymbol{v}$ in the patch k, we then denote by $\lambda^{e_d}_0$ the coarse univariate function associated with $\boldsymbol{v}$ on the edge e_d: this allows to rewrite the edge-based functions (4.7) in the patch Ω_k as

$$\Lambda^{e_1}_{\boldsymbol{v}}(\boldsymbol{x}) = \lambda^{e_1}_0(\hat{x}_1)\lambda^k_0(\hat{x}_2), \quad \Lambda^{e_2}_{\boldsymbol{v}}(\boldsymbol{x}) = \lambda^k_0(\hat{x}_1)\lambda^{e_2}_0(\hat{x}_2), \qquad \boldsymbol{x} \in \Omega_k.$$

Using next (3.25) we rewrite the coarse edge univariate functions in the form

$$\lambda^{e_d}_0(\hat{x}_d) = \sum_{j \ge 0} c^{e_d,k}_{0,j} \lambda^k_j(\hat{x}_d), \qquad d \in \{1,2\},$$

where we have $c^{e_d,k}_{0,0} = 1$ due to the interpolation property (3.3). (Note that if $k = k^-(e_d)$ then this decomposition is trivial, i.e. $c^{e_d,k}_{0,j} = 0$ for $j > 0$.) This allows to rewrite (4.15) as

$$\begin{aligned}
\Lambda^{\boldsymbol{v}}|_{\Omega_k}(\boldsymbol{x}) &= \lambda^{e_1}_0(\hat{x}_1)\lambda^k_0(\hat{x}_2) + \lambda^k_0(\hat{x}_1)\lambda^{e_2}_0(\hat{x}_2) - \lambda^k_0(\hat{x}_1)\lambda^k_0(\hat{x}_2) \\
&= \sum_{j \ge 0} c^{e_1,k}_{0,j} \lambda^k_j(\hat{x}_1)\lambda^k_0(\hat{x}_2) + \sum_{j \ge 0} c^{e_2,k}_{0,j} \lambda^k_0(\hat{x}_1)\lambda^k_j(\hat{x}_2) - \lambda^k_0(\hat{x}_1)\lambda^k_0(\hat{x}_2) \\
&= \sum_{j > 0} c^{e_1,k}_{0,j} \lambda^k_j(\hat{x}_1)\lambda^k_0(\hat{x}_2) + \sum_{j > 0} c^{e_2,k}_{0,j} \lambda^k_0(\hat{x}_1)\lambda^k_j(\hat{x}_2) + \lambda^k_0(\hat{x}_1)\lambda^k_0(\hat{x}_2).
\end{aligned}$$

Using again the interpolation property (3.3) this yields for $d \in \{1,2\}$

$$\Lambda^{\boldsymbol{v}}|_{\Omega_k}(\boldsymbol{x}) = \sum_{j > 0} c^{e_d,k}_{0,j} \lambda^k_j(\hat{x}_d) + \lambda^k_0(\hat{x}_d) = \lambda^{e_d}_0(\hat{x}_d) = \Lambda^{e_d}_{\boldsymbol{v}}(\boldsymbol{x}) \quad \text{for } \boldsymbol{x} \in e_d \tag{4.17}$$

which shows the continuity of $\Lambda^{\boldsymbol{v}}$ across the edge e_d, and hence on any $e \in \mathcal{E}(\boldsymbol{v})$. As $\Lambda^{\boldsymbol{v}}$ vanishes on the other edges $e \notin \mathcal{E}(\boldsymbol{v})$, it is continuous over the whole Ω.

We further observe that the function $\Lambda^{\boldsymbol{v}}$ vanishes outside the supports of the edge basis functions $\Lambda^e_{\boldsymbol{v}}$, namely we have $\operatorname{supp}(\Lambda^{\boldsymbol{v}}) \subset S^{\boldsymbol{v}}$ with

$$S^{\boldsymbol{v}} := \bigcup_{e \in \mathcal{E}(\boldsymbol{v})} S^e_{i^e(\boldsymbol{v})}, \tag{4.18}$$

indeed the latter domain contains the supports of the single-patch vertex functions,

$$\bigcup_{k\in\mathcal{K}(\boldsymbol{v})} S^k_{\boldsymbol{i}^k(\boldsymbol{v})} \subset S^{\boldsymbol{v}}, \tag{4.19}$$

see Figure 4.2.

For later purposes we define

$$\hat{h}_e := \min_{k\in\mathcal{K}(e)} \operatorname{diam}(\hat{s}^k_{i^k_\perp(e)}), \qquad h_e := \min_{k\in\mathcal{K}(e)} h_k \tag{4.20}$$

and

$$\hat{h}_{\boldsymbol{v}} := \min_{k\in\mathcal{K}(\boldsymbol{v}),d\in\{1,2\}} \operatorname{diam}(\hat{s}^k_{i^k_d(\boldsymbol{v})}), \qquad h_{\boldsymbol{v}} := \min_{k\in\mathcal{K}(\boldsymbol{v})} h_k. \tag{4.21}$$

We note that the local quasi-uniformity Assumption (3.28) and the regularity (3.1) yield $\hat{h}_g \sim \hat{h}_k$, as well as $h_g \sim H_k\hat{h}_g$, for any geometrical element $g = e$ or $\boldsymbol{v}$ and any contiguous patch $k \in \mathcal{K}(g)$. Using (3.7), (3.4) and the scaling relations (3.13) we also find that both the edge- and vertex-based functions satisfy the a priori bounds

$$\|\Lambda^e_i\|_{L^p(\Omega)} \lesssim h_e^{2/p} \quad \text{and} \quad \|\Lambda^{\boldsymbol{v}}\|_{L^p(\Omega)} \lesssim h_{\boldsymbol{v}}^{2/p}. \tag{4.22}$$

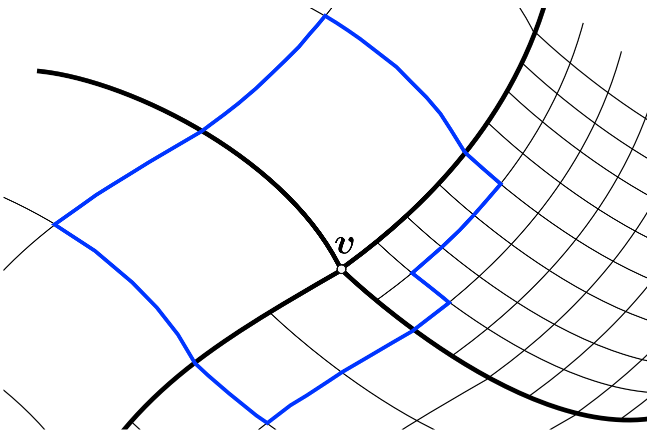

Figure 4.2. A vertex-based support domain $S^{\boldsymbol{v}}$ is shown for one vertex $\boldsymbol{v}$, as defined in (4.18), enclosed by the blue boundary. As above, bilinear splines are used as illustration.

Let us verify that the resulting collection indeed forms a basis of V^0_h.

Lemma 4.2. *The continuous functions defined above, namely*

$$\{\Lambda^k_{\boldsymbol{i}} : k \in \mathcal{K}, \boldsymbol{i} \in \boldsymbol{\mathcal{I}}^k_0\} \cup \{\Lambda^e_i : e \in \mathcal{E}, i \in \mathcal{I}^e_0\} \cup \{\Lambda^{\boldsymbol{v}} : \boldsymbol{v} \in \mathcal{V}\}, \tag{4.23}$$

form a basis for the conforming space $V^0_h = V^0_{\mathrm{pw}} \cap V^0$.

Proof. Let us decompose the set of single-patch indices into disjoint subsets

$$\boldsymbol{\mathcal{I}}^k = \boldsymbol{\mathcal{I}}^k_0 \cup \boldsymbol{\mathcal{I}}^k_{\mathcal{E},0} \cup \boldsymbol{\mathcal{I}}^k_{\mathcal{V}}$$

with $\boldsymbol{\mathcal{I}}^k_{\mathcal{V}} = \{\boldsymbol{i}^k(\boldsymbol{v}) : \boldsymbol{v} \in \mathcal{V}(k)\}$ and $\boldsymbol{\mathcal{I}}^k_{\mathcal{E},0} = \bigcup_{e\in\mathcal{E}(k)} \boldsymbol{\mathcal{I}}^k_e \setminus \boldsymbol{\mathcal{I}}^k_{\mathcal{V}}$. The linear independence of the collection (4.23) follows from the observation that (i) the continuous interior functions $\Lambda^k_{\boldsymbol{i}}$ are single-patch basis functions with $\boldsymbol{i} \in \boldsymbol{\mathcal{I}}^k_0$, (ii) the continuous edge-based functions Λ^e_j decompose into basis functions $\Lambda^k_{\boldsymbol{i}}$ with indices $\boldsymbol{i} \in \boldsymbol{\mathcal{I}}^k_{\mathcal{E},0}$ (and with $i_\parallel = j$ for $k = k^-(e)$), and (iii) the continuous vertex-based functions $\Lambda^{\boldsymbol{v}}$ additionally involve basis functions $\Lambda^k_{\boldsymbol{i}}$ with indices $\boldsymbol{i} \in \boldsymbol{\mathcal{I}}^k_{\mathcal{V}}$.

To verify that it forms a basis we remind that a discrete function $\phi \in V^0_{\rm pw}$ belongs to V^0_h if and only if it is continuous (that is, single valued) on the edges $e \in \mathcal{E}$ and on the vertices $\boldsymbol{v} \in \mathcal{V}$: given the interpolatory property (3.3), this amounts to a constraint on the single-patch boundary coefficients $\phi^k_{\boldsymbol{i}}$ with $\boldsymbol{i} \in \boldsymbol{\mathcal{I}}^k \setminus \boldsymbol{\mathcal{I}}^k_0$. We then verify that any value on the vertices can be obtained by choosing the coefficients of the vertex-based functions $\Lambda^{\boldsymbol{v}}$, and any function on an edge $e \in \mathcal{E}$ (belonging to the associated coarse space) can be obtained by selecting the coefficients of the edge-based functions Λ^e_j with $j \in \mathcal{I}^e_0$: this shows that any $\phi \in V^0_h$ can indeed be obtained as a combination of functions from the collection (4.23) ■

4.3. Projection operators on local broken and conforming subspaces

In order to define proper correction terms at the patch interfaces, we now introduce several projection operators on various local subspaces of the broken space $V^0_{\rm pw}$: first, we define a projection on the homogeneous single-patch space $V^0_k \cap H^1_0(\Omega_k)$,

$$I^k_0 : \Lambda^k_{\boldsymbol{i}} \longmapsto \begin{cases} \Lambda^k_{\boldsymbol{i}} & \text{if } \boldsymbol{i} \in \boldsymbol{\mathcal{I}}^k_0 \\ 0 & \text{otherwise} \end{cases} \tag{4.24}$$

where we remind that the set $\boldsymbol{\mathcal{I}}^k_0$ corresponds to patch-interior indices, see (4.6).

We then define two projection operators associated with an edge $e \in \mathcal{E}$: the first one is on the space spanned by the broken functions which do not vanish identically on e,

$$I^e : \Lambda^k_{\boldsymbol{i}} \longmapsto \begin{cases} \Lambda^k_{\boldsymbol{i}} & \text{if } k \in \mathcal{K}(e) \text{ and } \boldsymbol{i} \in \boldsymbol{\mathcal{I}}^k_e \\ 0 & \text{otherwise} \end{cases} \tag{4.25}$$

where we remind that the set $\boldsymbol{\mathcal{I}}^k_e$ corresponds to edge-based single-patch indices, see (4.10).

The second edge projection is on the space spanned by the edge-continuous basis functions:

$$P^e : \Lambda^k_{\boldsymbol{i}} \longmapsto \begin{cases} \Lambda^e_j & \text{if } k = k^-(e) \text{ and } \boldsymbol{i} \in \boldsymbol{\mathcal{I}}^-_e, \text{ with } j := i^k_\parallel \in \mathcal{I}^e \\ 0 & \text{otherwise.} \end{cases} \tag{4.26}$$

see (4.9), (4.10).

Next for each vertex $\boldsymbol{v} \in \mathcal{V}$ we define projection operators on different subspaces of $V^0_{\rm pw}$: one on the space spanned by the broken vertex functions

$$I^{\boldsymbol{v}} : \Lambda^k_{\boldsymbol{i}} \longmapsto \begin{cases} \Lambda^k_{\boldsymbol{i}} & \text{if } k \in \mathcal{K}(\boldsymbol{v}) \text{ and } \boldsymbol{i} = \boldsymbol{i}^k(\boldsymbol{v}) \\ 0 & \text{else} \end{cases} \tag{4.27}$$

where $\boldsymbol{i}^k(\boldsymbol{v})$ is the local index corresponding to $\boldsymbol{v}$, see (4.16).

Another projection is on the single vertex-continuous basis function

$$P^{\boldsymbol{v}} : \Lambda^k_{\boldsymbol{i}} \longmapsto \begin{cases} \Lambda^{\boldsymbol{v}} & \text{if } k = k^*(\boldsymbol{v}) \text{ and } \boldsymbol{i} = \boldsymbol{i}^k(\boldsymbol{v}) \\ 0 & \text{otherwise.} \end{cases} \tag{4.28}$$

where $k^*(\boldsymbol{v}) \in \mathcal{K}(\boldsymbol{v})$ is the patch associated to $\boldsymbol{v}$ as described in Section 3.5.

We also define a projection on the broken pieces of the vertex-continuous functions, namely

$$\bar{I}^{\boldsymbol{v}} : \Lambda^k_{\boldsymbol{i}} \longmapsto \begin{cases} \Lambda^{\boldsymbol{v}} \mathbb{1}_{\Omega_k} & \text{if } k \in \mathcal{K}(\boldsymbol{v}) \text{ and } \boldsymbol{i} = \boldsymbol{i}^k(\boldsymbol{v}) \\ 0 & \text{otherwise.} \end{cases} \tag{4.29}$$

Finally, we define projection operators on different spaces spanned by edge-vertex functions. Again, we define three operators: one that projects on the simple broken functions,

$$I^e_{\boldsymbol{v}} : \Lambda^k_{\boldsymbol{i}} \longmapsto \begin{cases} \Lambda^k_{\boldsymbol{i}} & \text{if } k \in \mathcal{K}(e) \cap \mathcal{K}(\boldsymbol{v}) \text{ and } \boldsymbol{i} = \boldsymbol{i}^k(\boldsymbol{v}) \\ 0 & \text{otherwise} \end{cases} \tag{4.30}$$

one on the edge-continuous functions which do not vanish on a given vertex

$$P^e_{\boldsymbol{v}} : \Lambda^k_{\boldsymbol{i}} \longmapsto \begin{cases} \Lambda^e_{\boldsymbol{v}} & \text{if } k = k^-(e) \in \mathcal{K}(\boldsymbol{v}) \text{ and } \boldsymbol{i} = \boldsymbol{i}^k(\boldsymbol{v}) \\ 0 & \text{otherwise} \end{cases} \tag{4.31}$$

and one on the broken pieces of the edge-continuous functions that do not vanish on the vertex:

$$\bar{I}^e_{\boldsymbol{v}} : \Lambda^k_{\boldsymbol{i}} \longmapsto \begin{cases} \Lambda^e_{\boldsymbol{v}} \mathbb{1}_{\Omega_k} & \text{if } k \in \mathcal{K}(e) \cap \mathcal{K}(\boldsymbol{v}) \text{ and } \boldsymbol{i} = \boldsymbol{i}^k(\boldsymbol{v}) \\ 0 & \text{otherwise.} \end{cases} \tag{4.32}$$

Below we will verify that these operators are indeed projection operators. For later reference we observe that for all $\phi \in V^0_{\mathrm{pw}}$, the above edge and vertex-based projections are localized in edge and vertex-based domains of the form (4.11) and (4.18):

$$\begin{cases} \big(\operatorname{supp}(P^e\phi) \cup \operatorname{supp}(I^e\phi)\big) \subset \bigcup_{j=0}^{n_e} S^e_j \\ \big(\operatorname{supp}(P^e_{\boldsymbol{v}}\phi) \cup \operatorname{supp}(\bar{I}^e_{\boldsymbol{v}}\phi)\big) \subset S^e_{i^e(\boldsymbol{v})} \subset S^{\boldsymbol{v}} \\ \big(\operatorname{supp}(P^{\boldsymbol{v}}\phi) \cup \operatorname{supp}(\bar{I}^{\boldsymbol{v}}\phi)\big) \subset S^{\boldsymbol{v}}. \end{cases} \tag{4.33}$$

From these definitions we infer some useful relations. First, we observe that

$$\sum_{e \in \mathcal{E}} I^e_{\boldsymbol{v}} = 2 I^{\boldsymbol{v}} \tag{4.34}$$

holds for all $\boldsymbol{v} \in \mathcal{V}$. Multiplying (4.15) with $\mathbb{1}_{\Omega_k}$ we further obtain an equality relating the operators (4.29) and (4.32) to the broken vertex-based projection (4.27):

$$\bar{I}^{\boldsymbol{v}} = \sum_{e \in \mathcal{E}} \bar{I}^e_{\boldsymbol{v}} - I^{\boldsymbol{v}}. \tag{4.35}$$

Another key relation is the decomposition of any broken function $\phi \in V^0_{\mathrm{pw}}$ as

$$\phi = \Big(\sum_{k \in \mathcal{K}} I^k_0 + \sum_{e \in \mathcal{E}} I^e_0 + \sum_{v \in \mathcal{V}} I^{\boldsymbol{v}} \Big) \phi \tag{4.36}$$

where we have set

$$I^e_0 \coloneqq I^e - \sum_{\boldsymbol{v} \in \mathcal{V}} I^e_{\boldsymbol{v}}. \tag{4.37}$$

By using the fact that the functions (4.23) form a basis for the conforming space $V^0_h = V^0_{\mathrm{pw}} \cap V^0$, we also define a local projection on the conforming subspace,

$$P : V^0_{\mathrm{pw}} \longrightarrow V^0_h, \quad \phi \longmapsto \Big(\sum_{k \in \mathcal{K}} I^k_0 + \sum_{e \in \mathcal{E}} P^e_0 + \sum_{\boldsymbol{v} \in \mathcal{V}} P^{\boldsymbol{v}} \Big) \phi. \tag{4.38}$$

where we have set

$$P^e_0 \coloneqq P^e - \sum_{\boldsymbol{v} \in \mathcal{V}} P^e_{\boldsymbol{v}}. \tag{4.39}$$

Lemma 4.3. *The operators $Q = I^k_0, \dots, \bar{I}^e_{\boldsymbol{v}}$ defined in (4.24)–(4.32) are all projection operators in the sense that $Q = Q^2$, and P defined in (4.38) is a projection operator onto the continuous space V^0_h.*

Proof. For the operators I_0^k, I^e, $I^{\boldsymbol v}$, $I^e_{\boldsymbol v}$ which map on specific sets of single-patch basis functions, the projection property is straightforward to verify. For an operator $P^g = P^e$, $P^{\boldsymbol v}$ or $P^e_{\boldsymbol v}$ which map on (fully or partially) continuous functions, the property follows from the fact that each of these continuous functions (say, Λ^g) admits a decomposition in the broken basis (3.14), of the form

$$\Lambda^g = \Lambda^{k(g)}_{\boldsymbol i(g)} + \sum_{k',\boldsymbol i'} c^g_{k',\boldsymbol i'}\Lambda^{k'}_{\boldsymbol i'}$$

with $P^g(\Lambda^{k(g)}_{\boldsymbol i(g)}) = \Lambda^g$ and $P^g(\Lambda^{k'}_{\boldsymbol i'}) = 0$, hence $P^g(\Lambda^g) = \Lambda^g$ holds indeed. For the operators $\bar I^g = \bar I^{\boldsymbol v}$ and $\bar I^e_{\boldsymbol v}$ which map on broken pieces of continuous functions, of the form $\Lambda^g|_{\Omega_k}$, the projection property follows from a similar observation. Finally, the projection property of P is verified by considering that each term in the sum (4.38) projects onto the continuous basis functions of interior, edge and vertex type in the collection (4.23). ■

Several useful properties can be derived from explicit expressions of the above projections.

Lemma 4.4. *Given $\phi \in V^0_{\rm pw}$ and $\boldsymbol x \in \Omega_k$, $k \in \mathcal K(e)$, the edge based projections read*

$$\begin{cases} (I^e\phi)|_{\Omega_k}(\boldsymbol x) = \phi|_{\Omega_k}(\boldsymbol p_e(\boldsymbol x))\lambda^k_{i^k_\perp(e)}(\hat x^k_\perp), \\ (P^e\phi)|_{\Omega_k}(\boldsymbol x) = \phi|_{\Omega_{k^-}}(\boldsymbol p_e(\boldsymbol x))\lambda^k_{i^k_\perp(e)}(\hat x^k_\perp) \end{cases} \tag{4.40}$$

where $X^k_e(\hat x^k_\parallel, \hat x^k_\perp) = \boldsymbol x$ as in (3.30), $k^- = k^-(e)$ and

$$\boldsymbol p_e(\boldsymbol x) \coloneqq X^k_e(\hat x^k_\parallel, \hat e^k_\perp) \tag{4.41}$$

is the point on the edge e that has the same parallel coordinate as $\boldsymbol x \in \Omega_k$. Similarly, the vertex based projections read

$$\bar I^{\boldsymbol v}\phi = \sum_{k\in\mathcal K(\boldsymbol v)} \phi|_{\Omega_k}(\boldsymbol v)\Lambda^{\boldsymbol v}\mathbb 1_{\Omega_k} \quad \text{and} \quad P^{\boldsymbol v}\phi = \phi|_{\Omega^*}(\boldsymbol v)\Lambda^{\boldsymbol v} \tag{4.42}$$

where $\Omega^* = \Omega_{k^*(\boldsymbol v)}$ and the edge-vertex based projections read

$$\bar I^e_{\boldsymbol v}\phi = \sum_{k\in\mathcal K(e)} \phi|_{\Omega_k}(\boldsymbol v)\Lambda^e_{\boldsymbol v}\mathbb 1_{\Omega_k} \quad \text{and} \quad P^e_{\boldsymbol v}\phi = \phi|_{\Omega_{k^-}}(\boldsymbol v)\Lambda^e_{\boldsymbol v}. \tag{4.43}$$

Proof. Write $\phi = \sum_{k\in\mathcal K, \boldsymbol i\in\boldsymbol{\mathcal I}^k}\phi^k_{\boldsymbol i}\Lambda^k_{\boldsymbol i}$. By definition, the projection $I^e\phi$ involves broken functions $\Lambda^k_{\boldsymbol i}$ with $\boldsymbol i = \boldsymbol i^k_e(j) = X^k_e(j, i^k_\perp(e))$ as in (4.10), i.e.

$$\Lambda^k_{\boldsymbol i^k_e(j)}(\boldsymbol x) = \lambda^k_j(\hat x^k_\parallel)\lambda^k_{i^k_\perp(e)}(\hat x^k_\perp) \quad \text{for } \boldsymbol x \in \Omega_k,\ j \in \{0, \dots, n_k\}$$

while $P^e\phi$ involves conforming functions of the form (4.7). In particular, we have

$$\begin{cases} (I^e\phi)|_{\Omega_k}(\boldsymbol x) = \displaystyle\sum_{\boldsymbol i\in\boldsymbol{\mathcal I}^k_e}\phi^k_{\boldsymbol i}\Lambda^k_{\boldsymbol i}(\boldsymbol x) = \Big(\sum_{j=0}^{n_k}\phi^k_{\boldsymbol i^k_e(j)}\lambda^k_j(\hat x^k_\parallel)\Big)\lambda^k_{i^k_\perp(e)}(\hat x^k_\perp) \\ (P^e\phi)|_{\Omega_k}(\boldsymbol x) = \displaystyle\sum_{j=0}^{n_e}\phi^-_{\boldsymbol i^-_e(j)}\Lambda^e_j(\boldsymbol x) = \Big(\sum_{j=0}^{n_{k^-}}\phi^-_{\boldsymbol i^-_e(j)}\lambda^-_j(\eta^k_e(\hat x^k_\parallel))\Big)\lambda^k_{i^k_\perp(e)}(\hat x^k_\perp) \end{cases} \tag{4.44}$$

and the expressions (4.40) follow from the interpolatory property (3.3) of the basis functions in the $\perp$ direction. For the vertex based projections we write

$$P^{\boldsymbol v}\phi = \phi^{k^*(\boldsymbol v)}_{\boldsymbol i^{k^*(\boldsymbol v)}(\boldsymbol v)}\Lambda^{\boldsymbol v}, \qquad \bar I^{\boldsymbol v}\phi = \sum_{k\in\mathcal K(\boldsymbol v)}\phi^k_{\boldsymbol i^k(\boldsymbol v)}\Lambda^{\boldsymbol v}\mathbb 1_{\Omega_k} \tag{4.45}$$

and

$$P^e_{\boldsymbol v}\phi = \phi^-_{\boldsymbol i^-(\boldsymbol v)}\Lambda^e_{\boldsymbol v}, \qquad \bar I^e_{\boldsymbol v}\phi = \sum_{k\in\mathcal K(e)}\phi^k_{\boldsymbol i^k(\boldsymbol v)}\Lambda^e_{\boldsymbol v}\mathbb 1_{\Omega_k}.$$

The expressions (4.42) and (4.43) follow from the relations $\phi^k_{\boldsymbol{i}^k(\boldsymbol{v})} = \phi|_{\Omega_k}(\boldsymbol{v})$, which again follows from the interpolation property (3.3) at the patch boundaries. ∎

The following properties, which will be needed to analyze the operators Π^ℓ, are immediate corollaries of Lemma 4.4

Lemma 4.5. *Let $\phi \in V^0_{\rm pw}$, and $e \in \mathcal{E}$. The equality*

$$P^e\phi(\boldsymbol{x}) = I^e\phi(\boldsymbol{x})$$

holds for all $\boldsymbol{x} \in \Omega_{k^-}$, and all $\boldsymbol{x} \in \Omega_{k^+}$ such that $\phi|_{\Omega_{k^-}}(\boldsymbol{p}_e(\boldsymbol{x})) = \phi|_{\Omega_{k^+}}(\boldsymbol{p}_e(\boldsymbol{x}))$ where $\boldsymbol{p}_e(\boldsymbol{x})$ is the projected point on e, see (4.41)*.*

Lemma 4.6. *Let $\phi \in V^0_{\rm pw}$ and $\boldsymbol{v} \in \mathcal{V}$. It holds:*

$$\text{if} \quad \phi|_{\Omega_k}(\boldsymbol{v}) = \phi|_{\Omega_{k'}}(\boldsymbol{v}) \text{ for all } k, k' \in \mathcal{K}(\boldsymbol{v}), \quad \text{then} \quad (P^{\boldsymbol{v}} - \bar{I}^{\boldsymbol{v}})\phi = 0.$$

Moreover, for all $e \in \mathcal{E}(\boldsymbol{v})$ it holds:

$$\bar{I}^{\boldsymbol{v}}\phi = \bar{I}^e_{\boldsymbol{v}}\phi \qquad \text{on } e \tag{4.46}$$

and

$$\text{if} \quad \phi|_{\Omega_k}(\boldsymbol{v}) = \phi|_{\Omega_{k'}}(\boldsymbol{v}) \text{ for all } k, k' \in \mathcal{K}(e), \quad \text{then} \quad (P^e_{\boldsymbol{v}} - \bar{I}^e_{\boldsymbol{v}})\phi = 0.$$

Proof. All these relations follow from the expressions (4.42)–(4.43). For the equality (4.46) we also use the relation (4.17). ∎

Another important property is that both the broken and conforming edge projections preserve the invariance along the parallel direction. This partially extends the preservation of directional invariance of the local projections stated in Lemma 3.1.

Lemma 4.7. *Let $\phi \in L^p(\Omega(e))$ be such that the pullbacks $\hat{\phi}^k := (\mathcal{F}^0_k)^{-1}(\phi|_{\Omega_k})$ satisfy $\hat{\partial}_\parallel\hat{\phi}^k = 0$ for $k \in \mathcal{K}(e)$. Then,*

$$\nabla^e_\parallel P^e\Pi^0_{\rm pw}\phi = \nabla^e_\parallel I^e\Pi^0_{\rm pw}\phi = \nabla^e_\parallel\Pi^0_{\rm pw}\phi = 0. \tag{4.47}$$

Proof. The last equality from (4.47)follows from Lemma 3.1. Apply then (4.40) to $\phi_h = \Pi^0_{\rm pw}\phi$ and observe that $\phi_h|_{\Omega^k}(\boldsymbol{p}_e(\boldsymbol{x}))$ is constant: the result follows. ∎

We further verify that these projection operators are locally stable.

Lemma 4.8. *Let $\phi \in L^p(\Omega)$, and let $Q^e = I^e$, P^e or P^e_0 be one of the broken or conforming projection operators associated with an edge $e \in \mathcal{E}$. Then $Q^e\Pi^0_{\rm pw}\phi$ vanishes outside the domains S^e_j, $j \in \mathcal{I}^e$, see* (4.11)*. Moreover, it holds*

$$\|Q^e\Pi^0_{\rm pw}\phi\|_{L^p(S^e_j)} \lesssim \|\phi\|_{L^p(E_e(S^e_j))} \quad \text{with } \; Q^e = I^e, P^e \text{ or } P^e_0 \tag{4.48}$$

where we remind E_e is the edge-based extension (4.12)*. Similarly, let $Q^{\boldsymbol{v}} = \bar{I}^{\boldsymbol{v}}$, $\bar{I}^e_{\boldsymbol{v}}$, $P^{\boldsymbol{v}}$ or $P^e_{\boldsymbol{v}}$ be one of the broken or conforming projection operators associated with a vertex $\boldsymbol{v}$. Then $Q^{\boldsymbol{v}}\Pi^0_{\rm pw}\phi$ vanishes outside the domain $S^{\boldsymbol{v}}$, and it holds*

$$\|Q^{\boldsymbol{v}}\Pi^0_{\rm pw}\phi\|_{L^p(S^{\boldsymbol{v}})} \lesssim \|\phi\|_{L^p(S^{\boldsymbol{v}})} \quad \text{with } \; Q^{\boldsymbol{v}} = \bar{I}^{\boldsymbol{v}}, \bar{I}^e_{\boldsymbol{v}}, P^{\boldsymbol{v}} \text{ or } P^e_{\boldsymbol{v}}. \tag{4.49}$$

Proof. Write $\phi_h := \Pi^0_{\rm pw}\phi = \sum_{k\in\mathcal{K},\boldsymbol{i}\in\mathcal{I}^k}\phi^k_{\boldsymbol{i}}\Lambda^k_{\boldsymbol{i}}$. The fact that $Q^e\phi_h$, resp. $Q^{\boldsymbol{v}}\phi_h$, vanishes outside the domains S^e_j, resp. $S^{\boldsymbol{v}}$, is easily verified using (4.33) and (4.39). Using the form (4.44) of $I^e\phi_h$ with the bound (3.19), we next compute

$$\|I^e\phi_h\|_{L^p(S^e_j)} \le \sum_{k\in\mathcal{K}(e),\boldsymbol{i}\in\mathcal{I}^k_e} |\phi^k_{\boldsymbol{i}}|\|\Lambda^k_{\boldsymbol{i}}\|_{L^p(S^e_j)} \lesssim \sum_{k\in\mathcal{K}(e),\boldsymbol{i}\in\mathcal{I}^k_e(S^e_j)} \|\phi\|_{L^p(S^k_{\boldsymbol{i}})} \tag{4.50}$$

so that (4.48) (for $Q^e = I^e$) follows from the bounded overlapping of the domains $S^k_{\boldsymbol{i}}$ and the inclusion (4.13). For $Q^e = P^e$ we use the form of $P^e\phi_h$ in (4.44) (the same computations also apply to $P^e_0\phi_h$ which involves fewer terms). With the bounds (3.21) and (4.22) with $h_e \sim h_k$ for $k \in \mathcal{K}(e)$, this yields

$$\|P^e\phi_h\|_{L^p(S^e_j)} \le \sum_{i\in\mathcal{I}^e} |\phi^-_{\boldsymbol{i}_e(i)}|\|\Lambda^e_i\|_{L^p(S^e_j)} \lesssim \sum_{i\in\mathcal{I}^e(S^e_j)} \|\phi\|_{L^p(S^-_{\boldsymbol{i}_e(i)})}$$

where the index set $\mathcal{I}^e(S^e_j)$ is defined in (4.12). The bound (4.48) for $Q^e = P^e$ then follows from the inclusion $S^-_{\boldsymbol{i}_e(i)} \subset S^e_i \subset E_e(\omega)$ for $i \in \mathcal{I}^e(\omega)$, and again the bounded overlapping of the domains $S^k_{\boldsymbol{i}}$. The bound (4.49) is proven with similar arguments: for instance, writing $\bar{I}^{\boldsymbol{v}}\phi_h = \sum_{k\in\mathcal{K}(\boldsymbol{v})}\phi^k_{\boldsymbol{i}^k(\boldsymbol{v})}\Lambda^{\boldsymbol{v}}\mathbb{1}_{\Omega_k}$ as in (4.45) and using again (4.22), we have

$$\|\bar{I}^{\boldsymbol{v}}\phi_h\|_{L^p(S^{\boldsymbol{v}})} \le \sum_{k\in\mathcal{K}(\boldsymbol{v})} |\phi^k_{\boldsymbol{i}^k(\boldsymbol{v})}|\|\Lambda^{\boldsymbol{v}}\|_{L^p(S^{\boldsymbol{v}})} \lesssim \sum_{k\in\mathcal{K}(\boldsymbol{v})} \|\phi\|_{L^p\left(S^k_{\boldsymbol{i}^k(\boldsymbol{v})}\right)}$$

so that (4.49) with $Q^{\boldsymbol{v}} = \bar{I}^{\boldsymbol{v}}$ follows from the inclusion $S^k_{\boldsymbol{i}^k(\boldsymbol{v})} \subset S^{\boldsymbol{v}}$, see (4.19). The cases $Q^{\boldsymbol{v}} = P^{\boldsymbol{v}}$, $\bar{I}^e_{\boldsymbol{v}}$ and $P^e_{\boldsymbol{v}}$ are handled in the same way. ■

5. L^p stable antiderivative operators

Our construction (2.10) for Π^1 relies on several local antiderivative operators, which are built using specific integration curves:

- a single-patch antiderivative Φ^k_d for $k \in \mathcal{K}$ and a direction $d \in \{1, 2\}$, associated with integration curves γ^k_d
- edge antiderivatives Φ^e_d for $e \in \mathcal{E}$ and a relative direction $d \in \{\|, \perp\}$, associated with integration curves γ^e_d
- a vertex antiderivative $\Phi^{\boldsymbol{v}}$ for $\boldsymbol{v} \in \mathcal{V}$, associated with integration curves $\gamma^{\boldsymbol{v}}$.

Given a vector valued function $\boldsymbol{u}$, these operators take the general form

$$\Phi(\boldsymbol{u})(\boldsymbol{x}) = \frac{1}{\hat{h}}\int_0^{\hat{h}}\int_{\gamma(\boldsymbol{x},a)} \boldsymbol{u}\cdot \mathrm{d}l\,\mathrm{d}a$$

where $\hat{h}$ is an averaging resolution in the spirit of [8] and for every value of the averaging parameter a, $\gamma(\boldsymbol{x}, a)$ is a generic curve connecting $\boldsymbol{x}$ and some starting point $\gamma_0(\boldsymbol{x}, a)$ which may or may not depend on $\boldsymbol{x}$. In particular, applied to gradients these will satisfy a relation of the form

$$\Phi(\nabla\phi)(\boldsymbol{x}) = \frac{1}{\hat{h}}\int_0^{\hat{h}}\int_{\gamma(\boldsymbol{x},a)} \nabla\phi\cdot \mathrm{d}l\,\mathrm{d}a = \phi(\boldsymbol{x}) - \frac{1}{\hat{h}}\int_0^{\hat{h}} \phi(\gamma_0(\boldsymbol{x}, a))\,\mathrm{d}a.$$

In a similar fashion, we will define bivariate antiderivative operators of the form

$$\Psi(f)(\boldsymbol{x}) = \frac{1}{\hat{h}} \int_0^{\hat{h}} \iint_{\sigma(\boldsymbol{x},a)} f \,\mathrm{d}\boldsymbol{z} \,\mathrm{d}a$$

which will be involved in the commuting projection Π^2.

5.1. Single-patch antiderivative operators

In the case of single-patch antiderivative operators Φ_d^k, the integration curve does not depend on a and for $\boldsymbol{x} \in \Omega_k$ it is fully contained in Ω_k. Writing $\hat{\boldsymbol{x}} = F_k^{-1}(\boldsymbol{x})$ we parametrize it as

$$\gamma_d^k(\boldsymbol{x}) = F_k(\hat{\gamma}_d(\hat{\boldsymbol{x}}, [0, \hat{x}_d])) \quad \text{with} \quad \hat{\gamma}_d(\hat{\boldsymbol{x}}, \cdot) : [0, \hat{x}_d] \ni z \longmapsto \begin{cases} (z, \hat{x}_2) & \text{if } d = 1 \\ (\hat{x}_1, z) & \text{if } d = 2. \end{cases}$$

Using the invariance of path integrals through 1-form pullback $(\mathcal{F}_k^1)^{-1} : \boldsymbol{u} \mapsto \hat{\boldsymbol{u}}^k$, this results in defining the directional antiderivative operators as

$$\Phi_1^k(\boldsymbol{u})(\boldsymbol{x}) := \int_0^{\hat{x}_1} \hat{u}_1^k(z_1, \hat{x}_2) \,\mathrm{d}z_1 \quad \text{and} \quad \Phi_2^k(\boldsymbol{u})(\boldsymbol{x}) := \int_0^{\hat{x}_2} \hat{u}_2^k(\hat{x}_1, z_2) \,\mathrm{d}z_2. \tag{5.1}$$

As already mentioned, these operators play a central role in the tensor-product construction of [13]. We review their main properties in our framework.

Lemma 5.1. *Let $\boldsymbol{u} = \nabla\phi$ with $\phi \in C^1(\overline{\Omega})$. It holds*

$$\Phi_d^k(\boldsymbol{u})(\boldsymbol{x}) = \phi(\boldsymbol{x}) - \phi(F_k(\bar{\boldsymbol{x}})) \quad \text{for } \boldsymbol{x} \in \Omega_k,$$

where $\bar{x}_d = 0$ and $\bar{x}_{d'} = \hat{x}_{d'}$ for the other component.

Proof. The proof is straightforward. ∎

Lemma 5.2. *The single-patch antiderivative operators are stable in L^p, namely*

$$\|\Phi_d^k(\boldsymbol{u})\|_{L^p(\Omega_k)} \lesssim \|\boldsymbol{u}\|_{L^p(\Omega_k)} \tag{5.2}$$

holds for $\boldsymbol{u} \in L^p(\Omega)$. Moreover, the local bound

$$\|\nabla_d^k \Pi_k^0 \Phi_d^k(\boldsymbol{u})\|_{L^p(S_{\boldsymbol{i}}^k)} \lesssim \|\boldsymbol{u}\|_{L^p(E_k(S_{\boldsymbol{i}}^k))} \tag{5.3}$$

holds on any domain $S_{\boldsymbol{i}}^k$ of the form (3.15), $\boldsymbol{i} \in \boldsymbol{\mathcal{I}}^k$, where E_k is the single-patch domain extension (3.16).

Proof. Using the scaling of (3.13), we work with the pullback $\hat{\Phi}_d^k(\hat{\boldsymbol{u}}^k)$ on the reference domain $\hat{\Omega}$. Without loss of generality, we consider $d = 1$, and with a Hölder inequality we bound

$$\begin{aligned} \|\hat{\Phi}_1^k(\hat{\boldsymbol{u}}^k)\|_{L^p(\hat{\Omega})}^p &= \iint_{\hat{\Omega}} \left| \int_0^{\hat{x}_1} \hat{u}_1^k(z, \hat{x}_2) \,\mathrm{d}z \right|^p \mathrm{d}\hat{\boldsymbol{x}} \\ &\leq \iint_{\hat{\Omega}} |\hat{x}_1|^{p-1} \int_0^{\hat{x}_1} |\hat{\boldsymbol{u}}^k(z, \hat{x}_2)|^p \,\mathrm{d}z \,\mathrm{d}\hat{\boldsymbol{x}} \leq \|\hat{\boldsymbol{u}}^k\|_{L^p(\hat{\Omega})}^2 \end{aligned} \tag{5.4}$$

and (5.2) follows from the scaling relations (3.13) and the bound $H_k \lesssim 1$. Turning to the local estimate we observe that for any fixed $\tilde{x}_1 \in [0, 1]$, the antiderivative

$$\tilde{\Phi}_1^k(\hat{\boldsymbol{u}}^k)(\hat{\boldsymbol{x}}) := \int_{\tilde{x}_1}^{\hat{x}_1} \hat{u}_1^k(z_1, \hat{x}_2) \,\mathrm{d}z_1$$

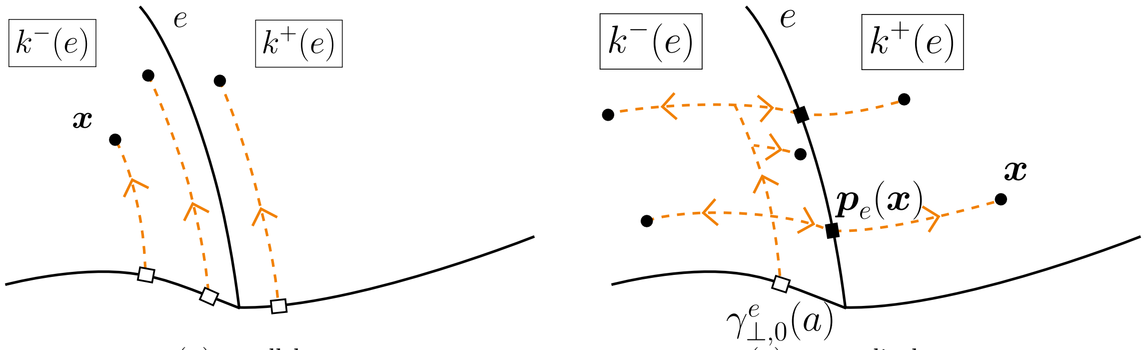

(A) parallel case (B) perpendicular case

FIGURE 5.1. Integration paths $\gamma^e_d(\boldsymbol{x}, a)$ defining the edge-based antiderivative operators Φ^e_d. In the case $d = \|$ (A) the curves connect various points $\boldsymbol{x}$ (curves for three different points are shown in this case) to different starting points $\gamma^e_{\|,0}(\boldsymbol{x})$, represented by white squares, which depend only on the perpendicular component $\hat{x}^k_\perp$ of the logical coordinate of $\boldsymbol{x} \in \Omega_k$, see (3.29). In the case $d = \perp$ (B) the curves depend on the averaging parameter a. For a given value of $a \in (0, \hat{h}_e)$ they connect every $\boldsymbol{x} \in \Omega(e)$ (curves for five different points are shown in this case) to the same starting point $\gamma^e_{\perp,0}(a)$ represented by a white square, see (5.7), possibly crossing the edge at $\boldsymbol{p}_e(\boldsymbol{x})$ represented by a black square, see (4.41).

satisfies $\hat{\nabla}_1 \hat{\Phi}^k_1(\hat{\boldsymbol{u}}^k) = \hat{\nabla}_1 \tilde{\Phi}^k_1(\hat{\boldsymbol{u}}^k)$, hence $\hat{\nabla}_1 \hat{\Pi}^0_k \hat{\Phi}^k_1(\hat{\boldsymbol{u}}^k) = \hat{\nabla}_1 \hat{\Pi}^0_k \tilde{\Phi}^k_1(\hat{\boldsymbol{u}}^k)$ by Lemma 3.1. Using the inverse estimate (3.6) and the local stability (3.20) we next bound

$$\|\hat{\nabla}_1 \hat{\Pi}^0_k \tilde{\Phi}^k_1(\hat{\boldsymbol{u}}^k)\|_{L^p(\hat{S}^k_{\boldsymbol{i}})} \lesssim \hat{h}_k^{-1} \|\hat{\Pi}^0_k \tilde{\Phi}^k_1(\hat{\boldsymbol{u}}^k)\|_{L^p(\hat{S}^k_{\boldsymbol{i}})} \lesssim \hat{h}_k^{-1} \|\tilde{\Phi}^k_1(\hat{\boldsymbol{u}}^k)\|_{L^p(\hat{E}_h(\hat{S}^k_{\boldsymbol{i}}))}.$$

We then observe that $\hat{E}_h(\hat{S}^k_{\boldsymbol{i}})$ is of diameter $\lesssim \hat{h}_k$, and we fix $\tilde{x}_1 \in \hat{S}^k_{i_1}$ which according to the locality properties (3.4)–(3.5), satisfies $|\hat{x}_1 - \tilde{x}_1| \lesssim \hat{h}_k$ for all $\hat{\boldsymbol{x}} \in \hat{E}_h(\hat{S}^k_{\boldsymbol{i}})$. We then compute as in (5.4): this gives

$$\|\tilde{\Phi}^k_1(\hat{\boldsymbol{u}}^k)\|^p_{L^p(\hat{E}_h(\hat{S}^k_{\boldsymbol{i}}))} \le \iint_{\hat{E}_h(\hat{S}^k_{\boldsymbol{i}})} |\hat{x}_1 - \tilde{x}_1|^{p-1} \int_{\tilde{x}_1}^{\hat{x}_1} |\hat{\boldsymbol{u}}^k(z, \hat{x}_2)|^p \,\mathrm{d}z \,\mathrm{d}\hat{\boldsymbol{x}} \le \hat{h}_k^p \|\hat{\boldsymbol{u}}^k\|^p_{L^p(\hat{E}_h(\hat{S}^k_{\boldsymbol{i}}))}$$

so that we have shown

$$\|\hat{\nabla}_1 \hat{\Pi}^0_k \hat{\Phi}^k_1(\hat{\boldsymbol{u}}^k)\|_{L^p(\hat{S}^k_{\boldsymbol{i}})} = \|\hat{\nabla}_1 \hat{\Pi}^0_k \tilde{\Phi}^k_1(\hat{\boldsymbol{u}}^k)\|_{L^p(\hat{S}^k_{\boldsymbol{i}})} \lesssim \|\hat{\boldsymbol{u}}^k\|_{L^p(\hat{E}_h(\hat{S}^k_{\boldsymbol{i}}))}.$$

Estimate (5.3) follows from the scaling (3.13) of 1-form pullbacks. ∎

5.2. Edge-based antiderivative operators

In a similar way, we define edge-based antiderivative operators Φ^e_d along $d \in \{\|, \perp\}$, the parallel and perpendicular directions relative to e. Both are supported in the patches adjacent to e and the construction is summarized in Figure 5.1.

For the parallel edge-based antiderivative operator $\Phi^e_\|$ the integration curve is similar to the single-patch one. For $\boldsymbol{x} \in \Omega_k$, $k \in \mathcal{K}(e)$, it is fully supported in Ω_k. Writing now $\hat{\boldsymbol{x}}^k = F_k^{-1}(\boldsymbol{x})$, we define it as

$$\gamma^e_\|(\boldsymbol{x}) = F_k(\hat{\gamma}^{e,k}_\|(\hat{\boldsymbol{x}}, [\eta^k_e(0), \hat{x}^k_\|])) \quad \text{with} \quad \hat{\gamma}^{e,k}_\|(\hat{\boldsymbol{x}}, \cdot) : [\eta^k_e(0), \hat{x}^k_\|] \ni z \longmapsto \hat{X}^k_e(z, \hat{x}^k_\perp)$$

where we remind that $\hat{x}^k_\parallel$ and $\hat{x}^k_\perp$ are the parallel and perpendicular coordinates relative to e, $\hat{X}^k_e$ is the reordering function (3.30) and η^k_e is the edge orientation function given by (4.4). Thus, the resulting parallel antiderivative is

$$\Phi^e_\parallel(\boldsymbol{u})(\boldsymbol{x}) := \int_{\gamma^e_\parallel(\boldsymbol{x})} \boldsymbol{u} \cdot \mathrm{d}l = \int_{\eta^k_e(0)}^{\hat{x}^k_\parallel} \hat{u}^k_\parallel(X^k_e(z, \hat{x}^k_\perp))\,\mathrm{d}z \tag{5.5}$$

for $\boldsymbol{x} \in \Omega_k$, $k \in \mathcal{K}(e)$ (without averaging as the curves do not depend on a). For the perpendicular edge-based antiderivative, we use an averaging step

$$\Phi^e_\perp(\boldsymbol{u})(\boldsymbol{x}) = \frac{1}{\hat{h}_e}\int_0^{\hat{h}_e} \Phi^e_{\perp,a}(\boldsymbol{u})(\boldsymbol{x})\,\mathrm{d}a \quad \text{with} \quad \Phi^e_{\perp,a}(\boldsymbol{u})(\boldsymbol{x}) = \int_{\gamma^e_\perp(\boldsymbol{x},a)} \boldsymbol{u}\cdot \mathrm{d}l \tag{5.6}$$

where $\hat{h}_e$ is defined in (4.20), and the integration curves are defined as follows:

For $\boldsymbol{x}$ on the coarse patch, the curve $\gamma^e_\perp(\boldsymbol{x}, a)$ is included in $\Omega_{k^-(e)}$. It is the mapping of the logical curve $\hat{\gamma}^{e,-}_\perp(\hat{\boldsymbol{x}}, a)$ defined for $z \in [-\hat{x}_\parallel, |\hat{x}_\perp - \tilde{a}|]$ by

$$\hat{\gamma}^{e,-}_\perp(\hat{\boldsymbol{x}}, a, \cdot) : z \longmapsto \begin{cases} X^-_e(\hat{x}_\parallel + z, \tilde{a}) & \text{for} \quad -\hat{x}_\parallel \le z \le 0 \\ X^-_e(\hat{x}_\parallel, \tilde{a} + z\,\mathrm{sign}(\hat{x}_\perp - \tilde{a})) & \text{for} \quad 0 \le z \le |\hat{x}_\perp - \tilde{a}|. \end{cases}$$

In particular the curve $\gamma^e_\perp(\boldsymbol{x}, a)$ connects $\boldsymbol{x}$ to the starting point

$$\gamma^e_{\perp,0}(a) = F_{k^-(e)}(X^-_e(0, \tilde{a})). \tag{5.7}$$

Here $\tilde{a}$ is the perpendicular coordinate at distance a from the edge, namely

$$\tilde{a} := \begin{cases} a & \text{if } \hat{e}^-_\perp = 0 \\ 1 - a & \text{if } \hat{e}^-_\perp = 1 \end{cases}, \tag{5.8}$$

where $\hat{e}^-_\perp$ is defined in (3.31). The antiderivative then reads

$$\Phi^e_{\perp,a}(\boldsymbol{u})(\boldsymbol{x}) := \int_0^{\hat{x}_\parallel} \hat{u}^-_\parallel(\hat{X}^-_e(z_\parallel, \tilde{a}))\,\mathrm{d}z_\parallel + \int_{\tilde{a}}^{\hat{x}_\perp} \hat{u}^-_\perp(\hat{X}^-_e(\hat{x}_\parallel, z_\perp))\,\mathrm{d}z_\perp, \text{ for } \boldsymbol{x} \in \Omega_{k^-}. \tag{5.9}$$

For $\boldsymbol{x}$ in the fine patch, the curve is defined in two pieces: the first one is included in $\Omega_{k^-(e)}$ and corresponds to the logical curve $\hat{\gamma}^{e,-}_\perp$ defined above: it connects the starting point (5.7) to the projection $\boldsymbol{p}_e(\boldsymbol{x})$ on the edge, see (4.41). The second piece is included in $\Omega_{k^+(e)}$, it connects $\boldsymbol{p}_e(\boldsymbol{x})$ to $\boldsymbol{x}$ and corresponds to a logical curve $\hat{\gamma}^{e,+}_\perp(\hat{\boldsymbol{x}}, \cdot)$ defined below. This amounts to summing

$$\Phi^e_{\perp,a}(\boldsymbol{u})(\boldsymbol{x}) := \Phi^e_{\perp,a}(\boldsymbol{u})(\boldsymbol{p}_e(\boldsymbol{x}))|_{\Omega_{k^-}} + \delta\Phi^e_\perp(\boldsymbol{u})(\boldsymbol{x}) \quad \text{for } \boldsymbol{x} \in \Omega_{k^+}, \tag{5.10}$$

where the first term is the path integral (5.9) on the patch $k^-(e)$, extended to the projected point (4.41) on the edge, here

$$\boldsymbol{p}_e(\boldsymbol{x}) = X^+_e(\hat{x}_\parallel, \hat{e}^+_\perp) = X^-_e(\eta_e(\hat{x}_\parallel), \hat{e}^-_\perp), \tag{5.11}$$

and the second term is a path integral in the fine patch $k^+(e)$, defined as

$$\delta\Phi^e_\perp(\boldsymbol{u})(\boldsymbol{x}) := \int_{\hat{e}^+_\perp}^{\hat{x}_\perp} \hat{u}^+_\perp(X^+_e(\hat{x}_\parallel, z_\perp))\,\mathrm{d}z_\perp \tag{5.12}$$

which corresponds to the local curve

$$\hat{\gamma}^{e,+}_\perp(\hat{\boldsymbol{x}}, \cdot) : [0, |\hat{x}_\perp - \hat{e}^+_\perp|] \ni z \longmapsto X^+_e(\hat{x}_\parallel, \hat{e}^+_\perp + z\,\mathrm{sign}(\hat{x}_\perp - \hat{e}^+_\perp)).$$

This two-term definition thus corresponds to an integration path that, for each value of the parameter a, connects every point $\boldsymbol{x} \in \Omega_k$, $k \in \mathcal{K}(e)$, to the common starting point $\gamma^e_\perp(0, a)$.

Notice that this property is also valid for boundary edges, since their unique patch is considered of coarse type by convention ($\mathcal{K}(e) = \{k^-(e)\}$).

Lemma 5.3. *For all $e \in \mathcal{E}$, $\phi \in C^1(\overline{\Omega})$, there exists a function $\tilde{\phi}_e \in \oplus_{k \in \mathcal{K}(e)} H^1(\Omega_k)$ for which the parallel edge antiderivative satisfies*

$$\Phi^e_{\parallel}(\nabla\phi)(\boldsymbol{x}) = \phi(\boldsymbol{x}) - \tilde{\phi}_e(\boldsymbol{x}) \quad \text{and} \quad \nabla^e_{\parallel}\tilde{\phi}_e = 0 \tag{5.13}$$

on $\Omega(e) := \bigcup_{k \in \mathcal{K}(e)} \Omega_k$. Moreover, the perpendicular edge antiderivative satisfies

$$\Phi^e_{\perp}(\nabla\phi)(\boldsymbol{x}) = \phi(\boldsymbol{x}) - \bar{\phi}_e \tag{5.14}$$

for a constant value $\bar{\phi}_e$, also on $\Omega(e)$.

Proof. For $\boldsymbol{u} = \nabla\phi$ the parallel antiderivative is the path integral of a gradient. Specifically, (5.5) yields (5.13) with $\tilde{\phi}_e(\boldsymbol{x}) = \phi(X^k_e(\eta^k_e(0), \hat{x}^k_{\perp}))$ for $\boldsymbol{x} \in \Omega_k$, $k \in \mathcal{K}(e)$. For all $a \in [0, \hat{h}_e]$ the perpendicular antiderivative is also the path integral of a gradient, hence for interior and boundary edges, we have $\Phi^e_{\perp,a}(\boldsymbol{u})(\boldsymbol{x}) = \phi(\boldsymbol{x}) - \phi(\gamma^e_{\perp,0}(a))$ where $\gamma^e_{\perp,0}(a)$ is the starting point defined in (5.7). The result follows from the averaging formula (5.6), with $\bar{\phi}_e = \frac{1}{\hat{h}_e}\int_0^{\hat{h}_e} \phi(\gamma^e_{\perp,0}(a))\,\mathrm{d}a$. ∎

In the following lemma we study the stability of these edge antiderivative operators in L^p, and establish a local estimate for the resulting edge-correction terms involved in (2.10).

Lemma 5.4. *Let $\boldsymbol{u} \in L^p(\Omega)$, and $e \in \mathcal{E}$. For $d \in \{\parallel, \perp\}$, the bound*

$$\|\Phi^e_d(\boldsymbol{u})\|_{L^p(\omega_e)} \lesssim \|\boldsymbol{u}\|_{L^p(\omega_e)} \tag{5.15}$$

holds on any set of the form

$$\omega_e = \bigcup_{k \in \mathcal{K}(e)} F_k(\hat{\omega}^k_e) \quad \text{with} \quad \hat{\omega}^k_e = \hat{\Omega} \cap \hat{X}^k_e([0,1] \times [\hat{e}^k_{\perp} - \rho\hat{h}_e, \hat{e}^k_{\perp} + \rho\hat{h}_e])$$

and $1 \le \rho \lesssim 1$. In particular, (5.15) holds on $S^e = \bigcup_{j \in \mathcal{I}^e} S^e_j$ the union of the edge-based domains (4.11).

Moreover, the edge correction term $\tilde{\Pi}^1_e\boldsymbol{u} = \sum_{d \in \{\parallel,\perp\}} \nabla^e_d(P^e - I^e)\Pi^0_{\mathrm{pw}}\Phi^e_d(\boldsymbol{u})$ vanishes outside S^e, and it satisfies the local bound

$$\|\tilde{\Pi}^1_e\boldsymbol{u}\|_{L^p(S^e_j)} \lesssim \|\boldsymbol{u}\|_{L^p(E_e(S^e_j))} \tag{5.16}$$

on any domain S^e_j, $j \in \mathcal{I}^e$, with E_e the edge-based domain extension (4.12).

Proof. The bound (5.15) for the parallel direction ($d = \parallel$) is proven just like (5.2) since the parallel antiderivative operator coincides with the single-patch (5.1) along the parallel direction, up to a possible change in the curve starting point and orientation. For the perpendicular direction ($d = \perp$), we first consider the k^- patch and again work with the pullback $\hat{\Phi}^e_{\perp}(\hat{\boldsymbol{u}}^-)(\hat{\boldsymbol{x}}) := \Phi^e_{\perp}(\boldsymbol{u})(\boldsymbol{x})$ where $\hat{\boldsymbol{u}}^- := (\mathcal{F}^1_{k^-})^{-1}\boldsymbol{u}$. For simplicity, we assume an orientation corresponding to $\hat{X}^-_e = I$, i.e., $\hat{\boldsymbol{x}} = (\hat{x}_{\parallel}, \hat{x}_{\perp})$, and $\hat{e}^-_{\perp} = 0$, i.e. $\tilde{a} = a$. Note that this also yields $\hat{\omega}^-_e = [0,1] \times [0, \rho\hat{h}_e]$. Using Hölder inequalities we compute

$$\begin{aligned}
\|\hat{\Phi}^e_{\perp}(\hat{\boldsymbol{u}}^-)\|^p_{L^p(\hat{\omega}^-_e)} &= \iint_{\hat{\omega}^-_e} \frac{1}{\hat{h}^p_e}\left|\int_0^{\hat{h}_e}\left(\int_0^{\hat{x}_{\parallel}} \hat{u}^-_{\parallel}(z_{\parallel}, a)\,\mathrm{d}z_{\parallel} + \int_a^{\hat{x}_{\perp}} \hat{u}^-_{\perp}(\hat{x}_{\parallel}, z_{\perp})\,\mathrm{d}z_{\perp}\right)\mathrm{d}a\right|^p \mathrm{d}\hat{\boldsymbol{x}} \\
&\lesssim \iint_{\hat{\omega}^-_e} \frac{|\hat{x}_{\parallel}|^{p-1}}{\hat{h}_e}\int_0^{\hat{h}_e}\int_0^{\hat{x}_{\parallel}} |\hat{u}^-_{\parallel}(z_{\parallel}, a)|^p\,\mathrm{d}z_{\parallel}\,\mathrm{d}a\,\mathrm{d}\hat{\boldsymbol{x}} \\
&\qquad + \iint_{\hat{\omega}^-_e}\int_0^{\hat{h}_e}\frac{|\hat{x}_{\perp} - a|^{p-1}}{\hat{h}_e}\int_a^{\hat{x}_{\perp}} |\hat{u}^-_{\perp}(\hat{x}_{\parallel}, z_{\perp})|^p\,\mathrm{d}z_{\perp}\,\mathrm{d}a\,\mathrm{d}\hat{\boldsymbol{x}} \\
&\lesssim \rho\|\hat{u}^-_{\parallel}\|^p_{L^p(\hat{\omega}^-_e)} + (\rho\hat{h}_e)^p\|\hat{u}^-_{\perp}\|^p_{L^p(\hat{\omega}^-_e)} \lesssim \|\hat{\boldsymbol{u}}^-\|^p_{L^p(\hat{\omega}^-_e)}.
\end{aligned} \tag{5.17}$$

The last inequality follows by dropping the constants and using the fact that $\hat{h}_e \le 1$ (this estimate seems a bit rough, but it is enough to show (5.15) and we shall further localize it to establish (5.16)). The scaling relations (3.13) for 0-form and 1-form pullbacks yield then

$$\|\Phi^e_\perp(\boldsymbol{u})\|_{L^p(\omega_e^-)} \sim H^{2/p}_{k^-}\|\hat{\Phi}^e_\perp(\hat{\boldsymbol{u}}^-)\|_{L^p(\hat{\omega}_e^-)} \lesssim H^{2/p}_{k^-}\|\hat{\boldsymbol{u}}^-\|_{L^p(\hat{\omega}_e^-)} \lesssim \|\boldsymbol{u}\|_{L^p(\omega_e)}. \tag{5.18}$$

On the k^+ patch we also assume an orientation corresponding to $\hat{X}^+_e = I$, i.e. $\hat{\boldsymbol{x}} = (\hat{x}_\parallel, \hat{x}_\perp)$, and $\hat{e}^+_\perp = 0$. We first consider the 0-form pullback of the integral term $\delta\Phi^e_\perp$ (5.10), and compute

$$\begin{aligned}
\|\widehat{\delta\Phi}^e_\perp(\hat{\boldsymbol{u}}^+)\|^p_{L^p(\hat{\omega}_e^+)} &= \iint_{\hat{\omega}_e^+} \left| \int_0^{\hat{x}_\perp} \hat{u}^+_\perp(\hat{x}_\parallel, z_\perp)\,\mathrm{d}z_\perp \right|^p \mathrm{d}\hat{\boldsymbol{x}} \\
&\le |\rho\hat{h}_e|^{p-1} \iint_{\hat{\omega}_e^+} \int_0^{\hat{x}_\perp} |\hat{u}^+_\perp(\hat{x}_\parallel, z_\perp)|^p \,\mathrm{d}z_\perp\,\mathrm{d}\hat{\boldsymbol{x}} \\
&\le |\rho\hat{h}_e|^p \|\hat{u}^+_\perp\|^p_{L^p(\hat{\omega}_e^+)} \lesssim \|\hat{\boldsymbol{u}}^+\|^p_{L^p(\hat{\omega}_e^+)}.
\end{aligned} \tag{5.19}$$

We next write $\hat{\Phi}^{e,*}(\hat{\boldsymbol{u}}^-)(\hat{\boldsymbol{x}}) := \Phi^e_\perp(\boldsymbol{u})(\boldsymbol{p}_e(\boldsymbol{x}))$, with $\boldsymbol{x} = F_{k^+}(\hat{\boldsymbol{x}})$, the pullback of the coarse matching term in (5.10). With our simple orientation the matching point (5.11) is $\boldsymbol{p}_e(\boldsymbol{x}) := F_{k^+}(\hat{x}_\parallel, 0) = F_{k^-}(\eta_e(\hat{x}_\parallel), 0)$. Without loss of generality we further assume the same orientation: $\eta_e(z) = z$ so that $\hat{\omega}^-_e = \hat{\omega}^+_e$. Since $\hat{\Phi}^{e,*}(\hat{\boldsymbol{u}}^-)(\hat{\boldsymbol{x}})$ corresponds to the first term in (5.10), it is a path integral on the coarse patch, given by (5.9). We thus have

$$\begin{aligned}
\|\hat{\Phi}^{e,*}(\hat{\boldsymbol{u}}^-)\|^p_{L^p(\hat{\omega}_e^+)} &= \iint_{\hat{\omega}_e^+} |\hat{\Phi}^e_\perp(\hat{\boldsymbol{u}}^-)(\hat{x}_\parallel, 0)|^p \,\mathrm{d}\hat{\boldsymbol{x}} \\
&= \iint_{\hat{\omega}_e^-} \frac{1}{\hat{h}_e^p} \left| \int_0^{\hat{h}_e} \left(\int_0^{\hat{x}_\parallel} \hat{u}^-_\parallel(z_\parallel, a)\,\mathrm{d}z_\parallel + \int_a^0 \hat{u}^-_\perp(\hat{x}_\parallel, z_\perp)\,\mathrm{d}z_\perp \right) \mathrm{d}a \right|^p \mathrm{d}\hat{\boldsymbol{x}} \\
&\lesssim \iint_{\hat{\omega}_e^-} \frac{|\hat{x}_\parallel|^{p-1}}{\hat{h}_e} \int_0^{\hat{h}_e} \int_0^{\hat{x}_\parallel} |\hat{u}^-_\parallel(z_\parallel, a)|^p \,\mathrm{d}z_\parallel\,\mathrm{d}a\,\mathrm{d}\hat{\boldsymbol{x}} \\
&\qquad + \iint_{\hat{\omega}_e^-} \int_0^{\hat{h}_e} \int_a^0 |\hat{u}^-_\perp(\hat{x}_\parallel, z_\perp)|^p \,\mathrm{d}z_\perp\,\mathrm{d}a\,\mathrm{d}\hat{\boldsymbol{x}} \\
&\lesssim \rho\|\hat{u}^-_\parallel\|^p_{L^p(\hat{\omega}_e^-)} + (\rho\hat{h}_e)^p\|\hat{u}^-_\perp\|^p_{L^p(\hat{\omega}_e^-)} \lesssim \|\hat{\boldsymbol{u}}^-\|^p_{L^p(\hat{\omega}_e^-)}.
\end{aligned} \tag{5.20}$$

With (5.19) and the scaling relations (3.13), this bound yields

$$\begin{aligned}
\|\Phi^e_\perp(\boldsymbol{u})\|_{L^p(\omega_e^+)} &\le \|\delta\Phi^e_\perp(\boldsymbol{u})\|_{L^p(\omega_e^+)} + \|\Phi^e_\perp(\boldsymbol{u})(\boldsymbol{p}_e(\cdot))\|_{L^p(\omega_e^+)} \\
&\lesssim H^{2/p}_{k^+}(\|\widehat{\delta\Phi}^{e,+}_\perp(\hat{\boldsymbol{u}}^+)\|_{L^p(\hat{\omega}_e^+)} + \|\hat{\Phi}^{e,*}(\hat{\boldsymbol{u}}^-)\|_{L^p(\hat{\omega}_e^+)}) \\
&\lesssim H^{2/p}_{k^+}(\|\hat{\boldsymbol{u}}^+\|_{L^p(\hat{\omega}_e^+)} + \|\hat{\boldsymbol{u}}^-\|_{L^p(\hat{\omega}_e^-)}) \lesssim \|\boldsymbol{u}\|_{L^p(\omega_e)}.
\end{aligned}$$

Together with (5.18), this proves the stability (5.15) in the perpendicular case.

Turning to the local bound (5.16), we observe that the inverse estimate (3.6) yields

$$\|\nabla^e_d(P^e - I^e)\Pi^0_{\mathrm{pw}}\Phi^e_d(\boldsymbol{u})\|_{L^p(S^e_j)} \lesssim h_e^{-1}\|(P^e - I^e)\Pi^0_{\mathrm{pw}}\Phi^e_d(\boldsymbol{u})\|_{L^p(S^e_j)}. \tag{5.21}$$

The local stability of P^e, I^e and Π^0_{pw}, see (4.48), allows us to write

$$\|(P^e - I^e)\Pi^0_{\mathrm{pw}}\Phi^e_d(\boldsymbol{u})\|_{L^p(S^e_j)} \lesssim \|\Phi^e_d(\boldsymbol{u})\|_{L^p(E_e(S^e_j)}$$

so that (5.16) would follow from a bound like $\|\Phi^e_d(\boldsymbol{u})\|_{L^p(E_e(S^e_j))} \lesssim h_e\|\boldsymbol{u}\|_{L^p(E_e(S^e_j))}$. A difficulty is that the latter cannot hold a priori, indeed both antiderivative operators rely on integration curves that are not localized in a domain of the form $E_e(S^e_j)$. Therefore, a localizing argument is needed. For the parallel term ($d =\parallel$) we can use a similar argument as the one that we used to prove (5.3) for the single-patch antiderivative: indeed one may again change the integration constant in $\Phi^e_{\parallel}(\boldsymbol{u})$, without changing the function $\nabla^e_{\parallel}(P^e - I^e)\Pi^0_{\rm pw}\Phi^e_{\parallel}(\boldsymbol{u})$: here this is made possible because the invariance with respect to the parallel variable is preserved not only by $\Pi^0_{\rm pw}$ but also by P^e and I^e, see Lemma 4.7. As a result one can define a localized antiderivative

$$\tilde\Phi^e_{\parallel}(\boldsymbol{u})(\boldsymbol{x}) = \int_{\eta^k_e(\tilde x^k_j)}^{\hat x^k_{\parallel}} \hat u^k_{\parallel}(X^k_e(z, \hat x^k_{\perp}))\,{\rm d}z$$

with $\tilde x^k_j \in \hat S^-_j$ a curvilinear coordinate corresponding to the edge piece $e \cap S^e_j$: by Lemma 4.7 we have $\nabla^e_{\parallel}(P^e - I^e)\Pi^0_{\rm pw}\Phi^e_{\parallel}(\boldsymbol{u}) = \nabla^e_{\parallel}(P^e - I^e)\Pi^0_{\rm pw}\tilde\Phi^e_{\parallel}(\boldsymbol{u})$ and a local estimate for this antiderivative (derived exactly in the same way as for the single-patch antiderivative) gives $\|\tilde\Phi^e_d(\boldsymbol{u})\|_{L^p(E_e(S^e_j))} \le h_e\|\boldsymbol{u}\|_{L^p(E_e(S^e_j))}$. This shows that the local bound (5.16) holds indeed for the parallel term.

For the perpendicular term we cannot use a similar localizing argument, as none of the projection operators P^e or I^e preserve an invariance along the perpendicular direction. Fortunately our design for the integration curves involved in $\Phi^e_{\perp}$ yields the following localizing property:

$$\boldsymbol{u} = 0 \ \text{ on } \ E_e(S^e_j) \quad \implies \quad (P^e - I^e)\Pi^0_{\rm pw}\Phi^e_{\perp}(\boldsymbol{u}) = 0 \ \text{ on } \ S^e_j. \tag{5.22}$$

To establish this property we assume for simplicity that the edge e has the same orientation in both patches, i.e. $\eta^+_e(x_{\parallel}) = x_{\parallel}$, and recall that $E_e(S^e_j)$ is Cartesian on both patches, with parallel coordinate in the same interval as a result of being continuous across e. Let us denote by $\alpha_{\parallel}$ the minimal parallel coordinate in both patches, so that any $\boldsymbol{x} \in E_e(S^e_j)$ satisfies $\hat x_{\parallel} \ge \alpha_{\parallel}$. For all $a \in [0, \hat h_e]$, we then observe that the curve $\gamma = \gamma^e_{\perp}(\boldsymbol{x}, a)$ is made of two connected parts: a first part $\Gamma^e_1(\boldsymbol{x}, a)$ with parallel coordinate $\hat\gamma_{\parallel} \le \alpha_{\parallel}$ (and included in the coarse patch Ω_{k^-}), and a second part $\Gamma^e_2(\boldsymbol{x}, a)$ with parallel coordinate $\hat\gamma_{\parallel} > \alpha_{\parallel}$. Because $|\tilde a - \hat e^k_{\perp}| = a \le \hat h_e$, see (5.8), (4.20), this latter part is included in $E_e(S^e_j)$ while the first part $\Gamma^e_1(\boldsymbol{x}, a)$ is fully outside. Moreover, this first part is independent of $\boldsymbol{x}$: $\Gamma^e_1(\boldsymbol{x}, a) = \Gamma^e_1(a)$. As a consequence we find that if $\boldsymbol{u} = 0$ on $E_e(S^e_j)$, then the antiderivative writes

$$\Phi^e_{\perp,a}(\boldsymbol{u})(\boldsymbol{x}) = \int_{\Gamma^e_1(a)\cup\Gamma^e_2(\boldsymbol{x},a)} \boldsymbol{u}\cdot{\rm d}l = \int_{\Gamma^e_1(a)} \boldsymbol{u}\cdot{\rm d}l, \qquad \boldsymbol{x} \in E_e(S^e_j),$$

which, by integration over $a \in [0, \hat h_e]$ yields a constant value, say $\Phi^e_{\perp}(\boldsymbol{u}) = C(\boldsymbol{u})$ on $E_e(S^e_j)$. According to Lemma 4.1, this shows that on the edge piece $e \cap S^e_j$, $\Pi^0_{\rm pw}\Phi^e_{\perp}(\boldsymbol{u})$ takes the same constant value $C(\boldsymbol{u})$: in particular it is continuous across e. Consider now $\boldsymbol{x} \in S^e_j$: Using Lemma 4.5 and the fact that the projected point $\boldsymbol{p}_e(\boldsymbol{x})$ on the edge is also in S^e_j, we find that $(P^e - I^e)\Pi^0_{\rm pw}\Phi^e_{\perp}(\boldsymbol{u}) = 0$ on S^e_j. The property (5.22) hence follows: we have indeed shown that

$$\begin{aligned} \boldsymbol{u} = 0 \ \text{ on } \ E_e(S^e_j) \quad &\implies \quad \Phi^e_{\perp}(\boldsymbol{u}) = cst \ \text{ on } \ E_e(S^e_j) \\ &\implies \quad \Pi^0_{\rm pw}\Phi^e_{\perp}(\boldsymbol{u}) = cst \ \text{ on } \ e \cap S^e_j \\ &\implies \quad (P^e - I^e)\Pi^0_{\rm pw}\Phi^e_{\perp}(\boldsymbol{u}) = 0 \ \text{ on } \ S^e_j. \end{aligned}$$

For a general $\boldsymbol{u} \in L^p(\Omega)$ decomposed as $\boldsymbol{u} = \boldsymbol{u}\mathbb{1}_{E_e(S^e_j)} + \boldsymbol{u}(1 - \mathbb{1}_{E_e(S^e_j)})$, this yields

$$(P^e - I^e)\Pi^0_{\rm pw}\Phi^e_{\perp}(\boldsymbol{u})(\boldsymbol{x}) = (P^e - I^e)\Pi^0_{\rm pw}\Phi^e_{\perp}(\boldsymbol{u}\mathbb{1}_{E_e(S^e_j)})(\boldsymbol{x}) \qquad \text{for } \boldsymbol{x} \in S^e_j$$

and allows us to bound

$$\begin{aligned} \|(P^e - I^e)\Pi^0_{\rm pw}\Phi^e_{\perp}(\boldsymbol{u})\|_{L^p(S^e_j)} &= \|(P^e - I^e)\Pi^0_{\rm pw}\Phi^e_{\perp}(\boldsymbol{u}\mathbb{1}_{E_e(S^e_j)})\|_{L^p(S^e_j)} \\ &\lesssim \|\Phi^e_{\perp}(\boldsymbol{u}\mathbb{1}_{E_e(S^e_j)})\|_{L^p(E_e(S^e_j))} \end{aligned} \tag{5.23}$$

by using (4.48). To complete the proof we finally observe that in the last antiderivative the integration curve $\gamma^e_{\perp}(\boldsymbol{x}, a)$ can be restricted to $E_e(S^e_j)$ which is of diameter $\lesssim h_e$. By repeating the steps in (5.17) and (5.20) with such a localized integration over z, we find

$$\|\Phi^e_\perp(\boldsymbol{u}\mathbb{1}_{E_e(S^e_j)})\|_{L^p(E_e(S^e_j))} \lesssim h_e\|\boldsymbol{u}\mathbb{1}_{E_e(S^e_j)}\|_{L^p(E_e(S^e_j))} = h_e\|\boldsymbol{u}\|_{L^p(E_e(S^e_j))}.$$

Together with (5.21) and (5.23) this proves the local bound (5.16) for the perpendicular term, and completes the proof. ∎

5.3. Vertex-based antiderivative operators

The vertex-based antiderivative $\Phi^{\boldsymbol{v}}(\boldsymbol{u})$ is defined on the patches contiguous to $\boldsymbol{v}$ in a similar way as the perpendicular edge-based antiderivative $\Phi^e_\perp$ from Section 5.2. Like the latter it involves an averaging step

$$\Phi^{\boldsymbol{v}}(\boldsymbol{u}) = \frac{1}{\hat{h}_{\boldsymbol{v}}}\int_0^{\hat{h}_{\boldsymbol{v}}} \Phi^{\boldsymbol{v}}_a(\boldsymbol{u})\,\mathrm{d}a, \qquad \Phi^{\boldsymbol{v}}_a(\boldsymbol{u})(\boldsymbol{x}) = \int_{\gamma^{\boldsymbol{v}}(\boldsymbol{x},a)} \boldsymbol{u}\cdot \mathrm{d}l \tag{5.24}$$

with $\hat{h}_{\boldsymbol{v}}$ defined in (4.21), and parameter-dependent integration curves $\gamma^{\boldsymbol{v}}(\boldsymbol{x}, a)$ of the same form as the curves $\gamma^e_\perp(\boldsymbol{x}, a)$ described in Section 5.2. Observe that in this construction, each curve was fully characterized by the central edge e, the choice of a coarse $(k^-(e))$ and a fine $(k^+(e))$ patch around e, and finally the choice of a starting edge on the coarse patch $k^-(e)$, where the starting points are located. To define the curves $\gamma^{\boldsymbol{v}}(\boldsymbol{x}, a)$ we can then specify these elements for each vertex, and for this we will use the decomposition (3.33) of the contiguous patches $k \in \mathcal{K}(\boldsymbol{v})$ in one or two sequences of adjacent nested patches $k = k^s_i(\boldsymbol{v})$ with $s \in \{l, r\}$ and $1 \le i \le n(\boldsymbol{v}, s)$. An illustration is provided in Figure 5.2 for interior vertices, and Figure 5.3 for boundary vertices.

On the two patches of a complete sequence, namely for $\boldsymbol{x} \in \Omega_k$ with $k = k^s_i(\boldsymbol{v})$ such that $n(\boldsymbol{v}, s) = 2$, we define the curve $\gamma^{\boldsymbol{v}}(\boldsymbol{x}, a)$ by taking (i) the edge $e = e^s(\boldsymbol{v})$ shared by the two patches $k^s_1(\boldsymbol{v})$ and $k^s_2(\boldsymbol{v})$ as the central edge, (ii) these respective patches as the coarse and fine patches associated with edge e, and finally (iii) the second edge contiguous to $\boldsymbol{v}$ in $k^s_1(\boldsymbol{v})$ as the starting edge for the curves. Note that if both patches adjacent to e have the same resolution, then it is possible that $k^s_1(\boldsymbol{v}) = k^+(e)$ and $k^s_2(\boldsymbol{v}) = k^-(e)$: in other words the orientation used to define the antiderivatives $\Phi^e_\perp$ and $\Phi^{\boldsymbol{v}}$ do not need to match. This covers the case of interior vertices, since their contiguous patches can always be decomposed in two complete sequences.

For the case of boundary vertices associated with single-patch sequences, namely for $\boldsymbol{x} \in \Omega_k$ with $k = k^s_1(\boldsymbol{v})$ such that $n(\boldsymbol{v}, s) = 1$, we observe that Ω_k has at least one edge contiguous to $\boldsymbol{v}$ which is a boundary edge $\partial\Omega$, say $e^s_b(\boldsymbol{v})$: we take this edge as the central edge e. Furthermore, we take the patch $k^s_1(\boldsymbol{v})$ as the coarse patch (no fine patch is involved here) and the second edge contiguous to $\boldsymbol{v}$ as the starting edge for the curves $\gamma^e_\perp(\boldsymbol{x}, a)$: we may denote this edge as $e^*(\boldsymbol{v})$, indeed if a second sequence of patches exists for $\boldsymbol{v}$ then this starting edge must be shared by $k^l_1(\boldsymbol{v})$ and $k^r_1(\boldsymbol{v})$.

The construction is then similar to what we had for the antiderivative $\Phi^e_\perp$: for interior vertices and boundary vertices, all the curves $\gamma^{\boldsymbol{v}}(\boldsymbol{x}, a)$, $\boldsymbol{x} \in \Omega(\boldsymbol{v})$, have a unique starting point $\gamma^{\boldsymbol{v}}_0(a)$ lying on the coarse edge $e^*(\boldsymbol{v})$ and at a logical distance a from the vertex $\boldsymbol{v}$.

This antiderivative operator satisfies several properties which can be directly inferred from those of the perpendicular edge antiderivative. The first one is similar to (5.14) and will be useful to prove commuting properties.

Lemma 5.5. *Let $\boldsymbol{v} \in \mathcal{V}$ be a vertex and $\boldsymbol{u} = \nabla\phi$ with $\phi \in C^1(\overline{\Omega})$. The equality*

$$\Phi^{\boldsymbol{v}}(\boldsymbol{u})(\boldsymbol{x}) = \phi(\boldsymbol{x}) - \phi^{\boldsymbol{v}}_0 \tag{5.25}$$

holds for all $\boldsymbol{x} \in \Omega(\boldsymbol{v})$, with a constant $\phi^{\boldsymbol{v}}_0 := \frac{1}{\hat{h}_{\boldsymbol{v}}}\int_0^{\hat{h}_{\boldsymbol{v}}} \phi(\gamma^{\boldsymbol{v}}_0(a))\,\mathrm{d}a$.

The second property is a local L^p stability estimate.

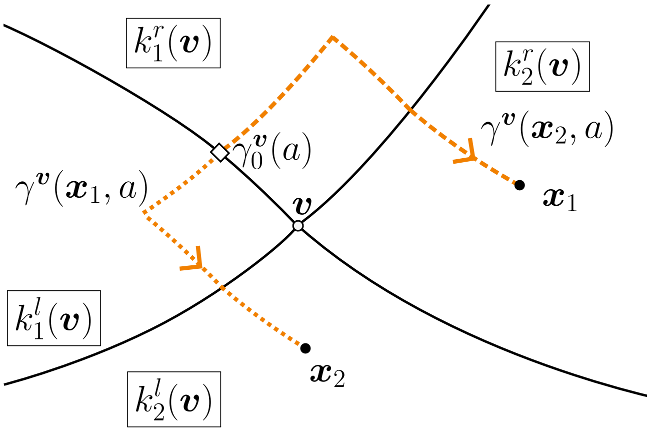

Figure 5.2. Integration paths $\gamma^{\boldsymbol{v}}(\boldsymbol{x}, a)$ for different points $\boldsymbol{x}_1$ and $\boldsymbol{x}_2$ involved in the vertex-based antiderivative operator $\Phi_a^{\boldsymbol{v}}$, for a given averaging parameter $a \in (0, \hat{h}_{\boldsymbol{v}})$. The common starting point $\gamma_0^{\boldsymbol{v}}(a)$ is represented by a white square.

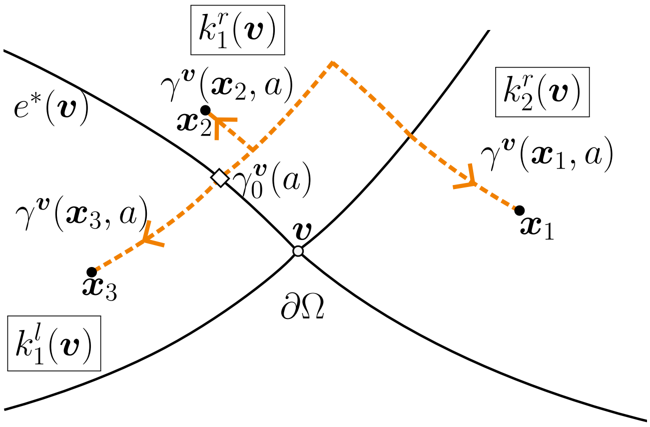

Figure 5.3. Integration paths $\gamma^{\boldsymbol{v}}(\boldsymbol{x}, a)$ defining the vertex-based antiderivative operators $\Phi^{\boldsymbol{v}}(\boldsymbol{u})$ for boundary vertices. Integration curves connect every $\boldsymbol{x} \in \Omega(\boldsymbol{v})$ to a common starting point $\gamma_0^{\boldsymbol{v}}(a)$.

Lemma 5.6. *For $\boldsymbol{u} \in L^p(\Omega)$, the bound*

$$\|\Phi^{\boldsymbol{v}}(\boldsymbol{u})\|_{L^p(S^{\boldsymbol{v}})} \lesssim h_{\boldsymbol{v}} \|\boldsymbol{u}\|_{L^p(S^{\boldsymbol{v}})}$$

holds on the vertex domain defined in (4.18)*.*

Proof. This estimate relies on two arguments. The first one is that for all $\boldsymbol{x} \in S^{\boldsymbol{v}}$ and all $a \in [0, \hat{h}_{\boldsymbol{v}}]$, the integration curve $\gamma^{\boldsymbol{v}}(\boldsymbol{x}, a)$ is contained in $S^{\boldsymbol{v}}$: this follows from the structure of $S^{\boldsymbol{v}}$ and the fact that $\hat{h}_{\boldsymbol{v}}$ defined in (4.21) is the minimal diameter of the edge-based supports that compose $S^{\boldsymbol{v}}$, see (4.18). The second argument is a bound similar to the one derived in (5.15) for the perpendicular case, as the integration curves $\gamma^{\boldsymbol{v}}(\boldsymbol{x}, a)$ are of the same form. Here no further localization argument is needed thanks to the inclusion $\gamma^{\boldsymbol{v}}(\boldsymbol{x}, a) \subset S^{\boldsymbol{v}}$, so that the desired bound simply follows from the fact that $S^{\boldsymbol{v}}$ is of diameter $\sim h_{\boldsymbol{v}}$. ∎

Lemma 5.7. *Let $\boldsymbol{u} \in L^p(\Omega)$. The vertex term $\tilde{\Pi}^1_{\boldsymbol{v}}\boldsymbol{u} = \nabla_{\rm pw}(P^{\boldsymbol{v}} - \bar{I}^{\boldsymbol{v}})\Pi^0_{\rm pw}\Phi^{\boldsymbol{v}}(\boldsymbol{u})$ vanishes outside $S^{\boldsymbol{v}}$, and it satisfies the local bound*

$$\|\tilde{\Pi}^1_{\boldsymbol{v}}\boldsymbol{u}\|_{L^p(S^{\boldsymbol{v}})} \lesssim \|\boldsymbol{u}\|_{L^p(S^{\boldsymbol{v}})}.$$

Proof. The first statement simply follows from the form of $P^{\boldsymbol{v}}$ and $\bar{I}^{\boldsymbol{v}}$, see (4.28)–(4.29), and the fact that $\Lambda^{\boldsymbol{v}}$ vanishes outside $S^{\boldsymbol{v}}$. To prove the local bound we use the inverse estimate (3.6) together with the stability bound (4.49) from Lemma 4.8, with $Q^{\boldsymbol{v}} = P^{\boldsymbol{v}}$ or $\bar{I}^{\boldsymbol{v}}$: for all $\phi \in L^p(\Omega)$, this gives

$$\|\nabla_{\rm pw}Q^{\boldsymbol{v}}\Pi^0_{\rm pw}\phi\|_{L^p(S^{\boldsymbol{v}})} \lesssim h_{\boldsymbol{v}}^{-1}\|Q^{\boldsymbol{v}}\Pi^0_{\rm pw}\phi\|_{L^p(S^{\boldsymbol{v}})} \lesssim h_{\boldsymbol{v}}^{-1}\|\phi\|_{L^p(S^{\boldsymbol{v}})}. \tag{5.26}$$

Setting $\phi = \Phi^{\boldsymbol{v}}(\boldsymbol{u})$, we find

$$\|\nabla_{\rm pw}(P^{\boldsymbol{v}} - \bar{I}^{\boldsymbol{v}})\Pi^0_{\rm pw}\Phi^{\boldsymbol{v}}(\boldsymbol{u})\|_{L^p(S^{\boldsymbol{v}})} \lesssim h_{\boldsymbol{v}}^{-1}\|\Phi^{\boldsymbol{v}}(\boldsymbol{u})\|_{L^p(S^{\boldsymbol{v}})} \lesssim \|\boldsymbol{u}\|_{L^p(S^{\boldsymbol{v}})}$$

where the last step follows from Lemma 5.6. ■

The next result will be useful to show projection properties.

Lemma 5.8. *If $\boldsymbol{u} \in V^1_h$, then*

- *$\Phi^k_d(\boldsymbol{u})$ belongs to the broken space $V^0_{\rm pw}$,*
- *for all $e \in \mathcal{E}$, $\Phi^e_{\parallel}(\boldsymbol{u})$ and $\Phi^e_{\perp}(\boldsymbol{u})$ belong to $V^0_{\rm pw}$,*
- *if e is an interior edge, $\Phi^e_{\parallel}(\boldsymbol{u})$ and $\Phi^e_{\perp}(\boldsymbol{u})$ are continuous across e,*
- *for all $\boldsymbol{v} \in \mathcal{V}$, $\Phi^{\boldsymbol{v}}(\boldsymbol{u})$ belongs to $V^0_{\rm pw}$ and is continuous across every $e \in \mathcal{E}(\boldsymbol{v})$.*

Proof. Let us first verify that when $\boldsymbol{u} \in V^1_{\rm pw}$, all its antiderivatives belong to $V^0_{\rm pw}$. In the single-patch and edge-parallel cases this is easily verified by observing that in (5.1) and (5.5) the (logical) integration is performed along the same dimension $\hat{x}_d$ as the integrated component $\hat{u}^k_d$. Since $\hat{u}^k$ is in the logical space $\hat{V}^1_k$ given by (3.2) we find that the logical antiderivative belongs to $\hat{V}^0_k$ indeed. In the edge-perpendicular case one must consider two cases, depending on whether $\boldsymbol{x}$ is in a patch Ω_k of coarse ($k = k^-(e)$) or fine type ($k = k^+(e)$). In the former case the logical antiderivative is given by the sum (5.9) where we see that each integral belongs to $\hat{V}^0_{k^-(e)}$ for the same reason as above (this holds for each value of a, and hence also after integration over a). In the latter case the logical antiderivative is a sum (5.10) where the second term is a logical integral (5.12) that clearly belongs to $\hat{V}^0_k$ (again for the same reason as above), and the first term is the restriction of a coarse antiderivative on the edge e. Therefore, as a function of the parallel variable $\hat{x}^k_{\parallel}$ it belongs to $\mathbb{V}^0_{k^-(e)}$, hence also to $\mathbb{V}^0_k$ due to the nestedness Assumption (3.24), and finally to $\hat{V}^0_k$ as a function of $\hat{\boldsymbol{x}}$. In the vertex case we can use the same argument, since vertex antiderivatives take locally the same form as edge-perpendicular antiderivatives. To see that these antiderivatives are continuous across the respective edges for $\boldsymbol{u} \in V^1_h$, we fix again a and observe that in each case, the corresponding integration curves depend continuously on $\boldsymbol{x}$ (in the Hausdorff distance between curves). For perpendicular curves crossing an interface this is enough to show the continuity of the antiderivative, and for parallel curves close to an interface the continuity follows from the continuity of the tangential component of the curl-conforming, piecewise continuous field $\boldsymbol{u}$. ■

5.4. **Edge-vertex antiderivative operators**

Given $\boldsymbol{v} \in \mathcal{V}$ and $e \in \mathcal{E}(\boldsymbol{v})$, the edge-vertex correction term from (2.10) involves two additional antiderivative operators defined on the domain $\Omega(e)$: a parallel one defined as

$$\Phi_{\parallel}^{e,\boldsymbol{v}}(\boldsymbol{u}) \coloneqq \Phi^{\boldsymbol{v}}(\boldsymbol{u}) \tag{5.27}$$

see (5.24), and a perpendicular one defined as

$$\Phi_{\perp}^{e,\boldsymbol{v}}(\boldsymbol{u}) \coloneqq \Phi_{\perp}^{e}(\boldsymbol{u}) \tag{5.28}$$

see (5.9)–(5.11).

Lemma 5.9. *Let $\boldsymbol{u} \in L^p(\Omega)$. For any $\boldsymbol{v} \in \mathcal{V}$ and $e \in \mathcal{E}(\boldsymbol{v})$, the edge-vertex correction $\tilde{\Pi}^1_{e,\boldsymbol{v}}\boldsymbol{u} = \sum_{d\in\{\parallel,\perp\}} \nabla^e_d(\bar{I}^e_{\boldsymbol{v}} - P^e_{\boldsymbol{v}})\Pi^0_{\mathrm{pw}}\Phi^{\boldsymbol{v},e}_d(\boldsymbol{u})$ vanishes outside $S^{\boldsymbol{v}} \cap \Omega(e)$, and it satisfies the local bound*

$$\|\tilde{\Pi}^1_{e,\boldsymbol{v}}\boldsymbol{u}\|_{L^p(S^{\boldsymbol{v}})} \lesssim \|\boldsymbol{u}\|_{L^p(S^{\boldsymbol{v}})}. \tag{5.29}$$

Remark 5.10. If e is a boundary edge, we know from Lemma 4.6 that $\bar{I}^e_{\boldsymbol{v}} = P^e_{\boldsymbol{v}}$, hence $\tilde{\Pi}^1_{e,\boldsymbol{v}} = 0$. Thus, we may consider only interior edges in the proof of Lemma 5.9.

Proof. The first statement is proven as in Lemma 5.7, using the fact that $\bar{I}^e_{\boldsymbol{v}}$ and $P^e_{\boldsymbol{v}}$ involve functions $\Lambda^e_{\boldsymbol{v}}$ which vanish outside $S^{\boldsymbol{v}} \cap \Omega(e)$, see (4.31)–(4.32) and (4.18). We next argue as for the bound (5.26) in the proof of Lemma 5.7, using here Lemma 4.8 with $Q^{\boldsymbol{v}} = P^e_{\boldsymbol{v}}$ and $\bar{I}^e_{\boldsymbol{v}}$: this allows us to write

$$\|\nabla^e_d(\bar{I}^e_{\boldsymbol{v}} - P^e_{\boldsymbol{v}})\Pi^0_{\mathrm{pw}}\Phi^{e,\boldsymbol{v}}_d(\boldsymbol{u})\|_{L^p(S^{\boldsymbol{v}})} \lesssim h^{-1}_{\boldsymbol{v}}\|\Phi^{e,\boldsymbol{v}}_d(\boldsymbol{u})\|_{L^p(S^{\boldsymbol{v}})}$$

for both the parallel and the perpendicular cases. In the parallel case where $\Phi^{e,\boldsymbol{v}}_{\parallel}(\boldsymbol{u}) = \Phi^{\boldsymbol{v}}(\boldsymbol{u})$, the proof is completed with the local bound of Lemma 5.6. In the perpendicular case where $\Phi^{e,\boldsymbol{v}}_{\perp}(\boldsymbol{u}) \coloneqq \Phi^e_{\perp}(\boldsymbol{u})$, we need a localizing argument similar to the one used to prove (5.16). Here the localizing property reads

$$\boldsymbol{u} = 0 \;\text{ on }\; S^{\boldsymbol{v}} \quad\implies\quad (\bar{I}^e_{\boldsymbol{v}} - P^e_{\boldsymbol{v}})\Pi^0_{\mathrm{pw}}\Phi^{e,\boldsymbol{v}}_{\perp}(\boldsymbol{u}) = 0$$

and the argument goes as follows: we first observe that for $\boldsymbol{x} \in S^{\boldsymbol{v}} \cap \Omega(e)$ and $a \in [0, \hat{h}_e]$, the curve $\gamma^e_{\perp}(\boldsymbol{x}, a)$ may have a piece outside $S^{\boldsymbol{v}}$ (in particular if the starting point $\gamma^e_{\perp,0}(\boldsymbol{x}, a)$ is not on an edge contiguous to $\boldsymbol{v}$) but this piece is the same (a logical line parallel to e) for all $\boldsymbol{x} \in S^{\boldsymbol{v}} \cap \Omega(e)$. From this we infer that if $\boldsymbol{u} = 0$ on $S^{\boldsymbol{v}}$, then the averaged integral $\Phi^{e,\boldsymbol{v}}_{\perp}(\boldsymbol{u}) = \Phi^e_{\perp}(\boldsymbol{u})$ takes a constant value on $S^{\boldsymbol{v}} \cap \Omega(e)$. In particular, it takes the same constant value on both domains $S^k_{\boldsymbol{i}^k(\boldsymbol{v})}$, $k = k^{\pm}(e)$, see (4.19), and as a consequence the corresponding coefficients $\phi^k_{\boldsymbol{i}^k(\boldsymbol{v})}$ of the broken projection $\phi = \Pi^0_{\mathrm{pw}}\Phi^{e,\boldsymbol{v}}_{\perp}(\boldsymbol{u})$ are the same for both $k = k^{\pm}(e)$. According to Lemma 4.6, this implies that $(\bar{I}^e_{\boldsymbol{v}} - P^e_{\boldsymbol{v}})\phi = 0$. Thus, we have shown that

$$\begin{aligned}
\boldsymbol{u} = 0 \;\text{ on }\; S^{\boldsymbol{v}} \quad &\implies\quad \Phi^{e,\boldsymbol{v}}_{\perp}(\boldsymbol{u}) = cst \;\text{ on }\; S^{\boldsymbol{v}} \cap \Omega(e) \\
&\implies\quad \Pi^0_{\mathrm{pw}}\Phi^{e,\boldsymbol{v}}_{\perp}(\boldsymbol{u})|_{\Omega^-(\boldsymbol{v})} = \Pi^0_{\mathrm{pw}}\Phi^{e,\boldsymbol{v}}_{\perp}(\boldsymbol{u})|_{\Omega_{k^+}(\boldsymbol{v})} \\
&\implies\quad (\bar{I}^e_{\boldsymbol{v}} - P^e_{\boldsymbol{v}})\Pi^0_{\mathrm{pw}}\Phi^{e,\boldsymbol{v}}_{\perp}(\boldsymbol{u}) = 0.
\end{aligned}$$

This localization property is then used as in the proof of (5.16). Here, the steps are

$$\begin{aligned}
\|(\bar{I}^e_{\boldsymbol{v}} - P^e_{\boldsymbol{v}})\Pi^0_{\mathrm{pw}}\Phi^{e,\boldsymbol{v}}_{\perp}(\boldsymbol{u})\|_{L^p(S^{\boldsymbol{v}})} &= \|(\bar{I}^e_{\boldsymbol{v}} - P^e_{\boldsymbol{v}})\Pi^0_{\mathrm{pw}}\Phi^{e,\boldsymbol{v}}_{\perp}(\boldsymbol{u}\mathbb{1}_{S^{\boldsymbol{v}}})\|_{L^p(S^{\boldsymbol{v}})} \\
&\lesssim \|\Phi^{e,\boldsymbol{v}}_{\perp}(\boldsymbol{u}\mathbb{1}_{S^{\boldsymbol{v}}})\|_{L^p(S^{\boldsymbol{v}})} \\
&\lesssim h_{\boldsymbol{v}}\|\boldsymbol{u}\|_{L^p(S^{\boldsymbol{v}})}
\end{aligned}$$

which, using an inverse estimate for $\nabla^e_{\perp}$ as above, allows us to complete the proof. ∎

5.5. Bivariate antiderivative operators

Our projection operator on V_h^2 involves bivariate antiderivative operators defined on functions $f \in L^p(\Omega)$. The first one is a single-patch antiderivative defined as

$$\Psi^k(f)(\boldsymbol{x}) := \int_0^{\hat{x}_1} \int_0^{\hat{x}_2} \hat{f}^k(z_1, z_2) \,\mathrm{d}z_2 \,\mathrm{d}z_1, \qquad \boldsymbol{x} \in \Omega_k,\ k \in \mathcal{K}, \tag{5.30}$$

where $\hat{f}^k := (\mathcal{F}_k^2)^{-1}(f|_{\Omega_k})$ is the 2-form pullback of f on the patch k. Outside Ω_k, we extend $\Psi^k(f)$ by zero.

The second one is an edge-based bivariate antiderivative defined as

$$\Psi^e(f)(\boldsymbol{x}) := \frac{1}{\hat{h}_e} \int_0^{\hat{h}_e} \iint_{\sigma^e(\boldsymbol{x},a)} f(\boldsymbol{z}) \,\mathrm{d}\boldsymbol{z} \,\mathrm{d}a, \qquad \boldsymbol{x} \in \Omega(e),\ e \in \mathcal{E} \tag{5.31}$$

(and $\Psi^e(f)(\boldsymbol{x}) := 0$ for $\boldsymbol{x} \notin \Omega(e)$) where $\sigma^e(\boldsymbol{x}, a) \subset \Omega(e)$ is the oriented surface whose boundary is the algebraic sum of three oriented curves,

$$\partial\sigma^e(\boldsymbol{x}, a) = \gamma_\perp^e(\boldsymbol{x}, a) - \gamma_\parallel^e(\boldsymbol{x}) + \tilde{\gamma}^e(\boldsymbol{x}, a).$$

Here $\gamma_\perp^e(\boldsymbol{x}, a)$ and $\gamma_\parallel^e(\boldsymbol{x})$ are the curves associated with the perpendicular and parallel edge-based antiderivatives in Section 5.2, while $\tilde{\gamma}^e(\boldsymbol{x}, a)$ is a closing curve following the edges of $\Omega(e)$.

An illustration is given in Figure 5.4-(a) for an interior edge e: For $\boldsymbol{x} \in \Omega_k$ and $k \in \mathcal{K}(e)$, we remind that $\gamma_\perp^e(\boldsymbol{x}, a)$ connects the point $\gamma_{\perp,0}^e(a)$, see (5.7), to $\boldsymbol{x}$, while $-\gamma_\parallel^e(\boldsymbol{x})$ connects the point $\boldsymbol{x}$ to $\gamma_{\parallel,0}^e(\boldsymbol{x})$. Since the starting point $\gamma_{\perp,0}^e(a)$ is on the edge $e_0^- := X_e^-(0, [0,1])$ and $\gamma_{\parallel,0}^e(\boldsymbol{x}) = X_e^k(\eta_e^k(0), \hat{x}_\perp^k)$ is on the edge $e_0^k := X_e^k(\eta_e^k(0), [0,1])$, we see that it is indeed possible to connect $\gamma_{\parallel,0}^e(\boldsymbol{x})$ to $\gamma_{\perp,0}^e(a)$ with a curve $\tilde{\gamma}^e(\boldsymbol{x}, a)$ that is included in the edges e_0^k, $k \in \mathcal{K}(e)$.

The third bivariate antiderivative is of edge-vertex type:

$$\Psi^{e,\boldsymbol{v}}(f)(\boldsymbol{x}) := \int_0^1 \iint_{\sigma^{e,\boldsymbol{v}}(\boldsymbol{x},\bar{a})} f(\boldsymbol{z}) \,\mathrm{d}\boldsymbol{z} \,\mathrm{d}\bar{a}, \qquad \boldsymbol{x} \in \Omega(e),\ \boldsymbol{v} \in \mathcal{V},\ e \in \mathcal{E}(\boldsymbol{v}) \tag{5.32}$$

(and $\Psi^{e,\boldsymbol{v}}(f)(\boldsymbol{x}) := 0$ for $\boldsymbol{x} \notin \Omega(e)$) where $\sigma^{e,\boldsymbol{v}}(\boldsymbol{x}, \bar{a})$ is the domain whose boundary is again the algebraic sum of three oriented curves, namely

$$\partial\sigma^{e,\boldsymbol{v}}(\boldsymbol{x}, \bar{a}) = \gamma_\perp^e(\boldsymbol{x}, \hat{h}_e\bar{a}) - \gamma^{\boldsymbol{v}}(\boldsymbol{x}, \hat{h}_{\boldsymbol{v}}\bar{a}) + \tilde{\gamma}^{e,\boldsymbol{v}}(\bar{a}).$$

Here $\gamma_\perp^e(\boldsymbol{x}, \hat{h}_e\bar{a})$ is the curve associated with the perpendicular edge-based antiderivative, it connects as above the point $\gamma_{\perp,0}^e(\hat{h}_e\bar{a})$ (defined by (5.7)) to $\boldsymbol{x}$, $-\gamma^{\boldsymbol{v}}(\boldsymbol{x}, \hat{h}_{\boldsymbol{v}}\bar{a})$ is the curve associated with the vertex-based antiderivative and $\boldsymbol{x}$ to the point $\gamma_0^{\boldsymbol{v}}(\hat{h}_{\boldsymbol{v}}\bar{a})$, and finally $\tilde{\gamma}^{e,\boldsymbol{v}}(\bar{a})$ is the curve that connects $\gamma_0^{\boldsymbol{v}}(\hat{h}_{\boldsymbol{v}}\bar{a})$ to $\gamma_{\perp,0}^e(\hat{h}_e\bar{a})$ and is included in the edges of the patches contiguous to $\boldsymbol{v}$. Observe that the latter curve does not depend on $\boldsymbol{x}$. An illustration is given in Figure 5.4-(b), again for an interior edge e.

Notice that contrary to the configurations depicted in Figure 5.4, the domain $\sigma^{e,\boldsymbol{v}}(\boldsymbol{x}, \bar{a})$ may be disjoint from $\boldsymbol{x}$, and even from the patch Ω_k containing $\boldsymbol{x}$: this may happen for instance in the case where $k = k^+(e)$, with starting points $\gamma_{\perp,0}^e(\hat{h}_e\bar{a})$ and $\gamma_0^{\boldsymbol{v}}(\hat{h}_{\boldsymbol{v}}\bar{a})$ located on the same edge $e' \neq e$ of $\Omega_{k^-(e)}$: in this case some parts of the curves $\gamma_\perp^e(\boldsymbol{x}, \hat{h}_e\bar{a})$ and $\gamma^{\boldsymbol{v}}(\boldsymbol{x}, \hat{h}_{\boldsymbol{v}}\bar{a})$ cancel each other, and the domain $\sigma^{e,\boldsymbol{v}}(\boldsymbol{x}, \bar{a})$ is in the patch $\Omega_{k^-(e)}$. Precisely it is the (mapped) Cartesian domain bounded by the two starting points in the direction perpendicular to e, and by e' and (the parallel coordinate of) $\boldsymbol{x}$ in the direction parallel to e.

The following properties will be useful.

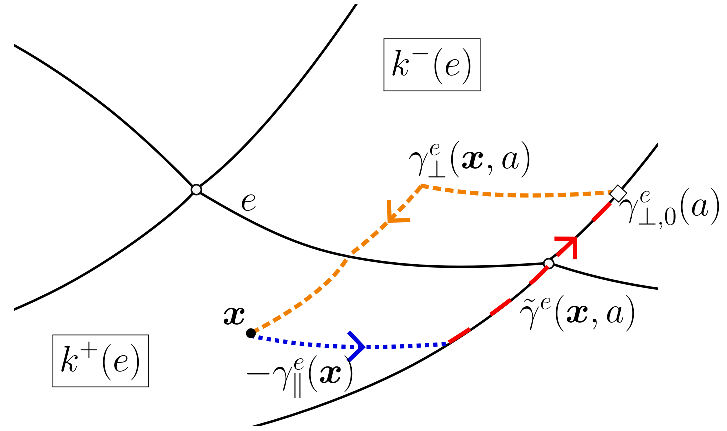

(A) edge case

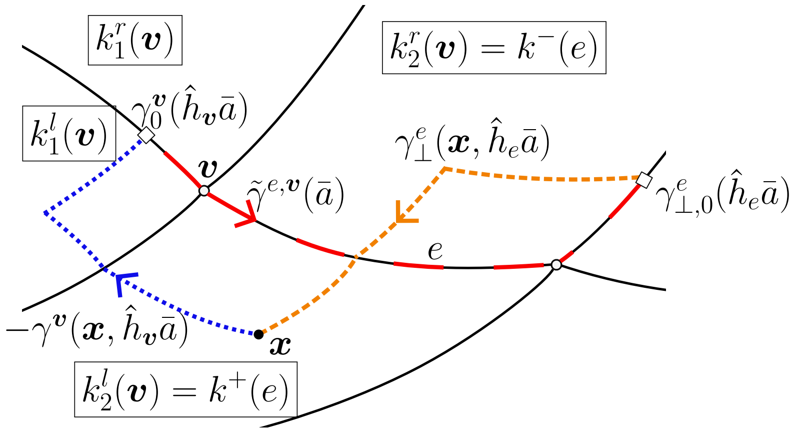

(B) edge-vertex case

FIGURE 5.4. Oriented curves delimiting the integration domains $\sigma^e(\boldsymbol{x}, a)$ (top) and $\sigma^{e,\boldsymbol{v}}(\boldsymbol{x}, \bar a)$ (bottom) involved in the bivariate antiderivative operators Ψ^e and $\Psi^{e,\boldsymbol{v}}$. On the top panel the curves for the edge-based antiderivative Ψ^e are shown for a given averaging parameter $a \in (0, \hat h_e)$ with starting point $\gamma^e_{\perp,0}(a)$ represented by a white square as in Figure 5.1. On the bottom panel the curves of the edge-vertex antiderivative $\Psi^{e,\boldsymbol{v}}$ are shown, for a given averaging parameter $\bar a \in (0,1)$. Again, we denote the starting points $\gamma^e_{\perp,0}(\hat h_e \bar a)$ and $\gamma^{\boldsymbol{v}}_0(\hat h_{\boldsymbol{v}} \bar a)$ of the respective perpendicular edge-based and vertex based antiderivative integration curves by white squares, as in Figure 5.1 and 5.2.

Lemma 5.11. *For $\boldsymbol{u} \in C^1(\overline{\Omega})$, $e \in \mathcal{E}$, $\boldsymbol{v} \in \mathcal{V}(e)$, we have*

$$\Psi^e(\operatorname{curl} \boldsymbol{u}) = \Phi^e_\perp(\boldsymbol{u}) - \Phi^e_\parallel(\boldsymbol{u}) + \tilde\Phi^e(\boldsymbol{u}) \quad \text{with} \quad \tilde\Phi^e(\boldsymbol{u})(\boldsymbol{x}) := \frac{1}{\hat h_e}\int_0^{\hat h_e}\int_{\tilde\gamma^e(\boldsymbol{x},a)} \boldsymbol{u}\cdot \mathrm{d}l\, \mathrm{d}a$$

and

$$\Psi^{e,\boldsymbol{v}}(\operatorname{curl} \boldsymbol{u}) = \Phi^{e,\boldsymbol{v}}_\perp(\boldsymbol{u}) - \Phi^{e,\boldsymbol{v}}_\parallel(\boldsymbol{u}) + \tilde\Phi^{e,\boldsymbol{v}}(\boldsymbol{u}) \quad \text{with} \quad \tilde\Phi^{e,\boldsymbol{v}}(\boldsymbol{u})(\boldsymbol{x}) := \int_0^1 \int_{\tilde\gamma^{e,\boldsymbol{v}}(\bar a)} \boldsymbol{u}\cdot \mathrm{d}l\, \mathrm{d}\bar a.$$

Moreover, the following relations holds:

$$\nabla^e_\parallel \tilde\Phi^e(\boldsymbol{u}) = 0 \qquad \text{and} \qquad \nabla_{\mathrm{pw}} \tilde\Phi^{e,\boldsymbol{v}}(\boldsymbol{u}) = 0. \tag{5.33}$$

Proof. By Stokes theorem, we have

$$\iint_{\sigma^e(\boldsymbol{x},a)} \operatorname{curl} \boldsymbol{u}(\boldsymbol{z})\, \mathrm{d}\boldsymbol{z} = \int_{\gamma_\perp^e(\boldsymbol{x},a)} \boldsymbol{u} \cdot \mathrm{d}l - \int_{\gamma_\parallel^e(\boldsymbol{x})} \boldsymbol{u} \cdot \mathrm{d}l + \int_{\tilde{\gamma}^e(\boldsymbol{x},a)} \boldsymbol{u} \cdot \mathrm{d}l$$

which, after averaging over a, shows the first equation, and

$$\iint_{\sigma^{e,\boldsymbol{v}}(\boldsymbol{x},\bar{a})} \operatorname{curl} \boldsymbol{u}(\boldsymbol{z})\, \mathrm{d}\boldsymbol{z} = \int_{\gamma_\perp^e(\boldsymbol{x},\hat{h}_e\bar{a})} \boldsymbol{u} \cdot \mathrm{d}l - \int_{\gamma^{\boldsymbol{v}}(\boldsymbol{x},\hat{h}_{\boldsymbol{v}}\bar{a})} \boldsymbol{u} \cdot \mathrm{d}l + \int_{\tilde{\gamma}^{e,\boldsymbol{v}}(\bar{a})} \boldsymbol{u} \cdot \mathrm{d}l$$

which, again, after taking the average, shows the second one while using (5.27) and (5.28). To complete the proof we observe that both curves $\tilde{\gamma}^{e,\boldsymbol{v}}(\bar{a})$ and $\tilde{\gamma}^e(\boldsymbol{x},a)$ are independent of $\hat{x}^k_\parallel$: for the latter curve this follows from the fact that it connects two starting points (namely, $\gamma^e_{\perp,0}(a)$ and $\gamma^e_{\parallel,0}(\boldsymbol{x})$, see Figure 5.1) which are independent of $\hat{x}^k_\parallel$ (for boundary edges this uses the convention that the adjacent patch is defined as the coarse one, $k = k^-(e)$). As a consequence the same invariance holds for the circulations $\tilde{\Phi}^{e,\boldsymbol{v}}(\boldsymbol{u})(\boldsymbol{x})$ and $\tilde{\Phi}^e(\boldsymbol{u})(\boldsymbol{x})$, which proves (5.33). ∎

Lemma 5.12. *Let $e \in \mathcal{E}$ and $\boldsymbol{v} \in \mathcal{V}(e)$. If $f \in V_h^2$, then both $\Psi^e(f)$ and $\Psi^{e,\boldsymbol{v}}(f)$ belong to V^0_{pw} and they are continuous across e.*

Proof. We prove the result for $\Psi^{e,\boldsymbol{v}}(f)$, as the same arguments apply to $\Psi^e(f)$ with minor changes. Given $\boldsymbol{x} \in \Omega(e)$ we let $k \in \mathcal{K}(e)$ be such that $\boldsymbol{x} \in \Omega_k$, and denote $\hat{\boldsymbol{x}}^k := F_k^{-1}(\boldsymbol{x})$. For $k' \in \mathcal{K}(\boldsymbol{v})$, we let

$$\hat{\sigma}_{k'}(\hat{\boldsymbol{x}}^k, \bar{a}) := F_{k'}^{-1}(\sigma^{e,\boldsymbol{v}}(\boldsymbol{x},\bar{a}) \cap \Omega_{k'}). \tag{5.34}$$

Notice that if $\Omega_{k'}$ intersects the domain $\sigma^{e,\boldsymbol{v}}(\boldsymbol{x},\bar{a})$, then either $k' = k$ or k' shares an edge e' with patch k and there is an integration curve γ that connects some starting point in $\Omega_{k'}$ to the point $\boldsymbol{x}$: by construction of the integration curves, this implies that the patch k' cannot have a finer resolution than k. By inspecting the possible configurations for the integration curves $\gamma^e_\perp(\boldsymbol{x}, \hat{h}_e\bar{a})$ and $\gamma^{\boldsymbol{v}}(\boldsymbol{x}, \hat{h}_{\boldsymbol{v}}\bar{a})$, we find that (5.34) can be expressed as an algebraic sum of Cartesian domains $\hat{\omega}_{k',m}(\hat{\boldsymbol{x}}^k) \in \hat{\Omega}$ as described below, with orientation $\epsilon_{k',m} = \pm 1$ for $m = 1, \ldots$ (for simplicity we drop the dependency on $\bar{a}$): on Ω_k, the antiderivative thus reads

$$\Psi^{e,\boldsymbol{v}}(f)(\boldsymbol{x}) = \sum_{k' \in \mathcal{K}(\boldsymbol{v})} \sum_m \epsilon_{k',m} \int_{\hat{\omega}_{k',m}(\hat{\boldsymbol{x}}^k)} \hat{f}^{k'}(\boldsymbol{z})\, \mathrm{d}\boldsymbol{z} \tag{5.35}$$

where $\hat{f}^{k'} := (\mathcal{F}^2_{k'})^{-1}(f)$ as above. For $k' = k$ it is possible to do this decomposition with domains $\hat{\omega}_{k',m}(\hat{\boldsymbol{x}}^k)$ of the form $[\alpha_1, \hat{\boldsymbol{x}}^k_1] \times [\alpha_2, \hat{\boldsymbol{x}}^k_2]$ and on an adjacent patch $k' \neq k$, of the form $\hat{X}^{k'}_{e'}([\alpha_1, \eta^{k'}_{e'}(\hat{\boldsymbol{x}}^k_\parallel)] \times [\alpha_2, \beta_2])$ where $\hat{\boldsymbol{x}}^k_\parallel$ is the component of $\hat{\boldsymbol{x}}^k$ that is parallel to e'. Using the properties of $\hat{V}^2_{k'}$ we then verify that the different integrals in (5.35), seen as functions of $\hat{\boldsymbol{x}}^k$, belong to $\hat{V}^0_k$: when $k' = k$ this follows from the tensor-product structure of $\hat{V}^2_k = \mathbb{V}^1_k \otimes \mathbb{V}^1_k$ and the fact that the indefinite integral maps $\mathbb{V}^1_k$ to $\mathbb{V}^0_k$. For the terms corresponding to the adjacent patches $k' \neq k$ this follows from the fact that the indefinite integrals only depend on the component of $\hat{\boldsymbol{x}}^k$ that is parallel to the shared edge, and from the above observation that the patch k' cannot have a finer resolution than k, hence our nestedness Assumption (3.24) reads $\mathbb{V}^0_{k'} \subset \mathbb{V}^0_k$. As a result, we find that $\Psi^{e,\boldsymbol{v}}(f)$ belongs indeed to V^0_{pw}. Finally, the continuity across e follows from the fact that the domains $\sigma^{e,\boldsymbol{v}}(\boldsymbol{x},\bar{a})$ depend continuously on $\boldsymbol{x}$ (in the sense of the Hausdorff distance). ∎

We conclude this section by studying the local stability of the correction terms (2.11) which involve these bivariate antiderivatives.

Lemma 5.13. *The edge correction term* $\tilde{\Pi}^2_e f = D^{2,e}(P^e - I^e)\Pi^0_{\mathrm{pw}}\Psi^e(f)$ *vanishes outside* $S^e = \bigcup_{j\in\mathcal{I}^e} S^e_j$*, and it satisfies a local bound*

$$\|\tilde{\Pi}^2_e f\|_{L^p(S^e_j)} \lesssim \|f\|_{L^p(E_e(S^e_j))} \tag{5.36}$$

for all $f \in L^p(\Omega)$ *and on any domain* S^e_j*,* $j \in \mathcal{I}^e$*, where* E_e *is the edge-based domain extension* (4.12)*.*

The edge-vertex correction term $\tilde{\Pi}^2_{e,\boldsymbol{v}} f = D^{2,e}(\bar{I}^e_{\boldsymbol{v}} - P^e_{\boldsymbol{v}})\Pi^0_{\mathrm{pw}}\Psi^{\boldsymbol{v},e}(f)$ *vanishes outside* $S^{\boldsymbol{v}}$*, and it satisfies the local bound*

$$\|\tilde{\Pi}^2_{e,\boldsymbol{v}} f\|_{L^p(S^{\boldsymbol{v}})} \lesssim \|f\|_{L^p(S^{\boldsymbol{v}})}. \tag{5.37}$$

Proof. The fact that these correction terms vanish outside the specified domains follows from the same reasons as their counterparts in Lemma 5.4, 5.7 and 5.9. We next study the local stability of our bivariate antiderivative operators, considering a function $f \in L^p(\Omega)$ supported in some domain ω. On some (possibly different) domain $\tilde{\omega} \subset \Omega(e)$, we have, using Hölder's inequality,

$$\begin{aligned} \|\Psi^e(f)\|^p_{L^p(\tilde{\omega})} &= \iint_{\tilde{\omega}} \frac{1}{\hat{h}^p_e}\left|\int_0^{\hat{h}_e} \iint_{\sigma^e(\boldsymbol{x},a)\cap\omega} f(\boldsymbol{z})\,\mathrm{d}\boldsymbol{z}\,\mathrm{d}a\right|^p \mathrm{d}\boldsymbol{x} \\ &\le \iint_{\tilde{\omega}} \frac{|\omega|^{p-1}}{\hat{h}_e}\int_0^{\hat{h}_e} \iint_{\sigma^e(\boldsymbol{x},a)\cap\omega} |f(\boldsymbol{z})|^p\,\mathrm{d}\boldsymbol{z}\,\mathrm{d}a\,\mathrm{d}\boldsymbol{x} \le |\tilde{\omega}||\omega|^{p-1}\|f\|^p_{L^p(\omega)}. \end{aligned} \tag{5.38}$$

To show the local bounds (5.36) and (5.37) we then argue as we did in the proof of Lemma 5.4 and 5.9. Here the inverse estimate (3.6) applied to the broken mixed derivative $D^{2,e}$ yields quadratic blow-up factors of order h_e^{-2}, which can be absorbed by a properly localized version of (5.38): the localizing arguments are then the same as those used for the path integrals in (5.16) and (5.29). ■

6. Commuting projection operators

In this section, we finalize the construction of our commuting projection operators sketched in Section 2, and we state our main results.

6.1. Projection operator on V^0_h

The projection on the first conforming space combines the projection $\Pi^0_{\mathrm{pw}} : L^p(\Omega) \to V^0_{\mathrm{pw}}$ on the broken multi-patch space with the fully discrete conforming projection $P : V^0_{\mathrm{pw}} \to V^0_h$, defined in (3.17) and (4.38) respectively. Thus, we set

$$\Pi^0 \coloneqq P\Pi^0_{\mathrm{pw}} : L^p(\Omega) \longrightarrow V^0_h, \tag{6.1}$$

whose projection properties are readily derived from those of Π^0_{pw} and P (see in particular Lemma 4.3).

Lemma 6.1. *The operator* (6.1) *is a projection onto the conforming space* V^0_h*.*

As described in Section 2, the projection Π^1 then involves single-patch projections which commute with the broken derivatives.

6.2. Single-patch commuting projection operators

On each patch a projection operator on V^1_k is defined following the tensor-product approach of [13], as

$$\Pi^1_k \boldsymbol{u} \coloneqq \sum_{d\in\{1,2\}} \nabla^k_d \Pi^0_k \Phi^k_d(\boldsymbol{u}) \tag{6.2}$$

where ∇_d^k is the patch-wise directional gradient (3.34) and Φ_d^k is the single-patch directional antiderivative (5.1). This definition corresponds to setting

$$\Pi_k^1 = \mathcal{F}_k^1 \hat{\Pi}_k^1 (\mathcal{F}_k^1)^{-1} \quad \text{with} \quad \hat{\Pi}_k^1 \hat{\boldsymbol{u}} := \begin{pmatrix} \partial_1 \hat{\Pi}_k^0 \big(\int_0^{\hat{x}_1} \hat{u}_1(z_1, \hat{x}_2)\, \mathrm{d}z_1 \big) \\ \partial_2 \hat{\Pi}_k^0 \big(\int_0^{\hat{x}_2} \hat{u}_2(\hat{x}_1, z_2)\, \mathrm{d}z_2 \big) \end{pmatrix} \in \hat{V}_k^1.$$

Similarly, a projection operator on V_k^2 is defined as

$$\Pi_k^2 f := D^{2,k} \Pi_k^0 \Psi^k(f) \tag{6.3}$$

where $D^{2,k}$ and Ψ^k are the single-patch mixed derivative and bivariate antiderivative operators, see (3.38) and (5.30). This amounts to writing

$$\Pi_k^2 = \mathcal{F}_k^2 \hat{\Pi}_k^2 (\mathcal{F}_k^2)^{-1} \quad \text{with} \quad \hat{\Pi}_k^2 \hat{f} := \partial_1 \partial_2 \hat{\Pi}_k^0 \left(\int_0^{\hat{x}_1} \int_0^{\hat{x}_2} \hat{f}(z_1, z_2)\, \mathrm{d}z_2\, \mathrm{d}z_1 \right) \in \hat{V}_k^2.$$

These single-patch operators satisfy some key properties which essentially follow from the arguments in [13].

Lemma 6.2. *The operators* (6.2) *and* (6.3) *are projections onto the respective spaces* V_k^1 *and* V_k^2*. For all* $\boldsymbol{u} \in L^p(\Omega)$ *and* $f \in L^p(\Omega)$*, the local bounds*

$$\|\Pi_k^1 \boldsymbol{u}\|_{L^p(S_{\boldsymbol{i}}^k)} \lesssim \|\boldsymbol{u}\|_{L^p(E_k(S_{\boldsymbol{i}}^k))}, \qquad \|\Pi_k^2 f\|_{L^p(S_{\boldsymbol{i}}^k)} \lesssim \|f\|_{L^p(E_k(S_{\boldsymbol{i}}^k))}$$

hold on any domain $S_{\boldsymbol{i}}^k$ *of the form* (3.15), $\boldsymbol{i} \in \boldsymbol{\mathcal{I}}^k$, *with* E_k *the single-patch domain extension* (3.16)*. Moreover, the commuting relations hold*

$$\nabla^k \Pi_k^0 \phi = \Pi_k^1 \nabla^k \phi \quad \textit{for all } \phi \in H^1(\Omega_k) \tag{6.4}$$

and

$$\operatorname{curl}^k \Pi_k^1 \boldsymbol{u} = \Pi_k^2 \operatorname{curl}^k \boldsymbol{u} \quad \textit{for all } \boldsymbol{u} \in H(\operatorname{curl}; \Omega_k). \tag{6.5}$$

Proof. The projection properties are straightforward to derive from the properties of the univariate sequence, and the local L^p bound on Π_k^1 has been established in Lemma 5.2 (sum the estimates (5.3) for $d = \{1, 2\}$). The bound on Π_k^2 is proven with the same arguments. To show the commuting property (6.4) we consider $\phi \in C^1(\overline{\Omega}_k)$ and observe that the path integral (5.1) of $\boldsymbol{u} = \nabla\phi$ along a logical dimension d reads $\Phi_d^k(\boldsymbol{u}) = \phi - \phi^*$ where $\phi^*(\boldsymbol{x}) := \phi(F_k(\hat{\boldsymbol{x}}^*))$ with $\hat{x}_d^* := 0$ and $\hat{x}_{d'}^* := \hat{x}_{d'}$ for the other component. In particular $\nabla_d^k \phi^* = 0$ and the preservation of directional invariance by Π_k^0 (see Lemma 3.1) yields $\nabla_d^k \Pi_k^0 \Phi_d^k(\boldsymbol{u}) = \nabla_d^k \Pi_k^0 \phi$. This shows (6.4) for $\phi \in C^1(\overline{\Omega}_k)$ and the result follows by density. The commuting relation (6.5) is shown with similar arguments, see [13] for more details. ■

Summing over the patches, we obtain projection operators Π_{pw}^1 and Π_{pw}^2 on the patch-wise spaces, see (2.8). These operators are obviously stable in L^p and they commute with the patch-wise, broken gradient and curl:

$$\Pi_{\mathrm{pw}}^1 \nabla\phi = \nabla_{\mathrm{pw}} \Pi_{\mathrm{pw}}^0 \phi, \qquad \phi \in H^1(\Omega) \tag{6.6}$$

and

$$\Pi_{\mathrm{pw}}^2 \operatorname{curl} \boldsymbol{u} = \operatorname{curl}_{\mathrm{pw}} \Pi_{\mathrm{pw}}^1 \boldsymbol{u}, \qquad \boldsymbol{u} \in H(\operatorname{curl}; \Omega).$$

Our next task is to modify Π_{pw}^1 so that it becomes a projection on the conforming space V_h^1 with commuting properties involving the projection Π^0 defined by (6.1).

6.3. The commuting projection operator on V_h^1.

A suitable projection operator on V_h^1 is obtained by adding correction terms to the single-patch projections (6.2). Thus, we set

$$\Pi^1 := \sum_{k\in\mathcal{K}} \Pi_k^1 + \sum_{e\in\mathcal{E}} \tilde{\Pi}_e^1 + \sum_{\boldsymbol{v}\in\mathcal{V}} \tilde{\Pi}_{\boldsymbol{v}}^1 + \sum_{\boldsymbol{v}\in\mathcal{V}, e\in\mathcal{E}(\boldsymbol{v})} \tilde{\Pi}_{e,\boldsymbol{v}}^1 \tag{6.7}$$

with edge correction terms

$$\tilde{\Pi}_e^1 : \begin{cases} L^p(\Omega) \longrightarrow V_{\mathrm{pw}}^1, \\ \boldsymbol{u} \longmapsto \displaystyle\sum_{d\in\{\|,\perp\}} \nabla_d^e (P^e - I^e)\Pi_{\mathrm{pw}}^0 \Phi_d^e(\boldsymbol{u}) \end{cases} \tag{6.8}$$

that involve the edge antiderivative operators (5.5) and (5.6)–(5.11), the patch-wise projection (3.18) on V_{pw}^0, the local (edge-based) conforming and broken projection operators (4.25), (4.26) and the edge-directional broken gradient operator (3.36), vertex correction terms

$$\tilde{\Pi}_{\boldsymbol{v}}^1 : \begin{cases} L^p(\Omega) \longrightarrow V_{\mathrm{pw}}^1, \\ \boldsymbol{u} \longmapsto \nabla_{\mathrm{pw}} (P^{\boldsymbol{v}} - \bar{I}^{\boldsymbol{v}})\Pi_{\mathrm{pw}}^0 \Phi^{\boldsymbol{v}}(\boldsymbol{u}) \end{cases} \tag{6.9}$$

that involve the vertex antiderivative operator (5.24), the vertex-based conforming and broken projection operators (4.27), (4.28) and the patch-wise gradient operator (3.35). Finally, the last terms are edge-vertex corrections

$$\tilde{\Pi}_{e,\boldsymbol{v}}^1 : \begin{cases} L^p(\Omega) \longrightarrow V_{\mathrm{pw}}^1, \\ \boldsymbol{u} \longmapsto \displaystyle\sum_{d\in\{\|,\perp\}} \nabla_d^e (\bar{I}_{\boldsymbol{v}}^e - P_{\boldsymbol{v}}^e)\Pi_{\mathrm{pw}}^0 \Phi_d^{\boldsymbol{v},e}(\boldsymbol{u}) \end{cases} \tag{6.10}$$

that involve the edge-vertex antiderivative operators (5.27) and (5.28), the edge-vertex broken and conforming projection operators (4.30) and (4.31), and again the edge-directional broken gradient operator (3.36).

6.4. The commuting projection operator on V_h^2.

A commuting projection V_h^2 is also obtained by adding correction terms to the single-patch projections (6.3). Specifically, it is defined as

$$\Pi^2 := \sum_{k\in\mathcal{K}} \Pi_k^2 + \sum_{e\in\mathcal{E}} \tilde{\Pi}_e^2 + \sum_{\boldsymbol{v}\in\mathcal{V}, e\in\mathcal{E}(\boldsymbol{v})} \tilde{\Pi}_{e,\boldsymbol{v}}^2 \tag{6.11}$$

with edge correction terms

$$\tilde{\Pi}_e^2 : \begin{cases} L^p(\Omega) \longrightarrow V_{\mathrm{pw}}^2, \\ f \longmapsto D^{2,e} (P^e - I^e)\Pi_{\mathrm{pw}}^0 \Psi^e(f) \end{cases}$$

and edge-vertex corrections

$$\tilde{\Pi}_{e,\boldsymbol{v}}^2 : \begin{cases} L^p(\Omega) \longrightarrow V_{\mathrm{pw}}^2, \\ f \longmapsto D^{2,e} (\bar{I}_{\boldsymbol{v}}^e - P_{\boldsymbol{v}}^e)\Pi_{\mathrm{pw}}^0 \Psi^{\boldsymbol{v},e}(f). \end{cases}$$

These terms involve the bivariate edge and edge-vertex antiderivatives (5.31) and (5.32), the patch-wise projection (3.18) on V_{pw}^0, the local broken and conforming projection operators (4.25), (4.26), (4.30) and (4.31) and the broken mixed derivative operator (3.39).

6.5. The main result

We are now in a position to state our main result for the grad-curl sequence (2.1): the operators Π^ℓ constructed above are commuting projections onto the spaces V_h^ℓ, and they are locally stable in L^p.

This result also holds for the curl-div sequence, and for the sequences with homogeneous boundary conditions: we refer to Sections A.1, B.1 and B.2 in the appendix for more details.

Our local estimates involve the single-patch extension E_k of the local domains $S_{\boldsymbol{i}}^k$ defined in (3.15), (3.16), as well as overlapping domains of edge and vertex types, namely

$$E_{\mathcal{E}}(S_{\boldsymbol{i}}^k) := \bigcup_{e\in\mathcal{E}, j\in\mathcal{I}^e(S_{\boldsymbol{i}}^k)} E_e(S_j^e) \quad \text{where} \quad \mathcal{I}^e(S_{\boldsymbol{i}}^k) := \{j \in \mathcal{I}^e : S_j^e \cap S_{\boldsymbol{i}}^k \neq \emptyset\}, \tag{6.12}$$

see (4.11) and (4.12), and

$$E_{\mathcal{V}}(S_{\boldsymbol{i}}^k) := \bigcup_{\boldsymbol{v}\in\mathcal{V}(S_{\boldsymbol{i}}^k)} S^{\boldsymbol{v}} \quad \text{where} \quad \mathcal{V}(S_{\boldsymbol{i}}^k) := \{\boldsymbol{v} \in \mathcal{V} : S^{\boldsymbol{v}} \cap S_{\boldsymbol{i}}^k \neq \emptyset\},$$

see (4.18). We gather these domains in a multi-patch domain extension

$$E_h(S_{\boldsymbol{i}}^k) := E_k(S_{\boldsymbol{i}}^k) \cup E_{\mathcal{E}}(S_{\boldsymbol{i}}^k) \cup E_{\mathcal{V}}(S_{\boldsymbol{i}}^k). \tag{6.13}$$

Observe that thanks to the grading Assumption (3.26), these extended domains overlap in a bounded way:

$$\#(\{(k', \boldsymbol{j}) : E_h(S_{\boldsymbol{j}}^{k'}) \cap E_h(S_{\boldsymbol{i}}^k) \neq \emptyset\}) \leq C \qquad \text{for } k \in \mathcal{K}, \boldsymbol{i} \in \boldsymbol{\mathcal{I}}^k \tag{6.14}$$

with a constant that only depends on the parameters κ_m from Section 3.

Theorem 6.3. *The operators Π^ℓ defined in* (6.1), (6.7) *and* (6.11) *are projection operators onto the respective spaces V_h^ℓ, $\ell = 0, 1, 2$. On any domain $S_{\boldsymbol{i}}^k$ with $k \in \mathcal{K}$ and $\boldsymbol{i} \in \boldsymbol{\mathcal{I}}^k$, they satisfy*

$$\|\Pi^\ell v\|_{L^p(S_{\boldsymbol{i}}^k)} \lesssim \|v\|_{L^p(E_h(S_{\boldsymbol{i}}^k))} \tag{6.15}$$

for $v \in L^p(\Omega)$, $1 \leq p \leq \infty$, with the domain extension defined in (6.13) *and constants that only depend on the parameters $\kappa_1, \ldots, \kappa_9$ described in Section 3. Moreover, the commuting relations*

$$\nabla \Pi^0 \phi = \Pi^1 \nabla \phi \quad \textit{and} \quad \operatorname{curl} \Pi^1 \boldsymbol{u} = \Pi^2 \operatorname{curl} \boldsymbol{u} \tag{6.16}$$

hold for all $\phi \in H^1(\Omega)$ and all $\boldsymbol{u} \in H(\mathrm{curl}; \Omega)$.

Remark 6.4. By using a density argument (see e.g. [37, Theorem 1.1]), one can show that the commuting relations (6.16) actually hold on larger spaces, that is for all $\phi \in W^{1,1}(\Omega)$ and all $\boldsymbol{u} \in W^1(\mathrm{curl}; \Omega)$, where for all $1 \leq p \leq \infty$ we define $W^p(\mathrm{curl}; \Omega) := \{\boldsymbol{u} \in L^p(\Omega) : \operatorname{curl} \boldsymbol{u} \in L^p(\Omega)\}$ equipped with the norm

$$\|\boldsymbol{u}\|_{W^p(\mathrm{curl};\Omega)} := (\|\boldsymbol{u}\|_{L^p(\Omega)}^p + \|\operatorname{curl} \boldsymbol{u}\|_{L^p(\Omega)}^p)^{\frac{1}{p}}.$$

We conclude this section by listing a few corollaries of Theorems 6.3. The first one is a global stability bound. It is easily derived using the bounded overlapping (6.14).

Corollary 6.5. *For $\ell = 0, 1, 2$, the bound*

$$\|\Pi^\ell v\|_{L^p(\Omega)} \lesssim \|v\|_{L^p(\Omega)}$$

holds for all $v \in L^p(\Omega)$, $1 \leq p \leq \infty$, with constants that only depend on the parameters $\kappa_1, \ldots, \kappa_9$ described in Section 3.

The second one is a direct consequence of the L^p stability and commuting sequence properties. (Notice that a local version also holds on domains $S_{\boldsymbol{i}}^k$.) For conciseness, we now write $d^0 = \nabla$ and $d^1 = \mathrm{curl}$, and accordingly denote $W^p(d^0; \Omega) = W^{1,p}(\Omega)$ and $W^p(d^1; \Omega) = W^p(\mathrm{curl}; \Omega)$.

Corollary 6.6. *Let $\ell = 0, 1$. The operators defined in* (6.1) *and* (6.7) *satisfy*

$$\|\Pi^\ell v\|_{W^p(d^\ell;\Omega)} \lesssim \|v\|_{W^p(d^\ell;\Omega)}, \quad v \in W^p(d^\ell;\Omega),$$

with constants that only depend on the parameters $\kappa_1, \dots, \kappa_9$ described in Section 3.

A third stability result follows by reasoning as in [3, Theorem 3.6]:

Corollary 6.7. *If a Poincaré–Friedrichs inequality holds,*

$$\|v\|_{L^2(\Omega)} \le c_{\mathrm{P}} \|d^\ell v\|_{L^2(\Omega)}, \quad v \in V^\ell \cap (\ker d^\ell)^\perp, \tag{6.17}$$

then the discrete spaces V_h^ℓ satisfy a Poincaré–Friedrichs inequality of the form

$$\|v\|_{L^2(\Omega)} \le c_{\mathrm{P}} c_\Pi \|d^\ell v\|_{L^2(\Omega)}, \quad v \in V_h^\ell \cap (\ker d^\ell|_{V_h^\ell})^\perp, \tag{6.18}$$

where c_Π only depends on the parameters $\kappa_1, \dots, \kappa_9$ from Section 3.

Important corollaries of Theorem 6.3 are well-posedness and a priori error estimates for FEEC approximations of Hodge Laplacian source problems of the form

$$\mathcal{L}\boldsymbol{u} = \boldsymbol{f} \quad \text{where} \quad \mathcal{L} = -\nabla \operatorname{div} + \operatorname{\mathbf{curl}} \operatorname{curl}$$

in mixed formulation, see Theorem 3.8, 3.9 and 3.11 of [3]. One further application regards the associated eigenvalue problem.

Corollary 6.8. *If the continuous sequence V satisfies the compactness property, then the FEEC approximation to the eigenvalue problem $\mathcal{L}\boldsymbol{u} = \lambda \boldsymbol{u}$ converges towards the exact one in the sense of Theorems 3.19 and 3.21 in* [3].

7. Proof of the main result

This section is devoted to the proof of Theorem 6.3, which we decompose in several lemmas.

7.1. Local L^p stability

Lemma 7.1. *Let $v \in L^p(\Omega)$ with $1 \le p \le \infty$, and $\ell \in \{0, 1, 2\}$. On any domain $S_{\boldsymbol{i}}^k$ with $k \in \mathcal{K}$ and $\boldsymbol{i} \in \boldsymbol{\mathcal{I}}^k$, the operators* (6.1), (6.7) *and* (6.11) *satisfy*

$$\|\Pi^\ell v\|_{L^p(S_{\boldsymbol{i}}^k)} \lesssim \|v\|_{L^p(E_h(S_{\boldsymbol{i}}^k))}$$

with the domain extension defined in (6.13).

Proof. We first consider the case $\ell = 0$ where $\Pi^0 = P\Pi^0_{\mathrm{pw}}$ is defined by (3.17), (4.38), and we write $\phi = v$. As in the proof of Lemma 4.8, we write $\phi_h = \Pi^0_{\mathrm{pw}}\phi = \sum_{k\in\mathcal{K}, \boldsymbol{j}\in\boldsymbol{\mathcal{I}}^k} \phi_{\boldsymbol{j}}^k \Lambda_{\boldsymbol{j}}^k$. Then $\Pi^0\phi = P\phi_h$ and the different terms corresponding to the decomposition (4.38), namely $I_0^k\phi_h$, $P_0^e\phi_h$ and $P^{\boldsymbol{v}}\phi_h$, can be bounded as follows. For the first term associated with interior coefficients, we argue as in (4.50) and write

$$\|I_0^k\phi_h\|_{L^p(S_{\boldsymbol{i}}^k)} \le \sum_{\boldsymbol{j}\in\boldsymbol{\mathcal{I}}^k(S_{\boldsymbol{i}}^k)} |\phi_{\boldsymbol{j}}^k| \|\Lambda_{\boldsymbol{j}}^k\|_{L^p(\Omega)} \lesssim \sum_{\boldsymbol{j}\in\boldsymbol{\mathcal{I}}^k(S_{\boldsymbol{i}}^k)} \|\phi\|_{L^p(S_{\boldsymbol{j}}^k)} \lesssim \|\phi\|_{L^p(E_k(S_{\boldsymbol{i}}^k))}. \tag{7.1}$$

For the second (edge-based) term we write

$$\|P_0^e\phi_h\|_{L^p(S_{\boldsymbol{i}}^k)} \le \sum_{j\in\mathcal{I}^e(S_{\boldsymbol{i}}^k)} \|P_0^e\phi_h\|_{L^p(S_j^e)} \lesssim \sum_{j\in\mathcal{I}^e(S_{\boldsymbol{i}}^k)} \|\phi\|_{L^p(E_e(S_j^e))} \lesssim \|\phi\|_{L^p(E_\mathcal{E}(S_{\boldsymbol{i}}^k))} \tag{7.2}$$

where the first inequality uses (6.12) and the fact that $P_0^e\phi_h$ vanishes outside the edge domains, the second one is (4.48) with $\phi = \phi_h = \Pi^0_{\mathrm{pw}}\phi$, and the last one follows from the bounded overlapping of the local domains. For the third (vertex-based) term we use similar arguments from Lemma 4.8, such as estimate (4.49), and write

$$\|P^{\boldsymbol{v}}\phi_h\|_{L^p(S^k_{\boldsymbol{i}})} \le \sum_{\boldsymbol{v}\in\mathcal{V}(S^k_{\boldsymbol{i}})} \|P^e_0\phi_h\|_{L^p(S^{\boldsymbol{v}})} \lesssim \sum_{\boldsymbol{v}\in\mathcal{V}(S^k_{\boldsymbol{i}})} \|\phi\|_{L^p(S^{\boldsymbol{v}})} \lesssim \|\phi\|_{L^p(E_{\mathcal{V}}(S^k_{\boldsymbol{i}}))}. \tag{7.3}$$

Summing (7.1), (7.2) and (7.3) yields the bound (6.15) for $\ell = 0$. For $\ell = 1$, writing $\boldsymbol{u} = v$ we use the same reasoning and assemble the local bounds on $\Pi^1_k\boldsymbol{u}$, $\tilde\Pi^1_e\boldsymbol{u}$, $\tilde\Pi^1_{\boldsymbol{v}}\boldsymbol{u}$ and $\tilde\Pi^1_{e,\boldsymbol{v}}\boldsymbol{u}$ that have been established in Lemma 6.2, 5.4, 5.7 and 5.9 respectively. For $\ell = 2$ we use the local bounds on $\Pi^2_k f$, $\tilde\Pi^2_e f$, and $\tilde\Pi^2_{e,\boldsymbol{v}} f$ that have been established in Lemma 6.2 and 5.13. ∎

7.2. Range property

Lemma 7.2. *For all $\phi, \boldsymbol{u}, f \in L^p(\Omega)$, $\Pi^0\phi$, $\Pi^1\boldsymbol{u}$ and $\Pi^2 f$ belong to the respective spaces V^0_h, V^1_h and V^2_h.*

Proof. The property for Π^0 has been established in Lemma 6.1. By construction, it is clear that Π^1 and Π^2 map into the respective broken spaces V^1_{pw} and V^2_{pw}. For Π^2 this is enough since $V^2_h = V^2_{\text{pw}}$, while for Π^1 we need to show that it also maps in $H(\text{curl};\Omega)$. This amounts to verifying that the tangential component of $\Pi^1\boldsymbol{u}$ is continuous across any edge $e \in \mathcal{E}$. For this we consider some unit tangent vector $\boldsymbol{\tau}_e$ and $k \in \mathcal{K}(e)$. Denoting by $\cdot|^k_e$ the restriction on e of the Ω_k piece of some broken field, we write

$$\boldsymbol{\tau}_e\cdot(\Pi^1\boldsymbol{u})|^k_e = A^k_e + B^k_e + C^k_e + D^k_e \quad\text{with}\quad \begin{cases} A^k_e = \boldsymbol{\tau}_e\cdot(\Pi^1_k\boldsymbol{u})|^k_e \\ B^k_e = \boldsymbol{\tau}_e\cdot\displaystyle\sum_{e'\in\mathcal{E}(k)}(\tilde\Pi^1_{e'}\boldsymbol{u})|^k_e \\ C^k_e = \boldsymbol{\tau}_e\cdot\displaystyle\sum_{\boldsymbol{v}\in\mathcal{V}(e)}(\tilde\Pi^1_{\boldsymbol{v}}\boldsymbol{u})|^k_e \\ D^k_e = \boldsymbol{\tau}_e\cdot\displaystyle\sum_{\substack{\boldsymbol{v}\in\mathcal{V}(e)\\ e'\in\mathcal{E}(\boldsymbol{v})}}(\tilde\Pi^1_{e',\boldsymbol{v}}\boldsymbol{u})|^k_e\ . \end{cases}$$

Here, we have restricted the vertex sums over $\mathcal{V}(e)$ (the vertex contiguous to e), since all the vertex and edge-vertex projection operators map into functions which vanish on e for $\boldsymbol{v} \notin \mathcal{V}(e)$ (this follows from the interpolation property of the basis functions at the patch boundaries). Using (3.37), i.e., $\nabla_{\text{pw}} = \nabla^e_\parallel + \nabla^e_\perp$ on $\Omega(e)$, and (4.5), that is $\boldsymbol{\tau}_e\cdot\nabla^e_\perp = 0$, we compute

$$A^k_e = \boldsymbol{\tau}_e\cdot\Pi^1_k\boldsymbol{u}|^k_e = \boldsymbol{\tau}_e\cdot(\nabla^e_\parallel\Pi^0_k\Phi^k_\parallel(\boldsymbol{u}))|^k_e = \boldsymbol{\tau}_e\cdot(\nabla^e_\parallel I^e\Pi^0_k\Phi^k_\parallel(\boldsymbol{u}))|^k_e$$

where the third equality follows from the fact that basis functions vanishing on e have also a vanishing parallel gradient on e. Here the single-patch antiderivative (5.1) is taken in the direction parallel to e, that is

$$\Phi^k_\parallel(\boldsymbol{u})(\boldsymbol{x}) = \int_0^{\hat x^k_\parallel}\hat u^k_\parallel(\hat X^k_e(z_\parallel,\hat x^k_\perp))\,\mathrm{d}z_\parallel \quad\text{with}\quad \hat{\boldsymbol{x}} = \hat X^k_e(\hat x^k_\parallel,\hat x^k_\perp) = (F_k)^{-1}(\boldsymbol{x}).$$

Then,

$$\begin{aligned} B^k_e &= \sum_{e'\in\mathcal{E}(k)}\boldsymbol{\tau}_e\cdot(\tilde\Pi^1_{e'}\boldsymbol{u})|^k_e \\ &= \boldsymbol{\tau}_e\cdot\sum_{e'\in\mathcal{E}(k)}\sum_{d\in\{\parallel,\perp\}}\nabla^{e'}_d(P^{e'} - I^{e'})\Pi^0_{\text{pw}}\Phi^{e'}_d(\boldsymbol{u})|^k_e \\ &= \bar B^k_e - \tilde A^k_e + \tilde B^k_e \end{aligned}$$

holds with

$$\begin{cases} \bar{B}^k_e = \boldsymbol{\tau}_e \cdot \nabla^e_\parallel P^e \Pi^0_{\mathrm{pw}} \Phi^e_\parallel(\boldsymbol{u}) \\ \tilde{A}^k_e = \boldsymbol{\tau}_e \cdot \nabla^e_\parallel I^e \Pi^0_{\mathrm{pw}} \Phi^e_\parallel(\boldsymbol{u}) \\ \tilde{B}^k_e = \boldsymbol{\tau}_e \cdot \sum_{\boldsymbol{v}\in\mathcal{V}(e)} \nabla^{e'(\boldsymbol{v})}_\perp (P^{e'(\boldsymbol{v})} - I^{e'(\boldsymbol{v})}) \Pi^0_{\mathrm{pw}} \Phi^{e'(\boldsymbol{v})}_\perp(\boldsymbol{u})|^k_e. \end{cases}$$

where $e'(\boldsymbol{v})$ is the edge $e' \neq e$ contiguous to $\boldsymbol{v}$ in Ω_k. Here we have used that $\boldsymbol{\tau}_e \cdot \nabla^{e'(\boldsymbol{v})}_\parallel = 0$, which follows from (4.5) and the fact that $\nabla^{e'(\boldsymbol{v})}_\parallel$ is colinear with $\nabla^e_\perp$ on Ω_k, indeed these edges correspond to different (orthogonal) logical axes, see (3.36). For an interior edge we see that $\bar{B}^k_e$ is continuous across e (in the sense that $\bar{B}^-_e = \bar{B}^+_e$) as the tangential derivative of a function continuous across e. By observing that $\Phi^e_\parallel(\boldsymbol{u})(\boldsymbol{x}) - \Phi^k_\parallel(\boldsymbol{u})(\boldsymbol{x}) = \int^0_{\eta^k_e(0)} \hat{u}^k_\parallel(X^k_e(z_\parallel, \hat{x}^k_\perp))\,\mathrm{d}z_\parallel$ is a function of $\hat{x}^k_\perp$ only, we can use Lemma 4.7 with $\phi = \Phi^e_\parallel(\boldsymbol{u}) - \Phi^k_\parallel(\boldsymbol{u})$ and infer that

$$\tilde{A}^k_e - A^k_e = \boldsymbol{\tau}_e \cdot \nabla^e_\parallel I^e \Pi^0_k(\Phi^e_\parallel(\boldsymbol{u}) - \Phi^k_\parallel(\boldsymbol{u})) = 0.$$

For the third term we compute, using again $\boldsymbol{\tau}_e \cdot \nabla_{\mathrm{pw}} = \boldsymbol{\tau}_e \cdot \nabla^e_\parallel$,

$$\begin{aligned} C^k_e &= \boldsymbol{\tau}_e \cdot \sum_{\boldsymbol{v}\in\mathcal{V}(e)} (\tilde{\Pi}^1_{\boldsymbol{v}} \boldsymbol{u})|^k_e \\ &= \boldsymbol{\tau}_e \cdot \sum_{\boldsymbol{v}\in\mathcal{V}(e)} \nabla^e_\parallel P^{\boldsymbol{v}} \Pi^0_{\mathrm{pw}} \Phi^{\boldsymbol{v}}(\boldsymbol{u})|^k_e - \boldsymbol{\tau}_e \cdot \sum_{\boldsymbol{v}\in\mathcal{V}(e)} \nabla^e_\parallel \bar{I}^{\boldsymbol{v}} \Pi^0_{\mathrm{pw}} \Phi^{\boldsymbol{v}}(\boldsymbol{u})|^k_e \\ &=: \bar{C}^k_e - \tilde{C}^k_e \end{aligned}$$

and for the last one we write, using (5.27) and (5.28),

$$\begin{aligned} D^k_e &= \boldsymbol{\tau}_e \cdot \sum_{\boldsymbol{v}\in\mathcal{V}(e), e'\in\mathcal{E}(\boldsymbol{v})} (\tilde{\Pi}^1_{e',\boldsymbol{v}} \boldsymbol{u})|^k_e \\ &= \boldsymbol{\tau}_e \cdot \sum_{\boldsymbol{v}\in\mathcal{V}(e)} \nabla^e_\parallel \bar{I}^e_{\boldsymbol{v}} \Pi^0_{\mathrm{pw}} \Phi^{\boldsymbol{v}}(\boldsymbol{u})|^k_e - \boldsymbol{\tau}_e \cdot \sum_{\boldsymbol{v}\in\mathcal{V}(e)} \nabla^e_\parallel P^e_{\boldsymbol{v}} \Pi^0_{\mathrm{pw}} \Phi^{\boldsymbol{v}}(\boldsymbol{u})|^k_e \\ &\qquad + \boldsymbol{\tau}_e \cdot \sum_{\boldsymbol{v}\in\mathcal{V}(e)} \nabla^{e'(\boldsymbol{v})}_\perp (\bar{I}^{e'(\boldsymbol{v})}_{\boldsymbol{v}} - P^{e'(\boldsymbol{v})}_{\boldsymbol{v}}) \Pi^0_{\mathrm{pw}} \Phi^{e'(\boldsymbol{v})}_\perp(\boldsymbol{u})|^k_e \\ &=: \tilde{D}^k_e - \bar{D}^k_e + \check{D}^k_e. \end{aligned}$$

According to (4.46) the equality $\bar{I}^{\boldsymbol{v}}\phi = \bar{I}^e_{\boldsymbol{v}}\phi$ holds on e: this yields $\tilde{C}^k_e = \tilde{D}^k_e$, moreover for $e' = e'(\boldsymbol{v})$ we have $P^{e'}\phi = P^{e'}_{\boldsymbol{v}}\phi$ and $I^{e'}\phi = \bar{I}^{e'}_{\boldsymbol{v}}\phi$ on e. This yields $\tilde{B}^k_e = -\check{D}^k_e$. Thus, we obtain that

$$\boldsymbol{\tau}_e \cdot (\Pi^1 \boldsymbol{u})|^k_e = \bar{B}^k_e + \bar{C}^k_e - \bar{D}^k_e \tag{7.4}$$

where these three terms are tangential derivatives of fields which are continuous across e (and hence are also continuous across e) if the latter is an interior edge. This shows that $\Pi^1\boldsymbol{u} \in H(\mathrm{curl};\Omega)$ and completes the proof. ∎

7.3. **Projection property**

Lemma 7.3. *For all $\boldsymbol{u} \in V^1_h$ and $f \in V^2_h$, we have $\Pi^1\boldsymbol{u} = \boldsymbol{u}$ and $\Pi^2 f = f$.*

Proof. We first consider Π^1 and observe that for all k, the restriction $\boldsymbol{u}|_{\Omega_k}$ belongs to the local space V^1_k. Hence, the projection property of the local projection operator gives $(\Pi^1_k \boldsymbol{u})|_{\Omega_k} = \boldsymbol{u}|_{\Omega_k}$: it follows that

$$\sum_{k\in\mathcal{K}} \Pi^1_k \boldsymbol{u} = \boldsymbol{u}.$$

We thus need to show that the correction terms $\tilde{\Pi}^1_e \boldsymbol{u}$, $\tilde{\Pi}^1_{\boldsymbol{v}} \boldsymbol{u}$ and $\tilde{\Pi}^1_{e,\boldsymbol{v}} \boldsymbol{u}$ all vanish for $\boldsymbol{u} \in V^1_h$. As for the first term we know from Lemma 5.8 that the parallel and perpendicular antiderivatives $\Phi^e_\parallel(\boldsymbol{u})$ and $\Phi^e_\perp(\boldsymbol{u})$ belong to $V^0_{\rm pw}$, hence they are left unchanged by the patch-wise projection $\Pi^0_{\rm pw}$. Moreover, again from Lemma 5.8, they are continuous across any interior edge e so that Lemma 4.5 allows us to write

$$(P^e - I^e)\Pi^0_{\rm pw}\Phi^e_d(\boldsymbol{u}) = 0, \qquad d \in \{\parallel, \perp\}.$$

We further observe that this equality also holds on boundary edges, this follows from the fact that $P^e = I^e$. As a result the edge correction terms vanish: $\tilde{\Pi}^1_e \boldsymbol{u} = 0$ for $\boldsymbol{u} \in V^1_h$. The same reasoning applies to the vertex correction term: according again to Lemma 5.8, the antiderivative $\Phi^{\boldsymbol{v}}(\boldsymbol{u})$ belongs to $V^0_{\rm pw}$ and it is continuous across any interior edge $e \in \mathcal{E}(\boldsymbol{v})$. Then Lemma 4.6 applies, which yields

$$(P^{\boldsymbol{v}} - \bar{I}^{\boldsymbol{v}})\Pi^0_{\rm pw}\Phi^{\boldsymbol{v}}(\boldsymbol{u}) = 0$$

and hence $\tilde{\Pi}^1_{\boldsymbol{v}} \boldsymbol{u} = 0$. Turning to the edge-vertex correction terms we infer from (5.27) and (5.28) that both $\Phi^{e,\boldsymbol{v}}_\parallel(\boldsymbol{u})$ and $\Phi^{e,\boldsymbol{v}}_\perp(\boldsymbol{u})$ are in $V^0_{\rm pw}$ and continuous across interior edges e. Applying again Lemma 4.6 yields then

$$(P^e_{\boldsymbol{v}} - \bar{I}^e_{\boldsymbol{v}})\Pi^0_{\rm pw}\Phi^{e,\boldsymbol{v}}_d(\boldsymbol{u}) = 0, \qquad d \in \{\parallel, \perp\},$$

which shows that $\tilde{\Pi}^1_{e,\boldsymbol{v}} \boldsymbol{u} = 0$ and finishes the proof. To show that Π^2 is a projection, we use a similar argument based on Lemma 5.12. ∎

7.4. Commuting property

Lemma 7.4. *The equality*

$$\Pi^1 \nabla \phi = \nabla \Pi^0 \phi \tag{7.5}$$

holds for all $\phi \in H^1(\Omega)$.

Remark 7.5. The commuting relation (7.5) also holds in the respective (larger) space $W^{1,1}(\Omega)$, as mentioned in Remark 6.4.

Proof. We consider $\boldsymbol{u} = \nabla\phi$, with $\phi \in C^1(\overline{\Omega})$: the result will then follow by a density argument, using the L^1 stability of the projection operators. Throughout this proof we write $\phi_h = \Pi^0_{\rm pw}\phi \in V^0_{\rm pw}$. For the volume terms, we have seen in (6.6) that the commutation of the patch-wise projection operators yield

$$\sum_{k \in \mathcal{K}} \Pi^1_k \boldsymbol{u} = \nabla_{\rm pw}\phi_h.$$

For the parallel edge correction terms we remind that (5.13) reads

$$\Phi^e_\parallel(\boldsymbol{u})(\boldsymbol{x}) = \phi(\boldsymbol{x}) - \tilde{\phi}_e(\boldsymbol{x})$$

on $\Omega(e)$, $e \in \mathcal{E}$, for some function $\tilde{\phi}_e$ independent of $\hat{x}^k_\parallel$. Hence, Lemma 4.7 yields

$$\nabla^e_\parallel(P^e - I^e)\Pi^0_{\rm pw}\Phi^e_\parallel(\boldsymbol{u}) = \nabla^e_\parallel(P^e - I^e)\phi_h.$$

Next for the perpendicular edge correction term, we use (5.14), namely

$$\Phi^e_\perp(\boldsymbol{u})(\boldsymbol{x}) = \phi(\boldsymbol{x}) - \bar{\phi}_e \tag{7.6}$$

(again on $\Omega(e)$) with a constant value $\bar{\phi}_e$. Since $\Pi^0_{\rm pw}$ preserves patch-wise constant functions, Lemma 4.5 gives $(P^e - I^e)\Pi^0_{\rm pw}\bar{\phi}_e = (P^e - I^e)\bar{\phi}_e = 0$. Hence, we have for any $e \in \mathcal{E}$

$$\nabla^e_\perp(P^e - I^e)\Pi^0_{\rm pw}\Phi^e_\perp(\boldsymbol{u}) = \nabla^e_\perp(P^e - I^e)\phi_h.$$

Writing again $\nabla^e_\parallel + \nabla^e_\perp = \nabla_{\rm pw}$ on $\Omega(e)$, it follows that

$$\tilde\Pi^1_e \boldsymbol{u} = \sum_{d\in\{\parallel,\perp\}} \nabla^e_d (P^e - I^e)\Pi^0_{\rm pw}\Phi^e_d(\boldsymbol{u}) = \nabla_{\rm pw}(P^e - I^e)\phi_h.$$

For the vertex correction we use (5.25), namely

$$\Phi^{\boldsymbol{v}}(\boldsymbol{u})(\boldsymbol{x}) = \phi(\boldsymbol{x}) - \phi^{\boldsymbol{v}}_0 \tag{7.7}$$

which holds on $\Omega(\boldsymbol{v})$ with a constant value $\phi^{\boldsymbol{v}}_0$. Thus, the statement result of Lemma 4.6 yields

$$\tilde\Pi^1_{\boldsymbol{v}} \boldsymbol{u} = \nabla_{\rm pw}(P^{\boldsymbol{v}} - \bar I^{\boldsymbol{v}})\Pi^0_{\rm pw}\Phi^{\boldsymbol{v}}(\boldsymbol{u}) = \nabla_{\rm pw}(P^{\boldsymbol{v}} - \bar I^{\boldsymbol{v}})\phi_h.$$

Finally, for the edge-vertex correction, the respective antiderivative operators (5.27) and (5.28) are of vertex and edge perpendicular type, hence they also satisfy relations of the form (7.6) and (7.7) on $\Omega(e)$, with constant terms $\bar\phi_e$ and $\phi^{\boldsymbol{v}}_0$. Thus, using the last statement of Lemma 4.6 we have

$$\tilde\Pi^1_{e,\boldsymbol{v}} \boldsymbol{u} = \sum_{d\in\{\parallel,\perp\}} \nabla^e_d (\bar I^e_{\boldsymbol{v}} - P^e_{\boldsymbol{v}})\Pi^0_{\rm pw}\Phi^{e,\boldsymbol{v}}_d(\boldsymbol{u}) = \nabla_{\rm pw}(\bar I^e_{\boldsymbol{v}} - P^e_{\boldsymbol{v}})\phi_h.$$

With the decomposition (4.36), i.e. $\phi_h = \big(\sum_{k\in\mathcal{K}} I^k_0 + \sum_{e\in\mathcal{E}} I^e_0 + \sum_{\boldsymbol{v}\in\mathcal{V}} I^{\boldsymbol{v}}\big)\phi_h$, this allows us to write $\Pi^1\boldsymbol{u} = \nabla_{\rm pw}\psi_h$ with

$$\begin{aligned}\psi_h &= \phi_h + \Bigg(\sum_{e\in\mathcal{E}}(P^e - I^e) + \sum_{\boldsymbol{v}\in\mathcal{V}}(P^{\boldsymbol{v}} - \bar I^{\boldsymbol{v}}) + \sum_{e\in\mathcal{E}}\sum_{\boldsymbol{v}\in\mathcal{V}}(\bar I^e_{\boldsymbol{v}} - P^e_{\boldsymbol{v}})\Bigg)\phi_h \\ &= \Bigg(\sum_{k\in\mathcal{K}} I^k_0 + \sum_{e\in\mathcal{E}}(I^e_0 + P^e - I^e) + \sum_{\boldsymbol{v}\in\mathcal{V}}(I^{\boldsymbol{v}} + P^{\boldsymbol{v}} - \bar I^{\boldsymbol{v}}) + \sum_{e\in\mathcal{E}}\sum_{\boldsymbol{v}\in\mathcal{V}}(\bar I^e_{\boldsymbol{v}} - P^e_{\boldsymbol{v}})\Bigg)\phi_h.\end{aligned}$$

We then observe that (4.34), (4.37) yield $\sum_e (I^e_0 - I^e) = -\sum_{e,\boldsymbol{v}} I^e_{\boldsymbol{v}} = -\sum_{\boldsymbol{v}} 2I^{\boldsymbol{v}}$, while (4.35) is $\bar I^{\boldsymbol{v}} = \sum_e \bar I^e_{\boldsymbol{v}} - I^{\boldsymbol{v}}$. With (4.39), i.e., $P^e - \sum_{\boldsymbol{v}} P^e_{\boldsymbol{v}} = P^e_0$, and the decomposition (4.38), this gives

$$\psi_h = \Bigg(\sum_{k\in\mathcal{K}} I^k_0 + \sum_{e\in\mathcal{E}} P^e + \sum_{\boldsymbol{v}\in\mathcal{V}} P^{\boldsymbol{v}} - \sum_{e\in\mathcal{E}}\sum_{\boldsymbol{v}\in\mathcal{V}} P^e_{\boldsymbol{v}}\Bigg)\phi_h = P\phi_h.$$

This shows that ψ_h is continuous on Ω, hence $\nabla_{\rm pw}\psi_h = \nabla\psi_h$, and finally we find $\Pi^1\nabla\phi = \nabla\psi_h = \nabla P\phi_h = \nabla P\Pi^0_{\rm pw}\phi = \nabla\Pi^0\phi$, which completes the proof. ∎

Lemma 7.6. *The equality*

$$\Pi^2 \operatorname{curl}\boldsymbol{u} = \operatorname{curl}\Pi^1\boldsymbol{u} \tag{7.8}$$

holds for all $\boldsymbol{u} \in H(\operatorname{curl};\Omega)$.

Remark 7.7. The commuting relation (7.8) also holds in the respective (larger) space $W^1(\operatorname{curl};\Omega)$ defined in Remark 6.4.

Proof. By a density argument we may consider $\boldsymbol{u} \in C^1(\overline\Omega)$. According to Lemma 6.2 we know that the single-patch projections commute with the patch-wise curl operator, namely

$$\operatorname{curl}^k \Pi^1_k\boldsymbol{u} = \Pi^2_k \operatorname{curl}\boldsymbol{u}.$$

Since every vertex correction term (6.9) is a patch-wise gradient, we also have

$$\operatorname{curl}_{\rm pw}\tilde\Pi^1_{\boldsymbol{v}}\boldsymbol{u} = 0.$$

For the edge correction terms (6.8), we use Lemma 3.4 with $\psi_d = (P^e - I^e)\Pi^0_{\rm pw}\Phi^e_d(\boldsymbol{u})$ and compute

$$\begin{aligned}\operatorname{curl}_{\rm pw}\tilde\Pi^1_e\boldsymbol{u} &= D^{2,e}(P^e - I^e)\Pi^0_{\rm pw}(\Phi^e_\perp(\boldsymbol{u}) - \Phi^e_\parallel(\boldsymbol{u})) \\ &= D^{2,e}(P^e - I^e)\Pi^0_{\rm pw}(\Phi^e_\perp(\boldsymbol{u}) - \Phi^e_\parallel(\boldsymbol{u}) + \tilde\Phi^e(\boldsymbol{u})) \\ &= D^{2,e}(P^e - I^e)\Pi^0_{\rm pw}\Psi^e(\operatorname{curl}\boldsymbol{u})\end{aligned}$$

where the second and third equalities follow from Lemma 5.11 and the parallel invariance preserving property of the operators $\Pi^0_{\rm pw}$, P^e and I^e, see Lemma 4.7: note that an invariance along $\hat{x}_\parallel$ leads indeed to the cancellation of the mixed derivative $D^{2,e}$ on each patch. For the edge-vertex correction terms (6.10) we use again Lemma 3.4 and write

$$\begin{aligned}\operatorname{curl}_{\rm pw}\tilde{\Pi}^1_{e,\boldsymbol{v}}\boldsymbol{u} &= D^{2,e}(\bar{I}^e_{\boldsymbol{v}} - P^e_{\boldsymbol{v}})\Pi^0_{\rm pw}(\Phi^{e,\boldsymbol{v}}_\perp(\boldsymbol{u}) - \Phi^{e,\boldsymbol{v}}_\parallel(\boldsymbol{u}))\\ &= D^{2,e}(\bar{I}^e_{\boldsymbol{v}} - P^e_{\boldsymbol{v}})\Pi^0_{\rm pw}(\Phi^{e,\boldsymbol{v}}_\perp(\boldsymbol{u}) - \Phi^{e,\boldsymbol{v}}_\parallel(\boldsymbol{u}) + \tilde{\Phi}^{e,\boldsymbol{v}}(\boldsymbol{u}))\\ &= D^{2,e}(\bar{I}^e_{\boldsymbol{v}} - P^e_{\boldsymbol{v}})\Pi^0_{\rm pw}\Psi^e(\operatorname{curl}\boldsymbol{u})\end{aligned}$$

where the second and third equalities follow from Lemma 5.11 and the preservation of constants by the operator $\Pi^0_{\rm pw}$, which are in the kernel of $\bar{I}^e_{\boldsymbol{v}} - P^e_{\boldsymbol{v}}$, see Lemma 4.6. Gathering the computations above and using the form of the Π^2 projection, we find

$$\begin{aligned}\operatorname{curl}\Pi^1\boldsymbol{u} &= \operatorname{curl}_{\rm pw}\Pi^1\boldsymbol{u}\\ &= \sum_{k\in\mathcal{K}}\operatorname{curl}^k\Pi^1_k\boldsymbol{u} + \sum_{e\in\mathcal{E}}\operatorname{curl}_{\rm pw}\tilde{\Pi}^1_e\boldsymbol{u} + \sum_{\boldsymbol{v}\in\mathcal{V}}\operatorname{curl}_{\rm pw}\tilde{\Pi}^1_{\boldsymbol{v}}\boldsymbol{u} + \sum_{\substack{\boldsymbol{v}\in\mathcal{V}\\ e\in\mathcal{E}(\boldsymbol{v})}}\operatorname{curl}_{\rm pw}\tilde{\Pi}^1_{e,\boldsymbol{v}}\boldsymbol{u}\\ &= \sum_{k\in\mathcal{K}}\Pi^2_k\operatorname{curl}\boldsymbol{u} + \sum_{e\in\mathcal{E}}\tilde{\Pi}^2_e\operatorname{curl}\boldsymbol{u} + \sum_{\substack{\boldsymbol{v}\in\mathcal{V}\\ e\in\mathcal{E}(\boldsymbol{v})}}\tilde{\Pi}^2_{e,\boldsymbol{v}}\operatorname{curl}\boldsymbol{u} = \Pi^2\operatorname{curl}\boldsymbol{u}.\end{aligned}$$

■

8. Conclusion

In this article we have proposed a new approach for constructing L^2 stable commuting projection operators on de Rham sequences of multipatch spaces, which allows patch-wise refinements with tensor-product structure.

Our construction involves single-patch projections that rely on the tensor-product structure of the single-patch spaces, and correction terms for the interfaces. Like the single-patch projections, the correction terms are composed of partial derivatives, local projections and antiderivative operators: the specificity of the latter is to involve projections on the local conforming and broken spaces associated with an interface.

Being local, our construction naturally yields projection operators which are stable in any L^p norm with $p \in [1, \infty]$. It also applies to de Rham sequences with homogeneous boundary conditions.

Looking ahead, an important objective will be to extend our construction to 3D domains and lift the four-patch restriction. Applying these theoretical findings to the design of stable numerical schemes is also a work in progress. Preliminary experiments conducted on curl-curl eigenvalue problems have yielded promising results, particularly when employing broken-FEEC schemes [18]: these and further studies will be described in a forthcoming article.

Acknowledgment

We would like to thank the anonymous reviewers for their careful reading of our manuscript, as well as for their insightful suggestions that helped us improve the analysis and results presented in this article.

Appendix A. The curl − div sequence

The curl-div sequence reads

$$\mathbb{R} \xrightarrow{\text{id}} V^{0,*} = H(\mathbf{curl};\Omega) \xrightarrow{\mathbf{curl}} V^{1,*} = H(\text{div};\Omega) \xrightarrow{\text{div}} V^{2,*} = L^2(\Omega) \xrightarrow{0} \{0\} \tag{A.1}$$

which can be related to the ∇ − curl sequence (2.1) by a standard rotation argument: We indeed observe that

$$\mathbf{curl}\,\phi = R\nabla\phi \quad \text{and} \quad \text{div}\,\boldsymbol{v} = \text{curl}\,R^{-1}\boldsymbol{v} \quad \text{with} \quad R = \begin{pmatrix} 0 & 1 \\ -1 & 0 \end{pmatrix}. \tag{A.2}$$

This leads to defining

$$\Pi^{0,*} := \Pi^0, \qquad \Pi^{1,*} := R\Pi^1 R^{-1}, \qquad \Pi^{2,*} := \Pi^2, \tag{A.3}$$

which allows to transfer the stability and commutation properties of the Π^ℓ projections to the curl-div sequence.

Analogously, the pushforward operators for the grad-curl sequence in (3.12) are also related to the ones of the curl-div sequence, namely

$$\begin{cases} \mathcal{F}_k^{0,*} : \hat{\phi} \longmapsto \phi := \hat{\phi} \circ F_k^{-1} \\ \mathcal{F}_k^{1,*} : \hat{\boldsymbol{u}} \longmapsto \boldsymbol{u} := (J_{F_k}^{-1} DF_k \hat{\boldsymbol{u}}) \circ F_k^{-1} \\ \mathcal{F}_k^{2,*} : \hat{f} \longmapsto f := (J_{F_k}^{-1} \hat{f}) \circ F_k^{-1}. \end{cases}$$

Using the matrix relation $RDF_k^{-T} = J_{F_k}^{-1} DF_k R$, we find indeed

$$\mathcal{F}_k^{0,*} = \mathcal{F}_k^0, \qquad \mathcal{F}_k^{1,*} = R\mathcal{F}_k^1 R^{-1}, \qquad \mathcal{F}_k^{2,*} = \mathcal{F}_k^2.$$

Following Section 3.2, we define the reference patch finite element spaces as

$$\hat{V}_k^{0,*} := \hat{V}_k^0 = \mathbb{V}_k^0 \otimes \mathbb{V}_k^0, \quad \hat{V}_k^{1,*} := R\hat{V}_k^1 = \begin{pmatrix} \mathbb{V}_k^0 \otimes \mathbb{V}_k^1 \\ \mathbb{V}_k^1 \otimes \mathbb{V}_k^0 \end{pmatrix}, \quad \hat{V}_k^{2,*} := \hat{V}_k^2 = \mathbb{V}_k^1 \otimes \mathbb{V}_k^1,$$

and upon pushing forward the patch-wise spaces with $V_k^{\ell,*} = \mathcal{F}_k^{\ell,*}(\hat{V}_k^{\ell,*})$, we define the global conforming spaces as

$$V_h^{0,*} = V_{\text{pw}}^{0,*} \cap H(\mathbf{curl};\Omega), \quad V_h^{1,*} = V_{\text{pw}}^{1,*} \cap H(\text{div};\Omega), \quad V_h^{2,*} = V_{\text{pw}}^{2,*} \cap L^2(\Omega) = V_{\text{pw}}^2.$$

These definitions allow us to extend the main result, namely Theorem 6.3, to this sequence:

Theorem A.1. *The operators $\Pi^{\ell,*}$ defined in* (A.3) *are projection operators onto the respective spaces $V_h^{\ell,*}$, $\ell = 0,1,2$. On any domain $S_{\boldsymbol{i}}^k$ with $k \in \mathcal{K}$ and $\boldsymbol{i} \in \boldsymbol{\mathcal{I}}^k$, they satisfy*

$$\|\Pi^{\ell,*} v\|_{L^p(S_{\boldsymbol{i}}^k)} \lesssim \|v\|_{L^p(E_h(S_{\boldsymbol{i}}^k))}$$

for all $v \in L^p(\Omega)$, $1 \le p \le \infty$, with the domain extension defined in (6.13) *and constants that only depend on the parameters $\kappa_1, \ldots, \kappa_9$ described in Section 3. Moreover, the commuting relations*

$$\mathbf{curl}\,\Pi^{0,*}\phi = \Pi^{1,*}\,\mathbf{curl}\,\phi \quad \textit{and} \quad \text{div}\,\Pi^{1,*}\boldsymbol{u} = \Pi^{2,*}\,\text{div}\,\boldsymbol{u}$$

hold for all $\phi \in H(\mathbf{curl};\Omega)$ and $\boldsymbol{u} \in H(\text{div};\Omega)$.

Remark A.2. Again, these commuting relations actually hold in larger spaces characterized by L^1 integrability, defined similarly as in Remark 6.4.

Proof. The stability follows from Theorem 6.3 and the fact that R and R^{-1} are isometries in any L^p. The range and projection properties for $\ell = 0, 2$ follow from Theorem 6.3 as the projectors and conforming spaces are equal. For $\ell = 1$, we first realize that the spaces $H(\mathrm{curl};\Omega)$ and $H(\mathrm{div};\Omega)$ have similar, but rotated, conformity conditions, i.e. continuity along tangent and normal vectors respectively. Since $V_k^{1,*} = \mathcal{F}_k^{1,*}(\hat{V}_k^{1,*}) = R\mathcal{F}_k^1(R^{-1}R\hat{V}_k^1) = RV_k^1$, we have

$$V_h^{1,*} = RV_{\mathrm{pw}}^1 \cap H(\mathrm{div};\Omega) = RV_h^1. \tag{A.4}$$

Thus, the range and projection properties are direct consequences of (A.4) and definition of $\Pi^{1,*}$. The commuting properties are again a consequence of Theorem 6.3 and the relations of differential operators in (A.2), i.e.

$$\Pi^{1,*}\,\mathbf{curl}\,\phi = R\Pi^1 R^{-1}\,\mathbf{curl}\,\phi = R\Pi^1\nabla\phi = R\nabla\Pi^0\phi = \mathbf{curl}\,\Pi^{0,*}\phi$$

and

$$\Pi^{2,*}\,\mathrm{div}\,\boldsymbol{v} = \Pi^2\,\mathrm{curl}\,R^{-1}\boldsymbol{v} = \mathrm{curl}\,\Pi^1 R^{-1}\boldsymbol{v} = \mathrm{curl}\,R^{-1}\Pi^{1,*}\boldsymbol{v} = \mathrm{div}\,\Pi^{1,*}\boldsymbol{v}. \qquad \blacksquare$$

Similarly, Theorem A.1 has the same corollaries as Theorem 6.3. In particular, Corollary 6.6 holds for $\Pi^{\ell,*}$ with $d^0 = \mathbf{curl}$ and $d^1 = \mathrm{div}$, and a second stability result follows by reasoning as in [3, Theorem 3.6]:

Corollary A.3. *If the spaces $V^{\ell,*}$ in the curl-div sequence* (A.1) *satisfy Poincaré–Friedrichs inequalities of the form* (6.17) *(with $V^\ell = V^{\ell,*}$ and $d^0 = \mathbf{curl}$, $d^1 = \mathrm{div}$), then the discrete spaces $V_h^{\ell,*}$ satisfy discrete Poincaré–Friedrichs inequalities of the form* (6.18) *with a constant c_Π that only depends on the parameters $\kappa_1, \dots, \kappa_9$ from Section 3.*

Appendix B. Homogeneous boundary conditions

We want to discuss the counterparts of sequences (2.1) and (A.1) with homogeneous boundary conditions, namely

$$0 \xrightarrow{0} V^0 = H_0^1(\Omega) \xrightarrow{\nabla} V^1 = H_0(\mathrm{curl};\Omega) \xrightarrow{\mathrm{curl}} V^2 = L^2(\Omega) \xrightarrow{\int} \mathbb{R} \tag{B.1}$$

and

$$0 \xrightarrow{0} V^0 = H_0(\mathbf{curl};\Omega) \xrightarrow{\mathbf{curl}} V^1 = H_0(\mathrm{div};\Omega) \xrightarrow{\mathrm{div}} V^2 = L^2(\Omega) \xrightarrow{\int} \mathbb{R}. \tag{B.2}$$

The constructions are very similar to the inhomogeneous cases, we just have to adapt some conventions we made earlier and add some explanations. In particular, the homogeneous boundary conditions are handled by removing boundary basis functions from the conforming basis of V_h^0 (with a consistent adaptation of the conforming projection P and its localized counterparts $P^e, P^{\boldsymbol{v}}, P^e_{\boldsymbol{v}}$), and by defining the antiderivative operators $\Phi^e_\perp$ and $\Phi^{\boldsymbol{v}}$ through integration curves that start from the homogeneous boundaries. In the following we focus on the first sequence (B.1), the other one being treated in the same way.

B.1. Notation and assumptions on the geometry

In the homogeneous case, instead of the convention that the single patch $\mathcal{K}(e)$ for boundary edges e is of coarse type, $k = k^-(e)$, as stated in Assumption 1, we now declare it to be of fine type, $k = k^+(e)$. Assumption 2 for boundary vertices $\boldsymbol{v}$ is then changed as follows: any $\boldsymbol{x} \in \Omega(\boldsymbol{v})$ can be connected to some boundary edge $e = e(\boldsymbol{x}) \in \mathcal{E}(\boldsymbol{v})$ with a monotonic curve of length $L \leq 2$ as is visualized in Figure B.1. Note that if $\boldsymbol{v}$ is a boundary vertex shared by three or four patches then it is now the finer patches of both sequences that must be adjacent, while the coarser ones do not need to be.

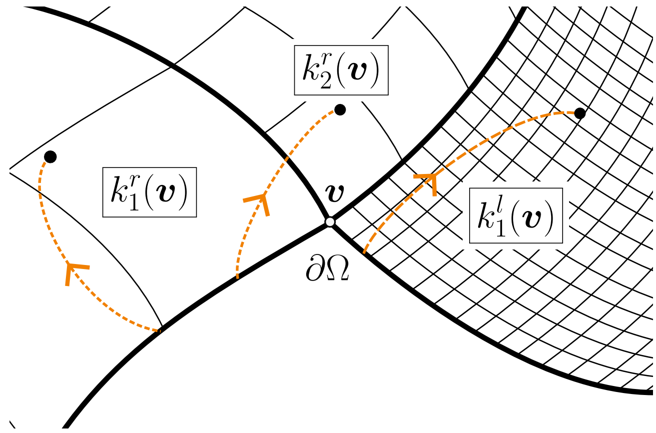

Figure B.1. Adjacent patches around a boundary vertex $\boldsymbol{v}$ and dashed curves connecting arbitrary points $\boldsymbol{x} \in \Omega(\boldsymbol{v})$ to one coarse edge $e^*(\boldsymbol{v})$ in the homogeneous case, according to Assumption 2. We show a decomposition of the form (3.33) for the adjacent nested patches.

B.2. Basis functions and conforming projectors

In the homogeneous case (B.1), the same basis from Section 4.2 can be used excluding the functions Λ_i^e and $\Lambda^{\boldsymbol{v}}$ associated with boundary edges and vertices.

This is consistent with the definitions of the conforming projectors as

- only a fine patch $k^+(e)$ has been associated to boundary edges e in Section B.1: we thus have $P^e = 0$.
- for boundary vertices where $k^*(\boldsymbol{v})$ is undefined, this leads to setting $P^{\boldsymbol{v}} = 0$.
- $P_{\boldsymbol{v}}^e = 0$ on homogeneous boundary edges where $k^-(e)$ is undefined

In total we have $P_0^e = P^e = 0$ for boundary edges and $P^{\boldsymbol{v}} = 0$ for boundary vertices, so that P defined by (4.38) is indeed a projection on the homogeneous conforming space $V_h^0 = V_{\text{pw}}^0 \cap H_0^1(\Omega)$.

In Lemma 4.4 we notice that in the homogeneous case (B.1) the patches $k^-(e)$ and $k^*(\boldsymbol{v})$ are undefined for boundary edges and vertices, so that the corresponding values of ϕ can be replaced by 0.

B.3. Antiderivative operators

The antiderivative operators defined in Section 5 are extended to the case of homogeneous boundary conditions, with the following changes.

Regarding edge-type antiderivative operators, for boundary edges where boundary patches are by convention of fine type $k^+(e)$, the curves $\gamma_\perp^e(\boldsymbol{x}, a)$ are all perpendicular to the boundary edge in the logical variables. In particular, they have many different starting points which all lie on the edge e (see Figure 5.1), hence on the boundary $\partial\Omega$.

Regarding vertex-type antiderivative operators associated with boundary vertices $\boldsymbol{v}$, we observe that the curves $\gamma^{\boldsymbol{v}}(\boldsymbol{x}, a)$ may start from different points $\gamma_0^{\boldsymbol{v}}(\boldsymbol{x}, a)$, but they all lie on the boundary $\partial\Omega$ as shown in Figure B.2.

In particular, we change some Lemmas of this section as follows:

Lemma 5.3: For a boundary edge e and $\boldsymbol{u} = \nabla\phi$ with $\phi \in C^1(\overline{\Omega})$, then it holds

$$\Phi_\perp^e(\boldsymbol{u})(\boldsymbol{x}) = \phi(\boldsymbol{x}). \tag{B.3}$$

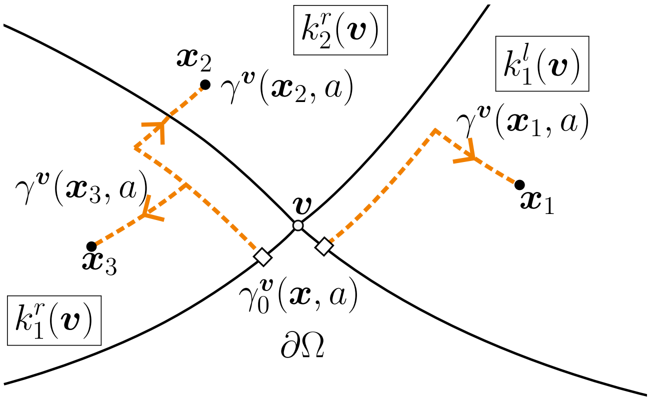

FIGURE B.2. Integration paths $\gamma^{\boldsymbol{v}}(\boldsymbol{x}, a)$ defining the vertex-based antiderivative operators $\Phi^{\boldsymbol{v}}(\boldsymbol{u})$ for boundary vertices. In the homogeneous case, different points $\boldsymbol{x} \in \Omega(\boldsymbol{v})$ may be connected to different starting points $\gamma_0^{\boldsymbol{v}}(\boldsymbol{x}, a)$, all on the boundary $\partial\Omega$.

The result follows from the fact that all curves $\gamma_\perp^e(\boldsymbol{x}, a)$ start from the boundary $\partial\Omega$ where $\phi = 0$.

Lemma 5.5: For a boundary vertex $\boldsymbol{v}$ and $\boldsymbol{u} = \nabla\phi$ with $\phi \in C^1(\overline{\Omega}) \cap H_0^1(\Omega)$, then

$$\Phi^{\boldsymbol{v}}(\boldsymbol{u})(\boldsymbol{x}) = \phi(\boldsymbol{x}) \quad \text{on } \Omega(\boldsymbol{v}). \tag{B.4}$$

Lemma 5.8:

- if e is a boundary edge, $\Phi_\parallel^e(\boldsymbol{u})$ and $\Phi_\perp^e(\boldsymbol{u})$ vanish on $\partial\Omega$
- if $\boldsymbol{v}$ is a boundary vertex, $\Phi^{\boldsymbol{v}}(\boldsymbol{u})$ vanishes on $\partial\Omega$.

This follows from the boundary vanishing properties of the antiderivatives in the case of homogeneous boundary edges and the fact that on $\partial\Omega$ all integration curves involved in these antiderivative operators are either of zero length (being normal to the boundary and starting from it), or tangent to the boundary: in this latter case they integrate the vanishing component of the function $\boldsymbol{u} \in V_h^1 \subset H_0(\mathrm{curl}; \Omega)$.

Lemma 5.11: The relations hold for $\boldsymbol{u} \in C^1(\overline{\Omega}) \cap H_0(\mathrm{curl}; \Omega)$. For boundary edges the circulation $\tilde{\Phi}^e(\boldsymbol{u})(\boldsymbol{x})$ may contains a contribution along e which depends on $\hat{x}_\parallel^k$ (because the adjacent patch k is considered as the fine patch, $k = k^+(e)$), but for $\boldsymbol{u} \in C^1(\overline{\Omega}) \cap H_0(\mathrm{curl}; \Omega)$ this contribution vanishes. The same argument can be used for $\tilde{\Phi}^{e,\boldsymbol{v}}(\boldsymbol{u})(\boldsymbol{x})$.

Lemma 5.12: The antiderivatives $\Psi^e(f)$ and $\Psi^{e,\boldsymbol{v}}(f)$ vanish on any boundary edge. Indeed, we observe that our definitions of integration curves associated with boundary edges and vertices lead to domains $\sigma^e(\boldsymbol{x}, a)$ and $\sigma_k^{e,\boldsymbol{v}}(\boldsymbol{x}, \bar{a})$ which are of zero measure for $\boldsymbol{x} \in e$ when $e \subset \partial\Omega$. Hence, $\Psi^e(f) = \Psi^{e,\boldsymbol{v}}(f) = 0$ on e.

B.4. The main result

Theorem 6.3 also holds for the sequences (B.1) where $\phi \in H_0^1(\Omega)$ and all $\boldsymbol{u} \in H_0(\mathrm{curl}; \Omega)$, and for the sequence (B.2) with the corresponding homogeneous spaces. The commuting relations (6.16) also extend to the larger spaces, i.e. they hold for all $\phi \in W_0^{1,1}(\Omega)$ and all $\boldsymbol{u} \in W_0^1(\mathrm{curl}; \Omega)$ where the latter space is the closure of $C_c^1(\Omega)$ in $W^1(\mathrm{curl}; \Omega)$.

Regarding the proofs in Section 7, we add the following remarks:

Lemma 7.2: We need to show that the tangential component of $\Pi^1 \boldsymbol{u}$ vanishes on boundary edges. Using the definitions of the conforming projectors in Section B.1, we realize that the terms in the decomposition (7.4) are tangential derivatives of fields that vanish on boundary edges. Hence, $\Pi^1 \boldsymbol{u} \in H_0(\mathrm{curl};\Omega)$.

Lemma 7.3: Similarly, we want to show that the correction terms vanish on boundary edges. This can directly be inferred form the properties we added to the antiderivative operators in Lemma 5.8, as they all already vanish on boundary edges.

Lemma 7.4: The equality holds for all $\phi \in H_0^1(\Omega)$ in the homogeneous case (B.1). As remarked, it also extends to the space $W_0^{1,1}(\Omega)$. The proof extends similarly, considering $\phi \in C^1(\overline{\Omega}) \cap H_0^1(\Omega)$, using $\bar{\phi}_e = 0$ and the relations (B.3) and (B.4) on homogeneous boundary edges.

Lemma 7.6: Again, the equality also holds for all $\boldsymbol{u} \in H_0(\mathrm{curl};\Omega)$ with extension to the larger space $W_0^1(\mathrm{curl};\Omega)$. The proof is verbatim, but considering $\boldsymbol{u} \in C^1(\overline{\Omega}) \cap H_0(\mathrm{curl};\Omega)$.

In the case of homogeneous boundary conditions, the commuting diagram (2.5) becomes:

$$
\begin{array}{ccccccccc}
\{0\} & \xrightarrow{\;0\;} & H_0^1(\Omega) & \xrightarrow{\;\nabla\;} & H_0(\mathrm{curl};\Omega) & \xrightarrow{\;\mathrm{curl}\;} & L^2(\Omega) & \xrightarrow{\;\int\;} & \mathbb{R} \\
\downarrow & & \downarrow \Pi^0 & & \downarrow \Pi^1 & & \downarrow \Pi^2 & & \downarrow \\
\{0\} & \xrightarrow{\;0\;} & V_h^0 & \xrightarrow{\;\nabla\;} & V_h^1 & \xrightarrow{\;\mathrm{curl}\;} & V_h^2 & \xrightarrow{\;\int\;} & \mathbb{R}
\end{array}
$$

Since the last commuting relation is non-trivial, let us state it formally.

Lemma B.1. *The equality*

$$\int_\Omega \Pi^2 f = \int_\Omega f$$

holds for all $f \in L^2(\Omega)$.

Proof. On each patch Ω_k, we decompose the pullback

$$\hat{f}^k := (\mathcal{F}_k^2)^{-1}(f|_{\Omega_k}) = \hat{f}_{\mathrm{mv}}^k + \hat{f}_0^k$$

into its mean value $\hat{f}_{\mathrm{mv}}^k := \fint_{\hat{\Omega}} \hat{f}^k$ and a remainder of zero integral, $\int_{\hat{\Omega}} \hat{f}_0^k = 0$. This yields a decomposition of f into

$$f = f_{\mathrm{mv}} + f_0 := \sum_{k\in\mathcal{K}} \mathcal{F}_k^2(\hat{f}_{\mathrm{mv}}^k) + \sum_{k\in\mathcal{K}} \mathcal{F}_k^2(\hat{f}_0^k),$$

where the integral preservation of the 2-form pushforward yields $\int_\Omega f_0 = 0$ and $\int_\Omega f_{\mathrm{mv}} = \int_\Omega f$. Without loss of generality we can assume that Ω is connected, so that $f_0 = \mathrm{curl}\,\boldsymbol{u}$ holds for some $\boldsymbol{u} \in H_0(\mathrm{curl};\Omega)$ (indeed the cohomology space $\{g \in L^2(\Omega) : \int_\Omega g = 0 \text{ and } \langle g, \mathrm{curl}\,\boldsymbol{v}\rangle_{L^2(\Omega)} = 0 \ \forall \boldsymbol{v} \in H_0(\mathrm{curl};\Omega)\}$ is trivial). Using the commuting property satisfied by the projection operators we then write

$$\int_\Omega \Pi^2 f_0 = \int_\Omega \Pi^2 \,\mathrm{curl}\,\boldsymbol{u} = \int_\Omega \mathrm{curl}\,\Pi^1 \boldsymbol{u} = \int_{\partial\Omega} n \times \Pi^1 \boldsymbol{u} = 0$$

where last equality follows from the fact that $\Pi^1 \boldsymbol{u} \in H_0(\mathrm{curl};\Omega)$. Since constants belong to the logical spaces $\hat{V}_k^2$ we further see that $f_{\mathrm{mv}} \in V_{\mathrm{pw}}^2 = V_h^2$: in particular the projection property yields $\Pi^2 f_{\mathrm{mv}} = f_{\mathrm{mv}}$. The result then follows by gathering the above findings:

$$\int_\Omega \Pi^2 f = \int_\Omega \Pi^2 f_{\mathrm{mv}} + \int_\Omega \Pi^2 f_0 = \int_\Omega f_{\mathrm{mv}} = \int_\Omega f. \qquad \blacksquare$$

References

[1] Douglas N. Arnold, Pavel B. Bochev, Richard B. Lehoucq, Roy A. Nicolaides, and Mikhail Shashkov, editors. *Compatible spatial discretizations*, volume 142 of *The IMA Volumes in Mathematics and its Applications*. Springer, 2006. Papers from the IMA Hot Topics Workshop on Compatible Spatial Discretizations for Partial Differential Equations held at the University of Minnesota, Minneapolis, MN, May 11–15, 2004.

[2] Douglas N. Arnold, Richard S. Falk, and Ragnar Winther. Finite element exterior calculus, homological techniques, and applications. *Acta Numer.*, 15:1–155, 2006.

[3] Douglas N. Arnold, Richard S. Falk, and Ragnar Winther. Finite element exterior calculus: From Hodge theory to numerical stability. *Bull. Am. Math. Soc.*, 47(2):281–354, 2010.

[4] Douglas N. Arnold and Johnny Guzmán. Local L^2-bounded commuting projections in FEEC. *ESAIM, Math. Model. Numer. Anal.*, 55(5):2169–2184, 2021.

[5] Yuri Bazilevs, Lourenço Beirão da Veiga, J. Austin Cottrell, Thomas J. R. Hughes, and Giancarlo Sangalli. Isogeometric analysis: approximation, stability and error estimates for h-refined meshes. *Math. Models Methods Appl. Sci.*, 16(7):1031–1090, 2006.

[6] Daniele Boffi. Finite element approximation of eigenvalue problems. *Acta Numer.*, 19:1–120, 2010.

[7] Daniele Boffi, Martin Costabel, Monique Dauge, Leszek Demkowicz, and Ralf Hiptmair. Discrete compactness for the p-version of discrete differential forms. *SIAM J. Numer. Anal.*, 49(1):135–158, 2011.

[8] Francesca Bonizzoni and Guido Kanschat. H^1-conforming finite element cochain complexes and commuting quasi-interpolation operators on Cartesian meshes. *Calcolo*, 58(2): article no. 18 (29 pages), 2021.

[9] Alain Bossavit. Whitney forms: a class of finite elements for three-dimensional computations in electromagnetism. *IEE Proc. A: Phys. Sci., Meas., Instrum.*, 135(8): article no. 1, 1988.

[10] Alain Bossavit. *Computational electromagnetism. Variational formulations, complementarity, edge elements*. Academic Press Inc., 1998.

[11] Annalisa Buffa, Jürgen Dölz, Stefan Kurz, Sebastian Schöps, Rafael Vázquez, and Felix Wolf. Multipatch approximation of the de Rham sequence and its traces in isogeometric analysis. *Numer. Math.*, 144(1):201–236, 2019.

[12] Annalisa Buffa, Eduardo M. Garau, Carlotta Giannelli, and Giancarlo Sangalli. On Quasi-Interpolation Operators in Spline Spaces. In Gabriel R. Barrenechea, Franco Brezzi, Andrea Cangiani, and Emmanuil H. Georgoulis, editors, *Building Bridges: Connections and Challenges in Modern Approaches to Numerical Partial Differential Equations*, Lecture Notes in Computational Science and Engineering, pages 73–91. Springer, 2016.

[13] Annalisa Buffa, Judith Rivas, Giancarlo Sangalli, and Rafael Vázquez. Isogeometric Discrete Differential Forms in Three Dimensions. *SIAM J. Numer. Anal.*, 49(2):818–844, 2011.

[14] Annalisa Buffa, Giancarlo Sangalli, and Rafael Vázquez. Isogeometric analysis in electromagnetics: B-splines approximation. *Comput. Methods Appl. Mech. Eng.*, 199(17):1143–1152, 2010.

[15] Annalisa Buffa, Giancarlo Sangalli, and Rafael Vázquez. Isogeometric methods for computational electromagnetics: B-spline and T-spline discretizations. *J. Comput. Phys.*, 257:1291–1320, 2014.

[16] Annalisa Buffa, Rafael Vázquez, Giancarlo Sangalli, and Lourenço Beirão da Veiga. Approximation estimates for isogeometric spaces in multipatch geometries. *Numer. Methods Partial Differ. Equations*, 31(2):422–438, 2015.

[17] Martin Campos Pinto. Moment Preserving Local Spline Projection Operators. *Computing*, 51(3):565–585, 2020.

[18] Martin Campos Pinto and Yaman Güçlü. Broken-FEEC discretizations and Hodge Laplace problems. `https://arxiv.org/abs/2109.02553`, 2021.

[19] Snorre H. Christiansen. Stability of Hodge decompositions in finite element spaces of differential forms in arbitrary dimension. *Numer. Math.*, 107(1):87–106, 2007.

[20] Snorre H. Christiansen and Ragnar Winther. Smoothed projections in finite element exterior calculus. *Math. Comput.*, 77(262):813–830, 2007.

[21] Carl de Boor. On local linear functionals which vanish at all B-splines but one. In *Theory of approximation. With applications (Calgary, 1975)*, pages 120–145. Academic Press Inc., 1976.

[22] Alexandre Ern, Thirupathi Gudi, Iain Smears, and Martin Vohralík. Equivalence of local- and global-best approximations, a simple stable local commuting projector, and optimal *hp* approximation estimates in $H(\mathrm{div})$. *IMA J. Numer. Anal.*, 42(2):1023–1049, 2022.

[23] Alexandre Ern and Jean-Luc Guermond. Mollification in Strongly Lipschitz Domains with Application to Continuous and Discrete De Rham Complexes. *Comput. Methods Appl. Math.*, 16(1):51–75, 2016.

[24] John A Evans, Michael A Scott, Kendrick M Shepherd, Derek C Thomas, and Rafael Vázquez. Hierarchical B-spline complexes of discrete differential forms. *IMA J. Numer. Anal.*, 40(1):422–473, 2020.

[25] Richard S. Falk and Ragnar Winther. Local Bounded Cochain Projections. *Math. Comput.*, 83(290):2631–2656, 2014.

[26] Yaman Güçlü, Said Hadjout, and Martin Campos Pinto. A broken FEEC framework for electromagnetic problems on mapped multipatch domains. `https://arxiv.org/abs/2208.05238`, 2022.

[27] Ralf Hiptmair. Canonical construction of finite elements. *Math. Comput.*, 68(228):1325–1346, 1999.

[28] Ralf Hiptmair. Finite elements in computational electromagnetism. *Acta Numer.*, 11:237–339, 2002.

[29] Florian Holderied, Stefan Possanner, and Xin Wang. Mhd-kinetic hybrid code based on structure-preserving finite elements with particles-in-cell. *J. Comput. Phys.*, 433: article no. 110143 (33 pages), 2021.

[30] Thomas J. R. Hughes, J. Austin Cottrell, and Yuri Bazilevs. Isogeometric analysis: CAD, finite elements, NURBS, exact geometry and mesh refinement. *Comput. Methods Appl. Mech. Eng.*, 194(39-41):4135–4195, 2005-10.

[31] Kjetil André Johannessen, Mukesh Kumar, and Trond Kvamsdal. Divergence-conforming discretization for Stokes problem on locally refined meshes using LR B-splines. *Comput. Methods Appl. Mech. Eng.*, 293:38–70, 2015.

[32] Jasper Kreeft, Artur Palha, and Marc Gerritsma. Mimetic framework on curvilinear quadrilaterals of arbitrary order. `https://arxiv.org/abs/1111.4304`, 2011.

[33] Francesco Patrizi. Isogeometric de Rham complex discretization in solid toroidal domains. `https://arxiv.org/abs/2106.10470`, 2021.

[34] Benedikt Perse, Katharina Kormann, and Eric Sonnendrücker. Geometric Particle-in-Cell Simulations of the Vlasov–Maxwell System in Curvilinear Coordinates. *SIAM J. Sci. Comput.*, 43(1):B194–B218, 2021.

[35] Joachim Schöberl. A multilevel decomposition result in h(curl). In *Proceedings from the 8th European Multigrid, Multilevel, and Multiscale Conference*, 2005. Edited by P.H.P. Wesseling and C.W. Oosterlee.

[36] Joachim Schöberl. A posteriori error estimates for Maxwell equations. *Math. Comput.*, 77(262):633–650, 2008.

[37] Roger Temam. *Navier-Stokes Equations: Theory and Numerical Analysis*. North-Holland, 1977.

[38] Deepesh Toshniwal and Thomas J. R. Hughes. Isogeometric discrete differential forms: Non-uniform degrees, Bézier extraction, polar splines and flows on surfaces. *Comput. Methods Appl. Mech. Eng.*, 376: article no. 113576 (44 pages), 2021.